Influence of Inflammatory Stimuli on the Peroxisomal Compartment of Mouse Macrophages

Inauguraldissertation

Zur Erlangung des Grades eines Doktors der Humanbiologie

Des Fachbereichs Medizin

Der Justus-Liebig-Universität Gießen

Vorgelegt von Kollas Andreas
Aus Bitburg

Gießen 2013

Aus dem Institut für Anatomie und Zellbiologie
Abteilung medizinische Zellbiologie II
Leitung: Frau Prof. Dr. Baumgart-Vogt

Gutachterin:
Frau Prof. Dr. Baumgart-Vogt

Gutachter
Herr Prof. Dr. Lochnit

Tag der Disputation
30.06.2016

1. Introduction

The result of this thesis is proposing an important role of the peroxisomal compartment in macrophages within inflammatory processes. It is based on previous findings of members of the Institute for Anatomy and Cell Biology, Department II, Medical Cell Biology, Justus-Liebig University, Gießen. The published studies link impaired peroxisome function with increased oxidative stress in inflammatory neuronal tissue and documented for the first time the presence of peroxisomes in alveolar macrophages [1]. A careful literature research at the beginning of this thesis revealed that there was only scarce knowledge about the role and function of peroxisomes in macrophages during inflammatory processes. Consequently, we searched if inflammatory stimuli affect the peroxisomal compartment in macrophages and what implications for the inflammatory response may emerge from impaired peroxisome function.

1.1 Peroxisomes

General aspects

Peroxisomes can be found in nearly all eukaryotic cells. For the first time they were described by Rhodin in 1954 who introduced the term “microbodies” [2], while their first biochemical characterisation was done in 1966 by De Duve and Baudhuin, who coined the name peroxisomes to these organelles, related to their content of hydrogen peroxide (H_2O_2) producing and degrading enzymes [3].

Peroxisomes are subcellular organelles surrounded by a single membrane and contain no own genome unlike mitochondria [4]. Shape, size (0.1-1.0 µM), number and metabolic functions of peroxisomes differ between different organism, organs and cell types [5]. Recent findings propose an Actinobacteria origin of the peroxisome. The study indicates a transfer of peroxisomal genes to the nucleus. During this process, peroxisomal genes were lost and got replaced by mitochondrial genes with similar function [6]. This could explain the unique peroxisome targeting and peroxisome protein import in comparison to the protein import of mitochondria or chloroplasts. Peroxisomes have the capability to import folded functional matrix proteins, proteins with attached cofactors and oligomerised matrix proteins into the organelle [7]. Consequently, the peroxisomal import machinery is able to transport larger cargo across the organelle membrane than mitochondria or chloroplasts.

According to their broad range of catabolic and anabolic functions, they are a multipurpose organelle, a kind of “Swiss army knife” (for a review see [8]). Additionally, peroxisomes have the capability to adapt to nutritional or environmental stimuli/changes [9]. At the moment more than 130 peroxisomal proteins are known [10]. Moreover, more than 30 so called peroxin (PEX…p) proteins have been discovered, 14 of them in mammals. Those with no homologues in mammals were discovered mainly in yeasts [8]. PEX proteins play an important role in peroxisomal biogenesis (for an overview see Tab. 1) and function. They are involved in peroxisomal matrix protein import. Dependent on their function, they are integrated into or attached to the peroxisomal membrane, cycle between peroxisomal membrane and the cytosol or are located in the peroxisomal matrix

Tab. 1: discovered peroxins and their characteristics.

Peroxin	Characteristics	Organism			
		Mammals	Yeasts	Plants	Fungi
PEX 1	ATPase of the AAA-family	**x**	**x**	**x**	**x**
PEX 2	zinc binding integral peroxisomal membrane protein, contains C3H4-motive	**x**	**x**	**x**	**x**
PEX 3	integral peroxisomal membrane protein, membrane protein import	**x**	**x**	**x**	**x**
PEX 4	peroxisome associated ubiquitin conjugating enzyme (E2)	**x**	**x**	**x**	**-**
PEX 5	PTS1-Receptor, located in cytoplasm and associated at the outside of peroxisomal membrane	**x**	**x**	**x**	**x**
PEX 6	ATPase of the AAA-family	**x**	**x**	**x**	**x**
PEX 7	PTS2-Receptor, located in cytoplasm and associated at the outside of the peroxisomal membrane	**x**	**x**	**x**	**x**
PEX 8	peripheral peroxisome membrane protein	**-**	**x**	**-**	**x**
PEX 9	integral peroxisomal membrane protein	**-**	**x**	**-**	**-**
PEX 10	zinc binding integral peroxisomal membrane protein, contains C3H4-motive	**x**	**x**	**x**	**x**
PEX 11	integral peroxisomal membrane protein, involved in fission processes	**x**	**x**	**x**	**x**
PEX 12	zinc binding integral peroxisomal membrane protein, contains C3H4-motive	**x**	**x**	**x**	**x**
PEX 13	integral peroxisomal membrane protein, contains SH3-domaine, part of the matrix protein receptor docking complex, binds Pex5p, Pex7p, Pex14p	**x**	**x**	**x**	**x**
PEX 14	peroxisomal membrane protein, class II binding motive for SH3-ligands, part of the matrix protein receptor docking complex, binds Pex5p, Pex7p, Pex13p	**x**	**x**	**x**	**x**
PEX 15	integral peroxisomal membrane protein	**-**	**x**	**-**	**-**
PEX 16	integral peroxisomal membrane protein, necessary for membrane biogenesis	**x**	**x**	**x**	**x**
PEX 17	peripheral membrane, binds Pex14p	**-**	**x**	**x**	**-**
PEX 18	mainly cytosolic, necessary for PTS2 import, highly homologue to PEX21	**-**	**x**	**-**	**-**
PEX 19	farnesylated protein, binds Pex3p, located in cytoplasm and associated at the outside of peroxisomal membrane	**x**	**x**	**x**	**x**
PEX 20	cytosolic protein, necessary for dimerisation and import of Fox3p	**-**	**x**	**-**	**x**
PEX 21	cytosolic protein, necessary for PTS-2 mediated protein import, highly homologue to PEX18	**-**	**x**	**-**	**-**
PEX 22	integral peroxisomal membrane protein, interacts with Pex4p	**-**	**x**	**x**	**x**
PEX 23	integral peroxisomal membrane protein	**-**	**x**	**-**	**x**
PEX 24	integral peroxisomal membrane protein	**-**	**x**	**-**	**x**
PEX 25	localised at the peroxisome, regulates peroxisome number and size	**-**	**x**	**-**	**-**
PEX 26	peroxisomal membrane protein, recycling of the PTS-1 receptor Pex5p	**x**	**-**	**-**	**x**
PEX 27	localised at the peroxisome, regulates peroxisome number and size	**-**	**x**	**-**	**-**
PEX 28	integral peroxisomal membrane protein, involved in dynamic processes of the peroxisome	**-**	**x**	**-**	**-**
PEX 29	integral peroxisomal membrane protein, involved in dynamic processes of the peroxisome	**-**	**x**	**-**	**-**
PEX 30	localised at the peroxisome, regulates peroxisome size	**-**	**x**	**-**	**-**
PEX 31	localised at the peroxisome, regulates peroxisome size	**-**	**x**	**-**	**-**
PEX 32	localised at the peroxisome, regulates peroxisome size	**-**	**x**	**-**	**-**
PEX 33	peroxisomal docking complex	**-**	**-**	**-**	**x**

1.1.1 Peroxisomal protein import and biogenesis

Up to now, peroxisomal protein import has been studied in yeasts and mammals. Peroxisomal proteins are synthesised at free ribosomes in the cytoplasm. The peroxisomal shuttling mechanism includes Pex5p and Pex7p [11, 12]. Pex5p is the binding partner of proteins directed to peroxisomes. Most of these proteins contain a specific targeting sequence at their carboxy-terminal end, the peroxisomal targeting sequence-1 (PTS-1). Historically, the PTS-1 is composed of the following consensus sequence (S/A/C) - (K/R/H) - (L/M). Since amino acid residues further up- or downstream of the original tripeptide influence the receptor binding capacity of the cargo protein, Brocard et al. proposed to define the PTS-1 as a dodecamer sequence recently [13]. In contrast, few peroxisomal proteins contain the amino-terminal PTS-2. The PTS-2 signal is more common in plants, whereas in *C. elegans* and *C. briggsae* PTS-2 dependent protein import seems to be completely absent [11, 12]. The consensus sequence is a degenerated nonapeptide:

(R) - (L/V/I/Q) – xx - (L/V/I/H) - (L/S/G/A) – x - (H/Q) - (L/A)

Pex7p recognises PTS-2 containing proteins. After the Pex7p-guided transport, the cargo protein gets cleaved during import by a peroxisomal matrix protein [14, 15].

During the PTS-1 initiated transport process, conformational changes of Pex5p at its N-terminus are induced after cargo binding, leading to interaction of the Pex5p/cargo complex with the import machinery at the peroxisomal membrane [12]. The import machinery consists mainly of Pex13p, Pex14p as well as the zinc RING finger proteins Pex2p, Pex10p and Pex12p [14]. Two hypotheses of cargo delivery are proposed. Either a complete transition of the Pex5p into the peroxisomal matrix (“extended shuttle hypothesis”) is suggested [16] or it is proposed, that Pex5p remains outside of the peroxisomal matrix, attached to the peroxisomal import machinery (“shuttle hypothesis”).

In humans two isoforms of Pex5p are known. These represent distinct splicing variants. The short form, Pex5S is exclusively involved in PTS-1 cargo-protein binding and transport. The long variant, Pex5L is also involved in targeted PTS-2 cargo protein transport. Pex5L initialises the binding of the transporter complex with the protein import machinery at the peroxisomal membrane by forming a complex with Pex7p and the corresponding cargo protein [15, 16]. In *S. cerevisiae* Pex18p and Pex21p and in fungi Pex20p play a similar role in cargo protein transport [17]. For an overview of peroxisomal matrix protein import and peroxisomal membrane protein import see Fig. 1.

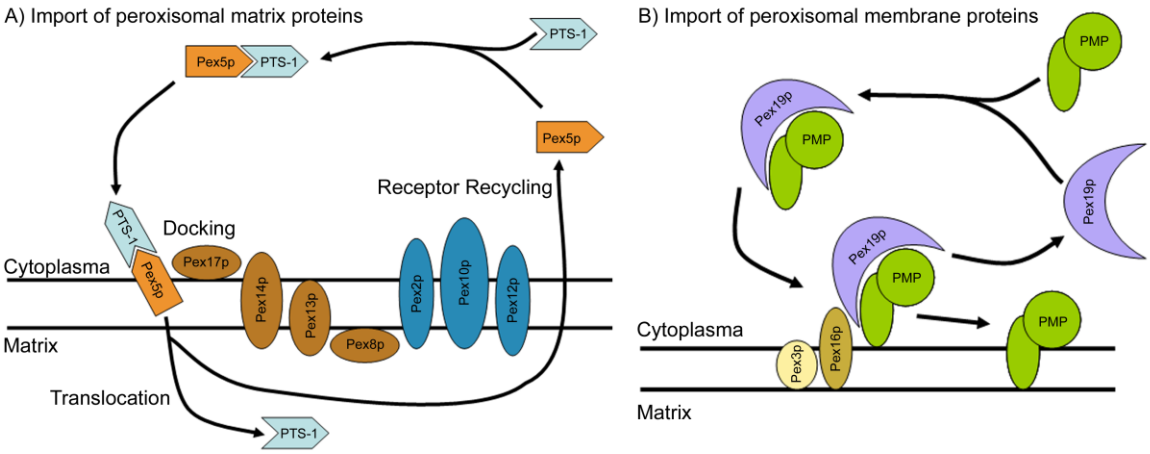

Fig. 1 Peroxisomal biogenesis according to Platta and Erdmann.
A) The cytoplasmic receptor Pex5p recognizes PTS-1 containing peroxisomal matrix proteins and guides them to the peroxisomal membrane. After docking at the sophisticated import complex (consisting of Pex17p, Pex14p, Pex13p and Pex8p) target proteins are imported while Pex5p is recycled by a complex containing Pex2p, Pex10p and Pex12p. B) New synthesized PMPs are guided and transported to the peroxisomal membrane by Pex19p. Integration into the peroxisomal membrane is Pex16p/Pex3p mediated, while Pex19p is recycled into the cytoplasm.

Integration of peroxisomal membrane proteins (PMPs) into the membrane of pre-existing peroxisomes is necessary for peroxisomal biogenesis. In mammals, fungi and plants the import complex consists of Pex19p, Pex3p and Pex16p (see Tab. 1 and Fig. 1) [13, 18]. In Yeasts (except *Yarrowia lipolytic*) and in *Caenorhabditis spec.* Pex16p seems to be absent [19]. PMPs originate from free cytoplasmic ribosomes. They contain a membrane targeting sequence (mPTS) with an inbuilt Pex19p-binding site and either a transmembrane domain or a protein binding site for membrane anchoring [14]. Pex19p is thought to be a protein receptor, cycling between cytoplasm and peroxisome. It binds PMPs in the cytoplasm, guides the PMPs to the peroxisomal membrane and interacts with Pex3p and Pex16p for PMP insertion [19, 20]. Loss of any of these three Pex proteins leads to a complete loss of peroxisomal membranes. It was hypothesised that the reintroduction of these proteins in appropriate knock out cells leads to the formation of peroxisomes *de novo* out of the ER [21, 22].

Peroxisomes do not only increase in size by import of matrix and membrane proteins but also proliferate by division which is induced by a broad variety of stimuli. The Pex protein Pex11p is involved in these processes, since deletion of PMP27, the yeast homologue of Pex11p, leads to significant reduction in peroxisome abundance, while over-expression showed a

massive increase of peroxisome abundance [20]. In mammals three isoforms of the Pex11p family are known (Pex11pα, Pex11pβ and Pex11pγ) that are thought to form homo-oligomers [21]. Yeast species harbour only a single Pex11p but contain several additional fission related proteins (Pex23p-Pex25p, Pex27p-Pex32p) (see Tab. 1). It was hypothesised, that oligomerisation might be a regulatory mechanism of Pex11p activity. Recently, Knoblach et al. showed in *S. cerevisiae* a phosphorylation dependent regulation of Pex11p [22]. For regular peroxisome division, further proteins are necessary, e.g. the dynamin-like large GTPase (DLP-1), its receptor Fis-1 and the mitochondrial fission factor (MFF) [23]. It is very noteworthy, that in mammals these proteins are involved in peroxisomal as well as mitochondrial division [24, 25]. Furthermore, in yeast, in fungi and in plants, dynamin-like GTPases and Fis-homologues are shared in peroxisomal and mitochondrial division [25-27].

1.1.2 Peroxisomes in cellular metabolism

Depending on organism, organ and cell type, peroxisomes are involved in a variety of distinct anabolic and catabolic processes, such as degradation of reactive oxygen species (ROS), β-oxidation of a broad set of lipid derivatives and α-oxidation of branched-chain fatty acids [28], as well as the biosynthesis of cholesterol, plasmalogens, phospholipids, isoprenoids, xenobiotics, pristanic acid and bile acids (see Tab. 2) [29-31]. Additionally, peroxisomes are involved in the glyoxylate cycle in plants [32], whereas they take part in penicillin biosynthesis in some fungi [33].

Tab. 2 Overview of metabolic activities in peroxisomes, according to Titorenko et al. [34]

Species	anabolic	catabolic
Yeast	Lysine	Methanol, β-oxidation of FA degradation of H_2O_2, glyoxylate cycle
Fungi	Penicillin	β-oxidation of FA, degradation of H_2O_2 glyoxylate cycle
Plant		Purine, reactions in photorespiration, β-oxidation of FA, degradation of H_2O_2 glyoxylate cycle
Mammals	Etherlipids Plasmalogens Cholesterol Bile acids Poly unsaturated fatty acids (PUFA)	Amino acids, Purine, Polyamine α-oxidation of FA β-oxidation of distinct lipid derivates, degradation of ROS (e.g. H_2O_2)
Human	Etherlipids Plasmalogens Cholesterole by β-oxidation enzymes Bile acids by β-oxidation enzymes PUFA by β-oxidation enzymes	Amino acids, Purine, Polyamine α-oxidation FA, β-oxidation of distinct lipid derivatives, degradation of ROS

1.1.3 Peroxisomes in ROS metabolism

As shown above, peroxisomes are involved in metabolic processes in which H_2O_2 is formed as by-product.

Fig. 2 gives an overview of the processes related to ROS production and degradation in peroxisomes. Main sources of H_2O_2 in peroxisomes are flavin oxidase activity (e.g. FA β-oxidation), dispropotionation of superoxide radicals and in plants the photorespiratory glycolate oxidase reaction (see Tab. 3) [35]. H_2O_2 is highly reactive and causes severe damage in all parts of the cell. To prevent intracellular damage, peroxisomes contain a large set of ROS degrading enzymes summarized in Tab. 4 [35].

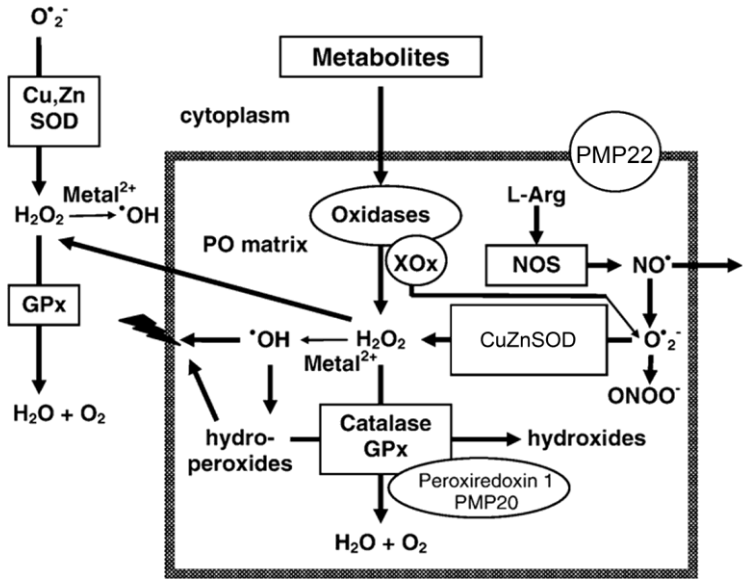

Fig. 2 Overview of ROS producing and degrading processes in peroxisomes.
Modified, according to Schrader and Fahimi, related enzymes are elucidated in Tab. 3 and Tab. 4

Tab. 3 ROS generating enzymes in peroxisomes

Enzyme	Substrate	ROS
(1) Acyl-CoA oxidases in rodents		
(a) Palmitoyl-CoA oxidase (ACOX1)	Long chain fatty acids	H_2O_2
(b) Trihydroxycoprostanoyl-CoA oxidase (ACOX 2)	Bile acid intermediates	H_2O_2
(c) Pristanoyl-CoA oxidase (ACOX3)	Methyl branched chain fatty acids	H_2O_2
(2) Urate oxidase	Uric acid	H_2O_2
(3) Xanthine oxidase	Xanthine	H_2O_2, $O_2^{\cdot -}$
(4) D-amino acid oxidase	D-Proline	H_2O_2
(5) Pipecolic acid oxidase	L-Pipecolic acid	H_2O_2
(6) D-aspartate oxidase D-aspartate	N-Methyl-D-aspartate	H_2O_2
(7) Sarosine oxidase	Sarcosine, pipecolate	H_2O_2
(8) L-alpha-hydroxy acid oxidase	Glycolate, lactate	H_2O_2
(9) Poly amine oxidase	N-Acetyl spermine/spermidine	H_2O_2
(10) inducible nitric oxide synthase (iNOS)	L-Arginine	$^{\cdot}NO$
(11) Plant sulfite oxidase	Sulfite	H_2O_2

Tab. 4 ROS degrading enzymes in the cell

Enzyme	Substrate	Cellular localisation
(1) Catalase	H_2O_2	Cytoplasm, nucleus, peroxisome
(2) Glutathione peroxidase 1	H_2O_2	All cell compartments (not lysosomes)
(3) Cu, Zn SOD	$O_2^{\cdot -}$	Cytoplasm, peroxisomes, nuleus
(4) Epoxide hydrolase	Epoxides	ER, cytoplasm and peroxisomes
(5) Peroxiredoxin I	H_2O_2	Cytoplasm, nucleus, mitochondria, peroxisomes
(6) Peroxiredoxin V (PMP20)	H_2O_2	Peroxisomes
(7) Plant ascorbate–glutathione cycle	H_2O_2	Peroxisomes, chloroplasts, cytoplasm, root nodule mitochondria (plants only)

1.1.4 Peroxisomes in lipid metabolism

1.1.4.1 Peroxisomal β-oxidation

Peroxisomes contain different anabolic and catabolic functions, like degradation of saturated and unsaturated medium, long- and very long-chain fatty acids and their derivates (e.g. α-oxidation, β-oxidation), synthesis of cholesterol, ether-phospholipids and polyunsaturated FA as well as leukotriens and prostaglandins, xenobiotics, and pristanic acid [5, 28, 31, 38-41]. The most prominent and best investigated pathway in peroxisomal metabolism is the degradation of fatty acids (FA). In mammals, FA-degradation is divided in a mitochondrial and a peroxisomal part both exhibiting different substrate specificities for FA degradation. The substrates of mitochondrial β-oxidation are limited to short (<C8), middle (C8-C12) und long chain FA (≤C20) In contrast substrates for peroxisomal β-oxidation are much more versatile including very long-chain FA (VLCFA, >C22), long- and medium-chain dicarboxylic FA (products of microsomal ω-oxidation) [28], prostaglandins, leukotriens, cholesterol side chain and steroids [5]. Therefore, the β-oxidation machinery in mitochondria and peroxisomes differ in their enzyme composition [42-46]. This division of tasks seems to be present mainly in mammals. In lower organisms like yeasts and plants FA β-oxidation is performed almost exclusively in peroxisomes [47].

Before degradation, FA are activated by binding to acyl-CoA which is a substrate specific reaction mediated by different acyl-CoA-synthetases [48]. In mammalian mitochondria the VLCFA related acyl-CoA-synthetase is missing [49], whereas it is present on the peroxisomal membrane. Peroxisomal import of VLCF acyl-CoA derivatives is thought to be mediated by peroxisomal ATP-binding-cassette transporter (ABC-transporter). ABC-transporter belong to the half adenosinetriphosphate transporter category D sub-family (ABCD). In mammals four family members are known. ABCD1 (adrenoleukodystrophy protein, ALDP), ABCD2 (the adrenoleukodystrophy-related protein, ALDRP), ABCD3 (the 70-kDa peroxisomal membrane protein PMP70) and ABCD4 (the PMP70-related protein P70) [50-53]. Data from the literature show, that most of the half transporters form dimers, it is hypothesized that this is also the case for peroxisomal ABCD-transporter [54].

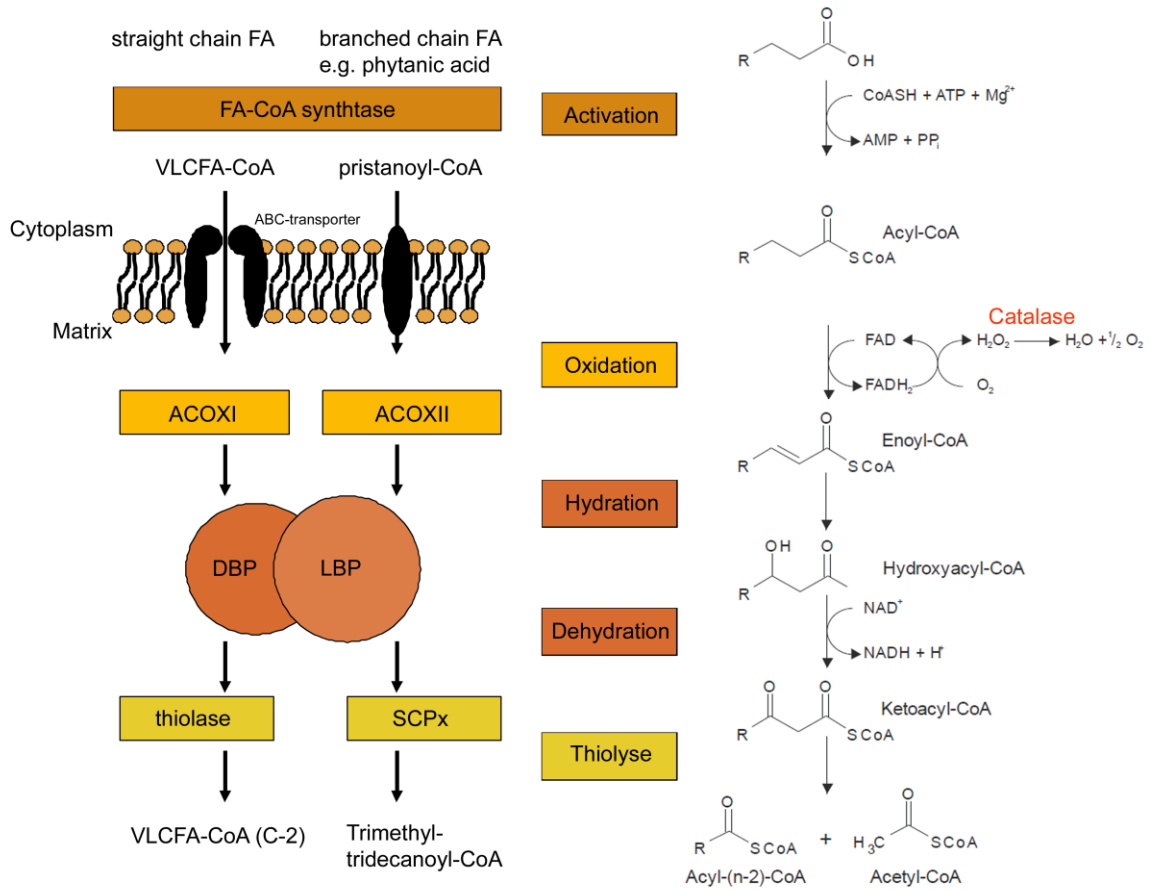

Fig. 3 Schematic overview of peroxisomal β-oxidation.
In peroxisomes very long chain fatty acids (VLCFA) and branched chain fatty acids are degraded. *Left*: degradation of straight chain VLCFA (e.g. cerotic acid) and degradation of branched chain fatty acid (e.g. phytanic acid). *Right*: peroxisomal β-oxidation step by step. *ACOX I/II* acyl-CoA oxidase I/II, *DBP* D-bifunctional protein, *LBP* L-bifunctional protein, *thiolase* 3-oxoacyl-CoA thiolase, *SCPx* Sterol carrier protein X

Basically, β-oxidation in mitochondria and peroxisomes consists of the same four subsequent steps: dehydrogenation, hydration, second dehydrogenation and thiolytic cleavage of acetyl-CoA. In humans, the rate limiting first step in β-oxidation is executed by either acyl-CoA-oxidase I (ACOXI, specific for straight chain VLCFA) or acyl-CoA-oxidase II (ACOXII, specific for CoA-esters of 2-methyl branched-chain fatty acids) [55, 56]. During this reaction electrons are transferred via $FADH_2$ to molecular oxygen. H_2O_2 is generated as by-product and is detoxified by catalase. The following two steps (hydration and second dehydration) are catalysed by two distinct bifunctional proteins (containing enoyl-CoA hydratase and 3-hydroxy-acyl-CoA dehydrogenase activity) which differ in their substrate specificity. D-bifuntional protein/enzyme (DBP/DBE) prefers VLC- and branched chain FA [57], whereas L-bifunctional protein/enzyme (LBP/LBE) sequesters also LCFA [58]. During the last step, one molecule of acetyl-CoA is detached from the activated FA by thiolytic cleavage.

For this purpose human peroxisomes contain two different 3-ketoacyl-CoA-thiolases. The straight-chain 3-oxoacyl-CoA thiolase (ACAA1) for 3-keto-acyl-CoA esters of VLCFA and the sterol carrier protein X (SCPx) for e.g. 2-methyl FA and 3-keto-acyl-CoA-esters of pristanic acid [59]. Three thiolases are described in rat and mouse: 3-ketoacyl-CoA thiolase A and B, a sterol carrier protein-2/3-ketoacyl-CoA thiolase (ScpX) as well as a thiolase involved in cholesterol synthesis [60, 61]. In mammals peroxisomal β-oxidation degrades FA down to a length of 6-8C followed by a transfer to mitochondria in form of carnitine-esters [62] or as free FA [63], for further degradation and ATP-production.

1.1.4.2 Peroxisomal α-oxidation

A special group of FA, 3-methyl branched FA carry a methyl group at their βC. Prior to peroxisomal β-oxidation, they have to undergo peroxisomal α-oxidation. During this process the first carbon atom is cleaved off and is released as CO_2 and the methyl group in the shortend derivative is then located at the αC position. Thereafter, the acyl-CoA FA is subject to peroxisomal β-oxidation. The most prominent representative of this group of FA in human physiology is phytanic acid. It is a degradation product of chlorophyll in ruminantia. Phytanic acid is obtained through the consumption of dairy products, especially milk and other ruminant animal fats. At the outside of peroxisomes phytanic acid is modified to its activated form phytanoyl-CoA by an acyl-CoA synthetase [64, 65]. After import into the peroxisomal matrix the phytanoyl-CoA is hydrolized by phytanoyol-CoA hydroxylase to 2-hydroxyphytanoyl-CoA [66]. Thereafter, 2-hydroxyphytanoyl-CoA lyase cleaves the intermediate to pristanal and formyl-CoA [67-69]. Finally, an aldehyde-dehydrogenase in peroxisomes catalyses pristanal to pristanic acid, which is further degraded by peroxisomal β-oxidation [70].

1.1.5 Peroxisomes and peroxisome proliferator-activated receptors

Peroxisomes play a substantial role in different metabolic pathways [63]. Impaired peroxisomal gene function leads to diseases of the Zellweger- or X-ALDP- spectrum. Furthermore, peroxisomes are involved in cellular defense against peroxides and ROS [71]. Ahlemeyer et al. have demonstrated that impaired peroxisomal function is linked to an increased ROS levels and inflammatory state in mouse brain which points out to a possible role of peroxisomes in chronic neurodegenerative diseases [72]. Therefore, the abundance and metabolism of peroxisomes and peroxisomal proteins has to be tightly regulated. Peroxisome proliferator-activated receptors (PPARs) are important regulators of peroxisomal abundance and metabolism. Until now, three distinct PPARs (PPARα, β/δ and γ) have been discovered. PPARs belong to the superfamily of steroid hormone receptors [73]. PPARα, -β/δ and -γ regulate a wide range of genes by ligand-dependent transcriptional gene activation and repression, fulfilling distinct functions in different tissues. Each PPAR has a characteristic tissue distribution.

- PPARα (alpha) is expressed in tissues with a high catabolic rate of fatty acids, such as brown and white adipose tissue. Furthermore in liver, kidney, heart, skeletal muscle and the retina [74, 75].
- PPARβ/δ (beta/delta) is ubiquitously expressed. Markedly in brain, kidney, liver, pancreas, heart, spleen and adipose tissue [74, 75].
- PPARγ (gamma): Two forms of PPARγ are known, PPARγ1 and PPARγ2. They originate from the same gene but contain different promoters and 5´exons. PPARγ1 is ubiquitously expressed, while PPARγ2 is mainly located in adipose tissue. (for review see [76]).

PPARs are predominantly located in the cytoplasm. After activation through a corresponding ligand, they dissociate from a corepressor, recruit coactivators, heterodimerise with other members of the nuclear receptor superfamily (like the retinoid X receptor) and translocate into the nucleus. There they recognise target DNA sequences, so called PPAR response elements (PPREs) and influence target gene transcription [77]. Ligands of PPARs are native FA, modified FA, metabolites and intermediates of FA metabolism [78]. Activation of PPARγ is an important therapeutic mechanism of antidiabetic drugs called thiazolidinediones (TZDs).
Additionally, PPARs influence the peroxisomal metabolism, since peroxisomal genes contain PPRE and are regulated by PPARs [79]. Moreover, recent data of our group suggest an important role of peroxisomes in balancing PPAR ligand homeostasis, since peroxisomes degrade PPAR ligands.

Besides their role in energy homeostasis, PPARs are involved in the regulation of the inflammatory response in monocytes/macrophages. Especially PPARα and -γ have been described in immunoregulatory cells, such as macrophages (MΦ) [80-82]. However, it is difficult to draw a conclusion about the role of distinct PPARs in inflammation, since they have shown pro-inflammatory as well as anti-inflammatory effects in different studies.

1.2 Macrophages

The first description of Macrophages (MΦ) (Greek: "large eaters") was in 1893 by the russian microbiologist Ilya Ilyich Mechnikov, who studied and worked several years in Gießen [83]. Depending on the blood building during ontogenesis of individuals, the origin of monocytes lies either in the yolk sac (embryo), the liver and spleen (foetus and newborn) or in the bone marrow [84]. Monocytes derive from pluripotent haematopoetic stem cells called colony-forming unit of the granulocyte and monocyte lineage (CFU-GM). Monocytes/MΦ are part of the innate immune system. They recognise, capture and destroy invading pathogens such as bacteria, pathogenic protozoa and fungi. Additionally, they are able to identify and neutralise tumour cells, virus-infected cells or apoptotic cells [85, 86]. Finally, monocytes and MΦ play an important role in humoral and cell mediated immune responses, as mediators between the innate and the adaptive immune system, since they are able to phagocyte invading pathogens and to present antigens to other cells of the adaptive immune system [87].

1.2.1 Development

During their development, monocytes differentiate progressively from monoblasts into promonocytes and monocytes within the bone marrow. At this developmental stage, monocytes leave the bone marrow into the peripheral blood stream and mature to MΦ (in tissue) [88]. Monocytes and MΦ comprise the mononuclear phagocyte system. During MΦ development, the differentiating hematopoetic stem cells lose their pluripotency and gain monocyte and MΦ specific features, such as the expression of IgG- and C3-receptors, phagocytotic activity, increasing lysosome abundance and transient peroxidase activity (see Fig. **4**) [89-92]. The development from stem cells to MΦ requires the availability of growth factors, like the macrophage colony-stimulating factor (M-CSF/CSF-1), the granulocyte-macrophage colony-stimulating factor (GM-CSF), interleukin-1, -3, -6 (IL-1, -3, -6) and interferon-γ (IFNγ) [93-97].

Under physiological conditions, a small percentage of monocytes leave the blood stream and enter the surrounding tissue and differentiate into resident MΦ, remaining in the tissue for several months [98]. During bacterial/viral infection, injury and/or inflammation, the production of monocytes in the bone marrow is increased and monocytes are attracted out of the blood stream into the affected tissue or organ due to the enhanced local expression and secretion of cytokines and chemoattractants [99]. Because of the stimulating cocktail of

growth factors, cytokines and chemokines monocytes differentiate into MΦ and abolish the cause of infection/inflammation.

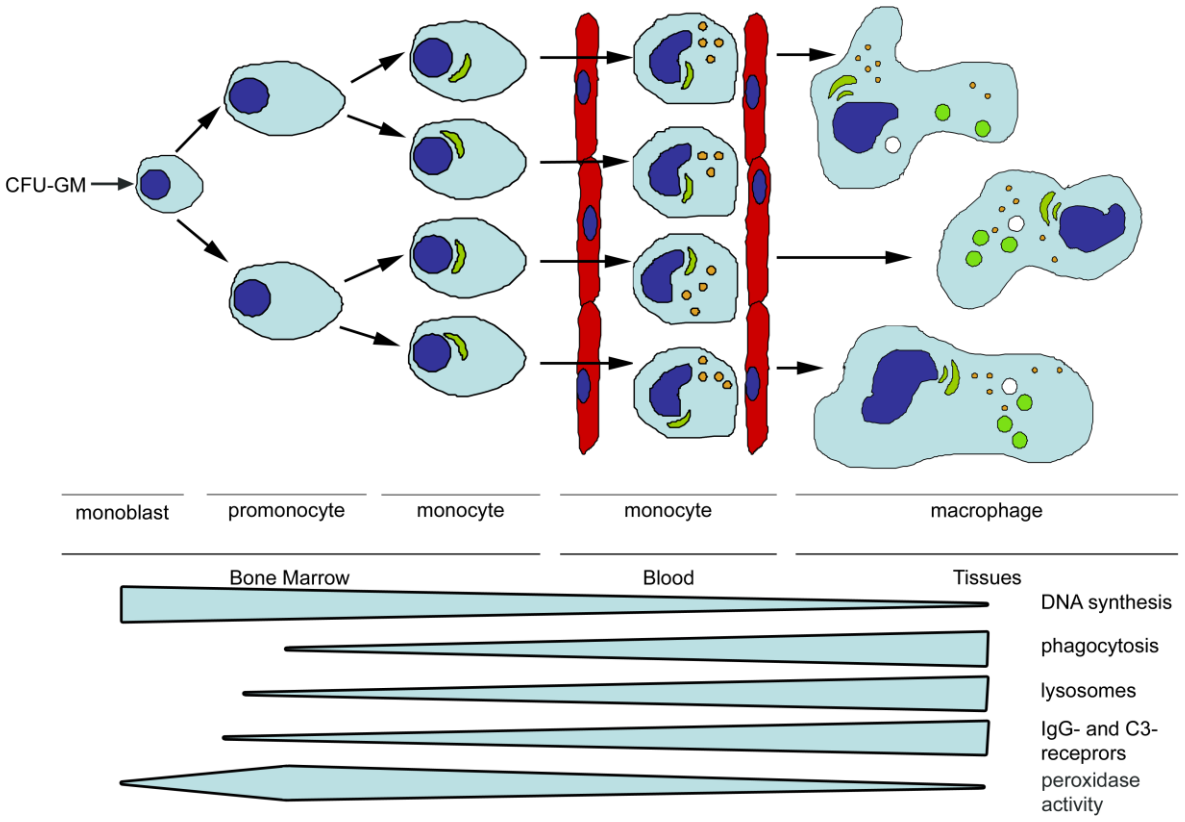

Fig. 4 Differentiation and characteristics of mononuclear phagocytic cells during development.
Origin and localisation of developing macrophages. The lower part exemplifies the gain and loss of typical features during development. According to Burke et al., 2002 [100].

Another important role of MΦ is the regulation of tissue-homeostasis. During embryogenesis, MΦ clear apoptotic areas, such as the skin between digits, coordinate organogenesis. The regulation of tissue-homeostasis persists in adult tissue, since MΦ are involved in wound healing, tissue repair and bone or organ remodelling [101-104]. Furthermore, MΦ participate in lipid homeostasis, e.g. cholesterol-metabolism [105] and in surfactant degradation in lungs [1].

1.2.2 Macrophages in bacterial Infection

In this chapter the composition of LPS will be described. Most of pathogenic bacteria in humans are gram-negative. MΦ detect these pathogens mainly based on the recognition of a unique component of the bacterial outer cell membrane, called lipopolysaccharide (LPS). LPS is a ligand of the CD14/Toll-like-receptor-4(TLR-4)/MD2 complex at the MΦ membrane. Ligand–complex interaction and signal transition by this receptor will be described in the chapter "the TLR family". Lipopolysaccharide is a highly conserved component of the bacterial membrane and crucial for cellular integrity of the bacteria, since loss of LPS leads to bacterial death [106]. LPS consists of three covalently linked units (see Fig. 5). The hydrophobic lipid A is the innermost unit of LPS, anchoring the LPS to the outer bacterial membrane. Lipid A consists of two glucosamine units with attached FAs and contains normally one phosphate group on each carbohydrate [107]. The central part of LPS consist of a core oligosaccharide (consisting of two subunits, an outer and an inner core), a short chain of sugar residues, which is highly diverse among bacterial species and

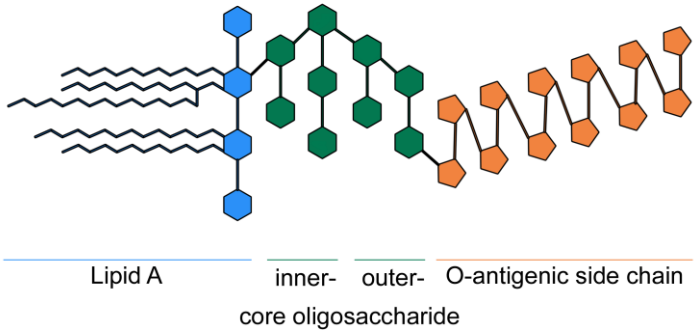

Fig. 5 Structure of LPS.

even within strains of species [108] and an O-antigenic side chain, a repetitive glycane polymer. This O-antigen is attached to the core oligosaccharide and comprises the outermost domain of the LPS molecule.

After LPS detection by TLR-4, resident MΦ induce a defensive response by attracting and activating other immune cells, including the recruitment of blood monocytes [109]. MΦ produce a massive amount of reactive oxygen species (ROS) and reactive nitrogen species (RNS), that is called oxidative burst [110, 111]. When activated, MΦ phagocyte [112-114] and digest pathogens [115, 116]. Moreover, MΦ secrete a variety of pro- and anti-inflammatory cytokines, modulating the host response to bacterial infection upon LPS stimulation (see Tab. 5 for details) [117, 118].

Tab. 5 MΦ secretory products in bacterial defence

Product	Function	Reference
Interleukine-1 (IL-1)	↑ proliferation and differentiation of T and B cells, ↑ IL-2, -8 and CSF production,	[119]
TNFα	↑ IL-6, -8, 9 and CSF production ↑ CR3	[120]
IL-6	Blocks LPS induced IL-1 and TNFα production	[121]
IL-8	↑ neutophil and monocyte activation chemotaxis	[122]
ROS/RNS	Killing bacteria by attacking lipids, proteins and DNA	[110, 111]
Lysozyme	Perforating the bacterial membrane	[123]
Complement factors	Opsonising bacteria for phagocytosis	[124]

1.2.3 The TLR family

The toll-like receptor 4 (TLR-4) is responsible for LPS recognition in monocytes/MΦ. TLR-4 belongs to the pattern recognition receptor (PRRs) superfamily and to the group of type I transmembrane proteins [125,126]. The receptor consists of three distinct domains. The outer domain contains leucine-rich repeats, which mediate the recognition of pathogen-associated molecular patterns (PAMP). The middle domain is a transmembrane domain, connecting the inner and outer domain. The inner domain is the Toll-IL receptor (TIR) domain, necessary for TLR dependent signal transduction [127]. Up to now, 13 different TLR family members have been discovered in mammals [128]. Their location within the cell differ as well as their ligand preferences (see Tab. 6), covering a broad spectrum of components of foreign pathogens referred to as PAMPs [125, 129]. In addition, endogenous ligands, such as heat shock proteins (HSPs), hyaluronate and heparan sulfate (extracellular matrix breakdown products), fibronectin, the high mobility group box 1 protein (HMGB1) and oxidised low-density lipoproteins (oxLDL) are known ligands for TLRs [130].

Tab. 6 Human TLRs, ligands and distribution (according to Kawai rt al. [127])

Receptor	Ligand(s)	Localisation
TLR-1	Triacyl lipopeptides, mycoplasma	Cell membrane
TLR-2	Diacyl lipopeptides from bacteria, peptidoglycan and lipoteichoic acid from Gram-positive bacteria, lipoarabinomannan from mycobacteria, zymosan from fungi, tGPI-mucin from *Trypanosoma cruzi* and the hemagglutinin protein from measles virus.	Cell membrane
TLR-3	dsRNA	Endosome
TLR-4	LPS	Cell membrane
TLR-5	flagellin	Cell membrane
TLR-6	forms heterodimer with TLR1 or TLR-2	Cell membrane
TLR-7	ssRNA	Endosome
TLR-8	Viral ssRNA	Endosome
TLR-9	unmethylated 2′-deoxyribo (cytidine-phosphate-guanosine) (CpG) DNA motifs	Endosome
TLR-10	unknown	Cell membrane
TLR-11	uropathogenic bacterial components (profiling)	Cell membrane
TLR-12	unknown	Unknown
TLR-13	unknown	Unknown

1.2.4 TLR-4 mediated signal transduction

As stated above, several different proteins (CD14, TLR-4, MDR2) are involved in LPS recognition. Moreover, the binding of LPS and the LPS-mediated signal transduction including alterations of gene transcription is a multistep process which is illustrated in Fig. 6.

1) LPS is bound by the LPS binding protein (LBP), a soluble protein in the interstitium.
2) The LPS/LBP interaction facilitates the binding of this complex to the membrane anchored CD14 molecule.
3) CD14 transfers the LPS/LBP-complex to TLR-4. A further soluble protein, MD-2, is associated to TLR-4, allowing the homodimerisation of TLR-4 after LPS binding [131].
4) Homodimerisation of TLR-4 is necessary for the early phase of the LPS-response via recruitment of TIR-domain containing adaptors (TIRAP) and subsequently MyD88. The early phase changes cellular gene transcription within minutes.
5) Signal transduction via recruitment of the IL-1 receptor-associated kinase (IRAK) and the TNF receptor-associated factor 6 (TRAF6) leads to activation of the nuclear transcription factor NFκB and the activating protein 1 (AP-1), inducing the transcription of pro-inflammatory cytokines, such as IL-6 and TNFα.
6) The late phase LPS response is induced after long term LPS exposure. The receptor complex LPS/LBP/CD14/TLR-4/MD-2 gets internalised, forming endosomes. Signal transduction is mediated by translocation of the associated membrane protein (TRAM) and the Toll/IL-1 receptor domain-containing adaptor-inducing IFN-β (TRIF)

recruitment . The following activation of NFκB leads to the activation of interferon regulatory factors (IRNs) [133].

By this two phase multistep LPS-response, a highly regulated pro-inflammatory cellular response is generated, leading to drastic morphologic changes, antimicrobial activity (oxidative burst), release of TNFα and other inflammatory cytokines for auto- and paracrine cellular communication.

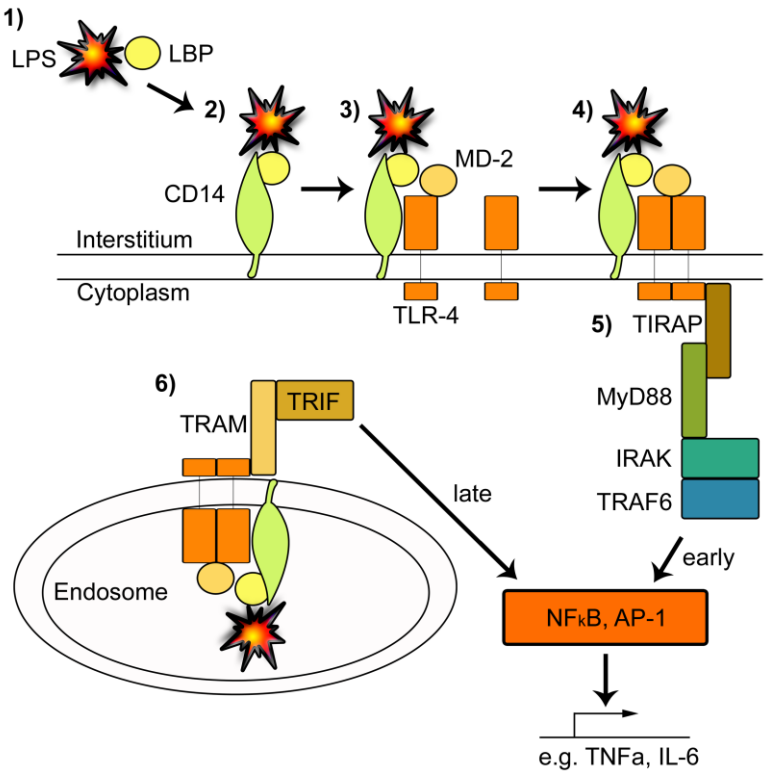

Fig. 6 TLR-4 mediated signal transduction.
After LPS binding by LBP (1), CD14 forms with LPS/LBP and TLR-4, MD-2 a complex which induce TLR-4 homodimerisation (2-4). The activated TLR-4 homodimer recruits successively the adaptor proteins TIRAP, MyD88, IRAK and TRAF6 (4, 5) leading to activation of transcription factors (e.g. NFκB, AP-1), initiating the early inflammatory response. Persisting LPS signalling leads to internalisation of the TLR-4 complex into endosomes and recruitment of TRAM and TRIF (6) and the initiation of the late response, activating transcription factors (e.g. NFκB).

1.2.5 TNFα signalling

First description of TNFα was in 1975. Application of TNFα caused tumour necrosis after LPS induction in a sarcoma mouse model [134]. Since then, the knowledge

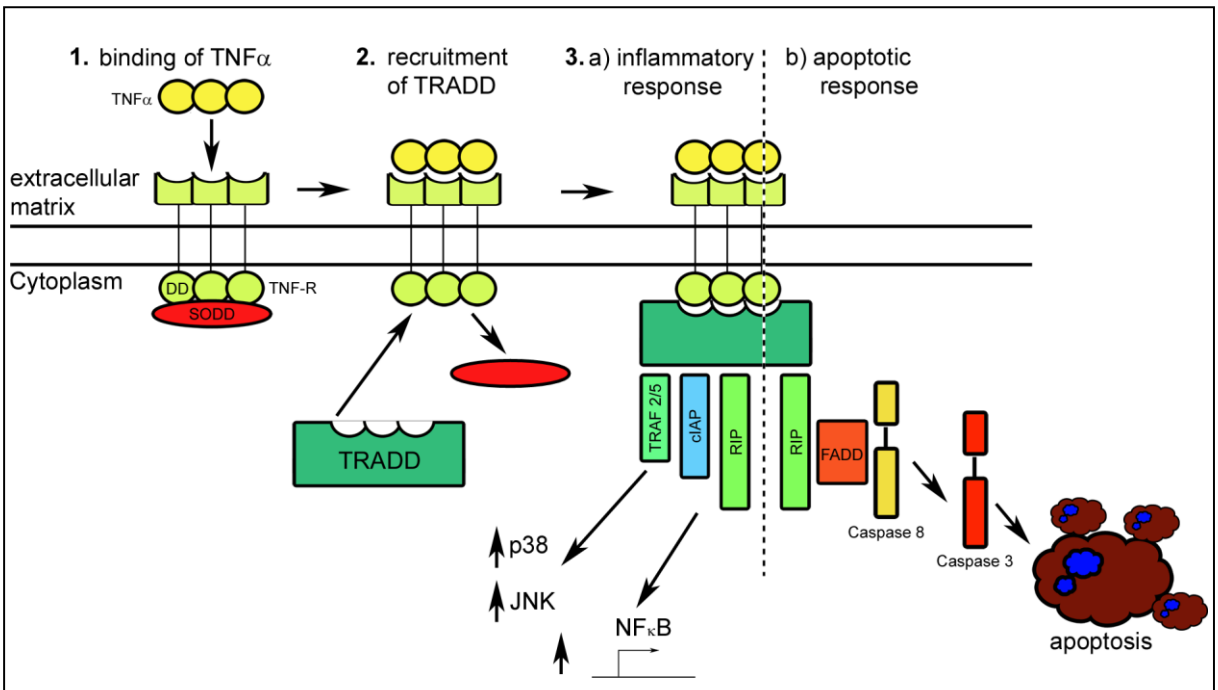

Fig. 7 TNFα signalling.
TNFα and TNFR-1 are trimers. 1) binding of TNFα to TNFR-1 leads to conformational changes of its cytoplasmic death domain (DD). 2) These changes allow the recruitment of adaptor proteins, that determine the cellular reactions to the TNFα, either the induction of an inflammatory response or leading to apoptosis. In both pathways, TRADD and RIP are recruited. A further recruitment of TRAF2/5 and cIAP induce the activation of the p38 and the JNK MAP-kinase pathways as well as activation of NFκB-dependent transcription of pro-inflammatory genes. In contrast, recruitment of FADD induces cleavage of procaspase-8, followed by cleavage of the execution caspase-3 leading to apoptosis.

about TNFα and its mediated effects has been grown continuously. Two TNFα receptors are known, TNFα receptor (TNFR)-1 and -2. TNFR-1 is involved in proliferation, inflammation and apoptotic signalling [135], while TNFR-2 is involved in tissue repair and angiogenesis [136, 137] but is less well characterised. Both receptors belong to the TNF receptor superfamily [138]. Family members are characterised by one to six cysteine rich repeats at their extracellular domain [139]. TNFR-1 and -2 possess four cysteine rich repeats, which are responsible for ligand binding (e.g. TNFα, lymphotoxin α) [139, 140]. TNFR-1 contains a so called death domain (DD) at its cytosolic end [141, 142]. The DD has no enzymatic activity at its own, but acts as docking platform for adaptor proteins. In contrast, TNFR-2 directly interacts with TNF receptor associated factors (TRAFs). TNFα induced TNFR-1 mediated signal transduction is depicted in Fig. 7.

Under physiological conditions, the DD of the TNFR1 homotrimer is masked by the silencer of death domain (SODD), preventing unintentional activation of the signalling cascade. After ligand binding, the receptor complex undergoes conformational changes, leading to the release of SODD and recruitment of DD-containing adaptor proteins. The first adaptor protein recruited is TNFR1-associated protein containing DD (TRADD) via DD-DD interaction [143, 144]. TRADD acts as assembly platform for further adaptor proteins. Depending on the recruited proteins, two different complexes are formed, complex I or II, initiating different signalling cascades.

Complex I (pro-inflammatory, anti-apoptotic) consists of the receptor interacting protein (RIP), the cellular inhibitor of apoptotic protein (cIAP) and the TNFR-1-associated factor 2 and/or 5 (TRAF 2/5) [143]. The formation of the complex I induces the anti-apoptotic MAP kinases p38 and JNK [145.147] and the pro-inflammatory response by activation of the NFκB-pathway [148, 149].

The formation of complex II leads to opposing reactions, such as apoptosis. In this case, the Fas associated protein with DD (FADD) is recruited by TRADD. FADD recruits the inactive procaspase-8 and/or -10 which undergoes activation by autocatalytic cleavage. The activated initiator caspases cleave the inactive proform of the executioner caspase-3. The activated caspase-3 cleaves cellular structure proteins as well as DNA [150-154].

1.2.6 NFκB signalling

NFκB is one of the most important signalling proteins in the centre of inflammatory processes [155]. Different inflammatory signalling cascades (e.g. TLR-signalling, TNFR-signalling, as shown above) are integrated at NFκB and induce and/or modulate the expression of inflammation related genes [156]. Additionally, recent data suggest an important role of NFκB signalling also in differentiation, cell survival and proliferation [157].

Besides regulatory elements, the core components of the NFκB pathway are the inhibitor of κB kinase- (IKK-) complex, the inhibitor of NFκB (IκB) and the nuclear transcription factor kappa B (NFκB) [158]. The general process of NFκB activation starts with a stimulus-induced activation of IKK (e.g. by LPS, TNFα). This leads to phosphorylation, ubiquitination and proteasomal degradation of IκB. The degradation of IκB releases NFκB which translocates into the nucleus and binds to its target genes and induces gene transcription. The process is summarised in Fig. 8.

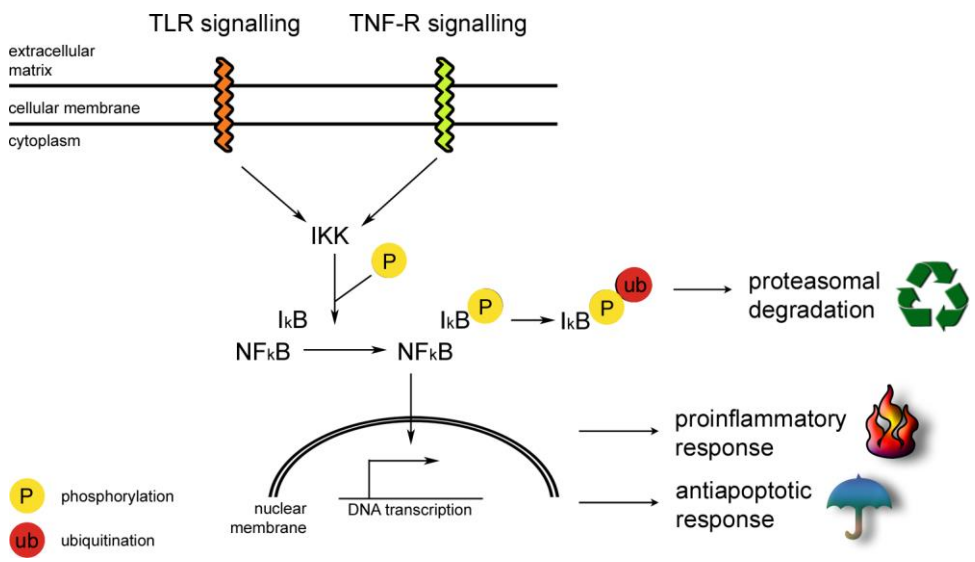

Fig. 8 Schematic overview of NFκB activation.

Up to now, five NFκB-protein family members are known, p50, p52, p65 (RelA), c-Rel and RelB . All of them contain an N-terminal Rel homology domain (RHD), necessary for hetero- and homodimerisation of NFκB family members as well as for DNA-binding at so called κB-binding sites within the promoter region of target genes. Only p65, c-Rel and RelB contain a transcription activation domain (TAD). The TAD is responsible for, nomen est omen, activation of target gene transcription [160]. In the unstimulated state, two proteins of the NFκB family (mostly p65/p50) form hetero-dimers that hetero-oligomerise with a member of the IκB family. The binding of an IκB protein to the NFκB dimer prevents the nuclear translocation of the NFκB by masking its nuclear translocation sequence. Three classical IκB family members are known: IκBα, IκBβ and IκBε (acting in the canonical NFκB pathway) [161], as well as their precursor proteins p100 and p105, which are involved in alternative NFκB signalling [162, 163]. Additionally, three atypical IκB proteins belong to the IκB family: IκBζ, IκBNS and Bcl-3. Their mode of activation and functions differ from the typical IκB family members [164-166].

After activation of the NFκB pathway, IκB is phosphorylated by activated IKK, gets ubiquitinated and is degraded in the 26S proteasome, thereby releasing the NFκB dimer for nuclear translocation and target gene transcription [167]. The IKK-complex is a trimer consisting of two homologue kinases IKKα and IKKβ and a regulatory subunit, the NFκB essential modulator (NEMO/IKKγ). Up to now, the complex mechanism of IKK activation is not completely resolved. In TLR signalling the information is mediated by MyD88, the adaptor proteins IRAK1/4 and TRAF6 leading to IKK activation via TAK1 and/or AP-1 [168, 169]. But how this activation is mediated in detail is still unknown. Different possible

mechanisms are discussed, like autophosphorylation, ubiquitination or an unknown upstream IKK-kinase. One explanation could be that TRAF6 acts as E3 ligase and cooperates with the E2 ligase Ubc13/Uev1A [170] or K63 [171]. But it is not yet possible to determine, if the ubiquitination of IKK takes place before or after IKK activation [172]. The activation of IKK during TNFR signalling is as mysterious as in TLR signalling. But it has been shown that TRAF2 and 5 are likely to be redundant in their functions. In knock out experiments deletion of one of both proteins did not lead to impaired NFκB activation only double knock out of both proteins affected TNFα signalling [173-175]. As mentioned above, activation of IKK by TNFR-1 signalling induces the expression of anti-apoptotic genes (e.g. cIAP, BclXL).

In addition to its central role in inflammatory response regulation, NFκB is also involved during the resolution of inflammation. It has been shown, that inflammatory gene transcription is inhibited after repeated or elongated LPS exposure [176]. Responsible for the resolution of inflammation are the NFκB family members Bcl-3 and p50. They also induce the transcription of the anti-inflammatory cytokine IL-10 and have a negative effect of IFNγ expression in natural killer cells [177]. The role of the NFκB signalling pathway in anti-inflammatory processes is further supported by the finding that IKKα-KO MΦ show increased release of pro-inflammatory chemo- and cytokines [178, 179].

1.2.7 Influence of inflammatory stimuli on the peroxisomal compartment

Up to now, little is known about the effect of inflammatory stimuli on the peroxisomal compartment of MΦ. There are reports which link impaired peroxisomal function to increased inflammatory response in different organs. Data from brains of patients suffering from adrenoleukodystrophy (X-ALD) show a higher inflammatory state [180]. Interestingly, blood monocytes from patients suffering from X-ALD show an elevated level of TNFα release [181]. Furthermore brains of twitcher mice, a mouse model for Krabs disease, show increased TNFα expression, leading to impaired peroxisome function [182]. In experimental encephalomyelitis, impaired peroxisomal function has been observed [183]. All these reports have in common, that inflammatory processess mediated by TNFα impairs peroxisomal function in the brain. Especially ROS degradation and myelin production were affected, leading to severe neuronal defects. It is suggested, that reduced PPARα expression during inflammation is a reason for the impaired peroxisome function in brain tissue.

In mouse liver, Hall et al. reported, that the inflammatory state depends on the expression level of peroxisomal β-oxidation proteins [184]. Taken into account the results of Khan et al. [185] who reported, that Kupffer cells are involved in endotoxin induced changes in the

peroxisomal compartment of hepatocytes. According to this, Contreras et al. gives further insights of peroxisomes in Kupffer cells during inflammatory processes in the liver [186]. It seems evident, that peroxisomes play a decisive role in inflammatory response modulation in liver.

However, there are few reports which directly link peroxisomes in MΦ to inflammation, e.g. Lanuzzel et al., who reported an increased TNFα release from blood monocytes in X-ALD patients [181] and the work of Karnati et al. who described the role of peroxisomes in mouse and human lung MΦ [1].

Taken together, it is obvious, that up to now knowledge about peroxisomes in MΦ is rare and we have just scratched at the surface on the role of peroxisomes in MΦ during inflammatory processes.

1.3 Atherosclerosis

Atherosclerosis (AS) and related cardiovascular diseases are one of the most important causes of death in western society [187]. Additionally, treatment of these diseases and their complications result in the highest costs in the public health system [188]. There are several risk factors, increasing the threat of cardiovascular diseases. The most important factors are age, male sex, obesity, smoking, hypertension, "Diabetes mellitus" and high serum cholesterol concentrations [189, 190].

AS is characterised by a local accumulation of (oxidized) lipids (lipoproteins, free fatty acids and cholesterol) and leukocytes in the large and medium large arteries, leading to chronic inflammation and subsequently to a thickening of the vessel wall. These areas of leukocyte aggregation and lipid deposition are called "plaques". Plaques tend to be destabilised by leukocytic action and rupture, leading to severe pathologic consequences such as cerebral ischemia or myocardial infarction (the progress of AS is reviewed in detail in [189-191]).

The initial event of AS is the appearance of "fatty streaks" beneath the endothelium of large and medium large arteries. The most important event in the formation of "fatty streaks" is the entrance of low density lipoproteins (LDL) into the intima, which lies beneath the endothelium of the vessel wall and subsequently recruiting monocytes and T-cells by factors released from endothelial cells. While LDL is in the blood stream, as part of the fatty acid (FA) and cholesterol delivery system, it is not affected by oxidative modifications, but after accessing the intima its components are susceptible to enzymatic and non-enzymatic modification. This ongoing reactions lead to the oxidative modification of the lipid and

protein moieties of the LDL, called oxidized LDL (oxLDL). Endothelial cells express cell-adhesion molecules (V-CAM, I-CAM, selectins) and secrete MΦ attractants (MCSF, MCP-1) as a response to the oxLDL in the intima, leading to MΦ and T-cells the recruitment [189-191]. The recruited MΦ recognise the oxLDL not via their LDL-receptors but via scavenger receptors (CD36, SR-A) and TLR-4. The uptake of oxLDL is not regulated .This uncontrolled uptake and storage of oxLDL by the MΦ leads to the formation of foam cells [189, 192].

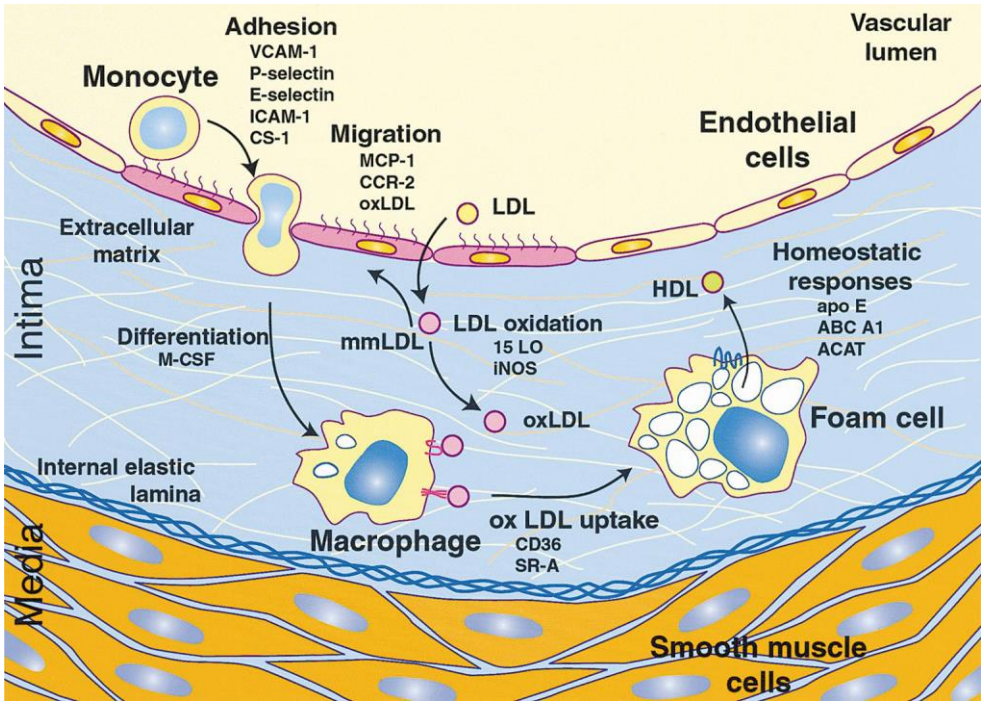

Fig. 9 Schematic overview of the initiating events of a atherosclerotic lesion.
From Glass and Witztum 2001 [189].
LDL in the intima is oxidatively modified. The oxLDL induces the expression of adhesion molecules in the endothelial cells, which attract free floating blood monocytes to attach. Monocytes migrate into the intima and differentiate into macrophages. Foam cell formation is driven by unregulated oxLDL uptake via scavenger receptors and storage.

A further step in plaque development is the immigration of smooth muscle cells (SMC) from the media across the lamina interna elastica into the intima of the vessel wall. The SMC proliferate and synthesize extracellular matrix proteins (e.g. Fibrin, Collagen, Proteoglycane) leading to the formation of a fibrous cap above the accumulating foam cells. Foam cells die by apoptotsis or necrosis due to their unregulated uptake of oxLDL and possibly due to free cholesterol in the plaque. This leads to the formation of a "necrotic core" within the plaque, which consists of cell debris and extracellular lipids. This stage of development is characterised by the constitution of the fibrous cap and MΦ and T-cells interaction leading to the establishment of a chronic inflammatory state. According to the inflammatory state of the intima and the above lying endothelium, further leukocytes are recruited to the plaque,

contributing to an ongoing growth of the plaque. In early stages this plaque growth is compensated by remodelling of the vessel wall. At later stages, the plaque growth into the vessel lumen, disturbing the blood flow and oxygen supply [189-191]. In an advanced plaque, MΦ express tissue factors inhibiting the production of matrix proteins by SMC and release matrix metallo proteases (MMP) degrading the existing extracellular matrix. Consequently, the fibrous cap gets destabilised. If the cap collapses, tissue factors are exposed to blood components, initiating the coagulation cascade with the recruitment of platelets and thrombus formation. The following pathologic events include cerebral apoplexy or myocardial infarction, depending on the affected artery [189-191].

It is very likely, that peroxisomes play an important role in storing and degrading oxidized elements of the phagocyted (ox)LDL particles given the broad substrate range of the peroxisomal β-oxidation system. They might also have an influence on the extend of macrophage activation after oxLDL consumption.

2. Objectives of this study

Macrophages play a central role in innate immunity by phagocytosis of pathogens and their role as antigen presenting cells in the adaptive immune system. Although it is known that macrophages contain peroxisomes, very little is known about the role and the function of peroxisomes in MΦ during inflammatory processes.

Main Objectives of the study were:

- To establish methodical protocols for the study of peroxisomes in macrophages
- To reveal the effects of pro-inflammatory stimuli on the peroxisomal compartment
- To compare the effects of LPS or oxLDL treatment on the peroxisomal compartment of macrophages
- To characterise the underlying signalling pathways involved in the regulation of peroxisomal genes after LPS stimulation
- To reveal the consequences of peroxisomal dysfunction on the inflammatory response of macrophages by the example of cultivated murine Pex11α KO MΦ

The results of this study provide reliable methods for peroxisome research in MΦ as well as first insights into the role of peroxisomes in MΦ during inflammatory processes. The gained knowledge provides a deeper understanding of intracellular processes in acute inflammation and the resolution of inflammation as well as the molecular pathogenesis of chronic inflammatory processes in peroxisomal disorders. Future studies will shed light on the influence of peroxisomes in chronic inflammatory processes such as neurodegenerative diseases or atherosclerosis.

3. Material and Methods

3.1 Material

3.1.1 Laboratory equipment

All equipment used during this thesis is listed at Tab. 7

Tab. 7: Laboratory equipment

Instruments	Company
AGFA Horizon Ultra Colour Scanner	AGFA Mortsel, Belgium
Biocell A10 water system	Milli Q-Millipore, Schwalbach, Germany
Biofuge Fresco	Heraeus, Hanau, Germany
Biofuge Pico	Heraeus, Hanau, Germany
Mini-Protean 3 System, electrophoresis apparatus	Bio-Rad, Heidelberg, Germany
Dias, microplate reader	Dynatech Laboratories, Alexandria, USA
Dish washing machine	Miele, Gütersloh, Germany
Gel-Doc 2000, gel documentation system	Bio-Rad, Heidelberg, Germany
Hera cell 240 incubator	Heraeus, Hanau, Germany
Hera safe, clean bench	Heraeus, Hanau, Germany
Scotsman AF-100, ice machine	Scotsman Ice Systems, Vernon Hills,USA
iCycler, PCR machine	Bio-Rad, Heidelberg, Germany
Leica DMRD, fluorescence microscope	Leica, Bensheim, Germany
Leica DC 480 camera	Leica, Bensheim, Germany
Leica TCS SP2, confocal laser scanning microscope	Leica, Heidelberg, Germany
Microwave oven	LG, Willich, Germany
Mini-Protean 3 cell, gel chamber	Bio-Rad, Heidelberg, Germany
Multifuge 3 SR centrifuge	Heraeus, Hanau, Germany
pH meter	IKA, Weilheim, Germany
Pipettes (2.5 µl, 20 µl, 100µl, 1000 µl)	Eppendorf, Hamburg, Germany
Potter-Elvehjem homogenizer	B.Braun, Melsungen, Germany
Power supplies - 200, 300 and 3000 Xi	Bio-Rad, Heidelberg, Germany
Pressure/Vacuum Autoclave FVA/3	Fedegari, Albuzzano, Italy
Sorvall Evolution RC centrifuge	Kendro, NC, USA
SmartspecTM 3000 spectrophotometer	Bio-Rad, Heidelberg, Germany
T25 basic homogenizer	IKA, Staufen, Germany
Trans-Blot SD, semidry transfer cell	Bio-Rad, Heidelberg, Germany
TRIO-thermoblock	Biometra, Göttingen, Germany
Ultra balance LA120 S	Sartorius, Göttingen, Germany
Ultra Turrax T25 basic homogenizer	Junke & Kunkel, Staufen, Germany
Vortex M10	VWR International, Darmstadt, Germany
Water bath, shaker GFL 1083	GFL, Burgwedel, Germany

3.1.2 Kits

All kits used in this thesis are listed in Tab. 8.

Tab. 8 List of used kits

Substance	Company
BD OptEIA, mouse TNF Elisa Set II	BD Biosciences, Heidelberg, Germany
Cytotoxicity Detection Kit^{plus}	Roche, Grenzach-Wyhlen, Germany
RNeasy® Mini Kit	Qiagen, Hilden, Germany

3.1.3 Chemicals

All chemicals used in this thesis are summarised in Tab. 9.

Tab. 9 List of chemicals

Substance	Company
12-Tetra-decanoyl-phorbol-13-acetate (TPA)	Sigma, Steinheim, Germany
Acrylamide	Roth, Karlsruhe, Germany
Agarose LE	Roche, Grenzach-Wyhlen, Germany
Alcian Blue 8Gx	Fluka, Neu-Ulm, Germany
Alizarin Red S	Fluka, Neu-Ulm, Germany
Ammonium persulfate (APS)	Roth, Karlsruhe, Germany
Ascorbic acid	Sigma, Steinheim, Germany
Bradford reagent	Sigma, Steinheim, Germany
Bromophenol blue	Riedel-de-Haën, Seelze, Germany
Calcium chloride	Merck, Darmstadt, Germany
Citric acid	Merck, Darmstadt, Germany
Ethanol	Riedel-de-Haën, Seelze, Germany
Ethidium bromide	Fluka, Neu-Ulm, Germany
Ethylene diamine tetraacetic acid (EDTA)	Fluka, Neu-Ulm, Germany
Dimethyl sulfoxide (DMSO)	Sigma, Steinheim, Germany
Formvar 1595 E	Serva, Heidelberg, Germany
Glutaraldehyde (GA)	Serva, Heidelberg, Germany
Glycine	Roth, Karlsruhe, Germany
Glycerol	Sigma, Steinheim, Germany
β-Glycerolphosphate	Sigma, Steinheim, Germany
4-(2-Hydroxyethyl)-1-piperazineethanesulfonic acid (HEPES)	Roth, Karlsruhe, Germany
Hydrogen peroxide (H_2O_2)	Merck, Darmstadt, Germany
L-Glutamate	Cambrex BioScience, MD, USA
Lipopolysaccharide (LPS)	Sigma, Steinheim, Germany
β-Mercaptoethanol	Sigma, Steinheim, Germany
Milkpowder, fat free	Roth, Karlsruhe, Germany
3-[N-Morpholino]-propanesulfonic acid (MOPS)	Serva, Heidelberg, Germany
Mowiol 4-88	Polysciences, Eppelheim, Germany
N-propyl-gallate	Sigma, Steinheim, Germany
Paraformaldehyde (PFA)	Sigma, Steinheim, Germany
Penicillin/Streptomycin	PAN Biotech, Aidenbach, Germany

Phenylmethanesulfonyl fluoride (PMSF)	Serva, Heidelberg, Germany
1,4 Piperazine bis 2-ethanosulfonic acid (PIPES)	Sigma, Steinheim, Germany
Ponceau S	Serva, Heidelberg, Germany
Potassium hexacyanoferrate	Merck, Darmstadt, Germany
Potassium hydrogen phosphate	Sigma, Steinheim, Germany
Potassium chloride	Sigma, Steinheim, Germany
Rotiphorese Gel 30	Roth, Karlsruhe, Germany
Protease Inhibitor Mix M	Serva, Heidelberg, Germany
RNaseZap	Sigma, Steinheim, Germany
Sodium carbonate	Merck, Darmstadt, Germany
Sodium chloride	Roth, Karlsruhe, Germany
Sodium hydrogen carbonate	Merck, Darmstadt, Germany
Sodium hydrogen phosphate	Sigma, Steinheim, Germany
Sodium hydroxide	Merck, Darmstadt, Germany
Sodium dodecyl sulfate (SDS)	Sigma, Steinheim, Germany
saccharose	Merck, Darmstadt, Germany
Tetramethylethylenediamine (TEMED)	Roth, Karlsruhe, Germany
Tris hydroxymethyl aminomethane (TRIS)	Merck, Darmstadt, Germany
Triton X-100	Sigma, Steinheim, Germany
Trypan blue	Sigma, Steinheim, Germany
Tween20	Fluka, Steinheim, Germany

3.1.4 Buffers and solutions

All buffers and solutions used for immunofluorescence microscopy are listed in Tab. 10.

Tab. 10 Buffers and solutions for immunofluorescence microscopy

Solution/Buffer	Components
10x PBS	1.5 M NaCl, 131 mM K_2HPO_4 , 50 mM KH_2PO_4, pH 7.4
Blocking buffer	4.0 % PBSA + 0.05 % Tween20
Dilution buffer	1.0 % PBSA + 0.05 % Tween20
Anti-fading agent	2.5 % N-propyl-gallate in PBS + 50.0 % glycerol
Mounting medium	25.0 % propylgalat in Mowiol 4-88

All buffers, solutions and general materials used for Western Blot analysis are listed in Tab. 11.

Tab. 11 Buffers, solutions and general materials for Western blot analysis

Solution/Buffer	Components
Homogenisation Buffer (HB)	250 mM saccharose, 5.0 mM MOPS Before use, add 0.1 % ethanol, 1.0 mM EDTA, 0.2 mM DTT, 1.0 mM 6 mM aminocapron acid, 2.0 protease inhibitor mix (according to the manual)
Buffer A (resolving gel)	1.5 M Tris-HCL, pH 8.8 + 0.4 % SDS
Buffer B (stacking gel)	0.5 M Tris-HCL, pH 6.8 + 0.4 % SDS
12 % separation gel	8.0 ml 30 % acrylamide + 10.0 ml buffer A + 2.0 ml ddH_2O + 15.0 µl TEMED + 130.0 µl 10 % APS
Stacking gel	1.25 ml 30 % acrylamide + 5.0 ml buffer B + 5.0 ml ddH2O + 15.0 µl TEMED + 130.0 µl 10 % APS
10x TBS	100 mM Tris + 150 mM NaCl in 1000 ml of ddH2O, adjust to pH 8.0
1x TBST, Washing buffer	10 mM Tris/HCl, 15 mM NaCl, 0.05 % Tween20
SDS Sample buffer, Laemmli buffer	0.5 M Tris-HCL pH 6.8, 10 % SDS 3.55 ml ddH_2O + 1.25 ml 0.5 M Tris-HCl pH 6.8 + 2.5 ml Gycerol +2.0 ml 10 % (W/V) SDS + a spatula tip of Bromphenol blue before use add 5.0 % β-Mercaptoethanol
5.0 % Blocking buffer	5.0 % fat free milk in TBST
10.0 % Blocking buffer	10.0 % fat free milk in TBST
5x Elektrophoresis buffer	250 mM Tris + 2 M glycin + 1.0 % SDS
BioMax MR-films	Kodak, Stuttgart, Germany
Dental READYMATIC Developer	Kodak, Stuttgart, Germany
Dental READYMATIC Fixer	Kodak, Stuttgart, Germany
Immobilon ® P PVDF membranes	Millipore, Schwalbach, Germany
Immun Star™-AP substrate	Bio-Rad, Heidelberg, Germany
NuPage transfer buffer	Invitrogen, Karlsruhe ,Germany
Precesion StrepTactin -AP conjugate	Bio-Rad, Heidelberg, Germany
Precision Plus™ protein standards, dual color	Bio-Rad, Heidelberg, Germany
Precision Plus™ protein standards, unstained	Bio-Rad, Heidelberg, Germany
Protean ® XL size filter paper	Bio-Rad, Heidelberg, Germany

All buffers and solutions used for molecular biology are listed in Tab. 12.

Tab. 12 Buffers and Solutions for molecular biology

Solution/Buffer	Components
10x TAE buffer	40 mM Tris base + 20 mM acetic acid + 1 mM EDTA, pH 7.6
RNA-loading dye	16.0 µl saturated aqueous bromophenol blue + 80 µl 500 mM EDTA pH 8.0 + 720 µl 37 % formaldehyde + 4.0 ml 10x gel buffer fill up to 10 ml with ddH_20
10x RNA transfer buffer	200 mM MOPS + 50 mM sodium acetate + 10 mM EDTA, pH 7.0

3.1.5 Cell culture material and media

All media and materials used for cell culture are listed in Tab. 13.

Tab. 13: Cell culture materials

General materials and culture media	Company
3-(4,5-Dimethyl-2-thiazolyl)-2,5-diphenyl-2H-tetrazolium bromide (MTT)	Sigma-Aldrich, Munich, Germany
Accutase	PAA, Pasching, Austria
Cell culture dishes (35mm, 60mm, 100mm)	Sarstedt, Nürnbrecht, Germany
Cover slips	Menzel-Gläser, Braunschweig, Germany
Dulbecco's Modified Eagle's Medium (DMEM)	PAA, Pasching, Austria
Fetal calf serum (FCS)	PAA, Pasching, Austria
Filter tips and canules	Braun, Melsungen, Germany
Molecular weight markers (DNA, RNA)	Fermentas, St.Leon-Rot, Germany
Multi-well cell culture plates (6-, 12-, 24- wells)	Sarstedt, Nürnbrecht, Germany
Roswell Park Memorial Institute medium (RPMI) -1640	PAA, Pasching, Austria

3.1.6 PCR primer and reagents

The following oligo-nucleotides were synthesised by Operon, Cologne, Germany and were used as primers for RT-PCR.

Tab. 14: Primer pairs for RT-PCR

Gene target	Sense primer (5´-3´) Antisense primer (5´-3´)	PCR Produkt [bp]	Annealing Temp. [°C]
28s rRNA	CCTTCGATGTCGGCTCTTCCTAT GGCGTTCAGTCATAATCCCACAG	254	65
Pro-inflammatory response			
COX2	GCAAATCCTTGCTGTTCC GGAGGAAGGGCCCTGGTG	364	60
iNOS	CTATCTTGAAGCCCCGCTACTA ATGTCCTGAACGTAGACCTTGG	475	60
TNFα	TGTCTACTGAACTTCGGGGTGA GGCAGAGAGGAGGTTGACTTTC	378	62
HO-1	GCACTATGTAAAGCGTCTCCACGAG CCAGGCAAGATTCTCCCTTACAGAG	610	64
peroxisomal fission			
PEX11α	TCAGCTGCTGTGTTCTCAGTCCTT GTACTTAGGAGGGTCCCGAGAGGA	420	64
DLP-1	CGGTGGTGCT AGG ATT TGT T GCA CCA TTT CAT TT GTC ACG	368	60
H_2O_2 degradation			
Catalase	GGAGAGGAAACGCCTGTGTGA GTCAGGGTGGACGTCAGTGAAA	103	60
fatty acid degradation/transport			
Thiolase	TCAGGTGAGTGATGGAGCAG CACACAGTAGACGGCCTGAC	241	60
ABCD3	CTGGGCGTGAAATGACTAGATTGG AGCTGCACATTGTCCAAGTACTCC	523	56
peroxisomal protein import			
PEX13	GACCACGTAGTTGCAAGAGCAGAGT CTGAGGCAGCTTGTGTGTTCTACTG	717	64
PEX14	CACTGGCCTCTGTCCAAGAGCTA CTGACAGGGGAGATGTCACTGCT	298	65

All reagents used for quantitative or reverse transcriptase PCR are listed in Tab. 15.

Tab. 15: RT-PCR reagents

PCR reagents	Company
10x DNase-I reaction buffer	Invitrogen, Karlsruhe, Germany
10x PCR buffer	Invitrogen, Karlsruhe, Germany
5x First strand buffer	Invitrogen, Karlsruhe, Germany
DNase-I, amplification grade, 1 U/u	Invitrogen, Karlsruhe, Germany
dNTP mix (10mM each)	Invitrogen, Karlsruhe, Germany
DTT 0.1 M	Invitrogen, Karlsruhe, Germany
EDTA 25 mM	Invitrogen, Karlsruhe, Germany
Low DNA mass ladder	Invitrogen, Karlsruhe, Germany
Oligo (dT) primer	Invitrogen, Karlsruhe, Germany
RNase OUT™ (40 units/µl)	Invitrogen, Karlsruhe, Germany
SuperScript™ II reverse transcriptase	Invitrogen, Karlsruhe, Germany
Taq DNA polymerase	Invitrogen, Karlsruhe, Germany

3.1.7 Primer pairs for quantitative PCR

The primer pairs used for qPCR are listed in Tab. 16

Tab. 16 List of qPCR primer pairs

Gene Target	Sense primer (5´-3´) Antisense primer (5´-3´)	PCR Produkt [bp]	Annealing Temp. [°C]
Pro-inflammatory response			
COX2	cctcctggaacatggactca agaagcgtttgcggtactca	173	61
iNOS	ccaagccctcacctacttcc gggttgttgctgaacttcca	156	61
TNFα	cctgtagcccacgtcgtag gggagtagacaaggtacaaccc	148	61
Housekeeping gene			
Gnb2l	actcccacttcgttagtgagt cccttgtgagatcccagag	100	61
Rpl37	gctaaacgcaccaagaaggtc gccactgttttcatgcaggaa	197	61
Hprt	agtcccagcgtcgtgattag tttccaaatcctcggcataatga	88	61

3.1.8 Software

For image processing and evaluation, we used the following software:

- imageJ: Rasband, W.S., ImageJ, U. S. National Institutes of Health, Bethesda, Maryland, USA, http://rsb.info.nih.gov/ij/, 1997-2009.
- AdobePhotoshop CS2 Version 9.0

For statistical analysis of the data, we used Microsoft® Excel 2003, SP3

3.1.8 Antibodies and inhibitors

All primary antibodies used during this thesis are listed in Tab. 17.

Tab. 17: Primary antibodies for Western blot analysis and immunofluorescence staining

Primary antibodies	host	dilution		source
		WB	IF	
MΦ activation marker				
CD68, mouse, monoclonal	rat	1:1,000	-	AbD Serotec, Düsseldorf, Germany
H_2O_2 degradation				
Catalase, mouse, polyclonal	rabbit	1:30,000	1:5,000	D. I. Crane, Brisbane, AUS
peroxisomal protein import				
Pex13p, mouse, polyclonal	rabbit	1:15,000	-	D. I. Crane, Brisbane, AUS
Pex14p, mouse, polyclonal	rabbit	1:30,000	1:5,000	D. I. Crane, Brisbane, AUS
peroxisomal fatty acid transport/degradation				
Peroxisomal 3-keto-Acyl CoA-Thiolase (thiolase), mouse, polyclonal	rabbit	1:15,000	-	P. P. van Veldhoven, Leuven, Belgium
ABCD3, mouse polyclonal	rabbit	1:2,000	-	A. Völkl, Heidelberg, Germany
autophagosomal marker				
LC-3	mouse	1:1,000	1:500	Biozol, Eching, Germany
apoptose marker				
Cleaved Caspase-3, Mouse, polyclonal		1:1,000	-	Cell Signaling, Danvers, USA

All secondary antibodies used during this thesis are listed in Tab. 18 and Tab. 19.

Tab. 18: Secondary antibodies for Western blot analysis and immunofluorescence staining

secondary antibodies	species	dilution		source
		WB	IF	
α-rabbit IgG, alkaline phosphatase bound	goat	1:30,000	-	Sigma-Aldrich, Hamburg, Germany
α-mouse IgG, alkaline phosphatase bound	goat	1:30,000	-	Sigma-Aldrich, Hamburg, Germany
α-rat IgG, alkaline phosohatase bound	goat	1:30,000	-	Sigma-Aldrich, Hamburg, Germany
α-rabbit IgG, Alexa Fluor 488	donkey	-	1:300	Molecular Probes, Karlsruhe, Germany
α-mouse IgG, Alexa Fluor 633	donkey	-	1:300	Invitrogen, Karlsruhe, Germany

Tab. 19: Counterstaining of nuclei for immunofluorescence

dye	dilution	source
DAPI, Hoechst 22358	1:300	
Toto-3 iodide	1:300	Molecular Probes, Karlsruhe, Germany

Inhibitors of inflammatory signalling pathways are listed in Tab. 20.

Tab. 20 Inhibitors

Inhibitor	function	company
Celastrol	Inhibits NFκB signalling	InvivoGen, Toulouse, France
CLI-095	Prevents LPS binding to TLR-4	InvivoGen, Toulouse, France
SPD-304	Prevents TNFα-TNF-R interaction	Sigma, Steinheim, Germany

3.2 Animals

3.2.1 Mice

Specified pathogen free (SPF) C57Bl/6J wild type mice were purchased for experimental purposes from Charles River Laboratories (Sulzfeld, Germany). They were kept on a normal laboratory diet and water *ad libitum* and housed in cages under standardised environmental conditions (12 hours light/dark cycle, 23°C ± 1°C and 55 % ± 1 % relative humidity). The mice were transported to our institute two days prior to the experiments.

PEX11α KO mice were kept at the central animal facility (University Gießen) until MΦ isolation. Animals were delivered the day before isolation and kept overnight under standardized environmental conditions (12 hours light/dark cycle, 23°C ± 1°C and 55 % ± 1 % relative humidity).

3.3 Primary cells and cell lines

3.3 1 RAW 264.7

This mouse macrophage cell line was established from an Abelson leukaemia virus [193]. The cell line was originally bought at ATCC and was a kind gift of our collaborator Dr. S. Immenschuh (Institut für Transfusionsmedizin, Medizinische Hochschule Hannover).

3.3.2 Primary mouse alveolar macrophages

These cells were freshly isolated from C57BL/6J mice by alveolar lavage as described by Zhang et al. [194]. After cervical dislocation of the mice, the fur at the cervical region was removed, the skin was cut open and the trachea was exposed. Thereafter, a canula with an attached 1.0 ml syringe was inserted into the trachea and 0.5 ml of prewarmed PBS/0.5 mM EDTA was instilled into the trachea, withdrawn and the lavage was collected in a 15 ml falcon tube. The instillation and lavage steps were repeated 10 times and the collected lavage was centrifuged for 10 min at 400 g. Cells were counted with a Neubauer counting chamber. A cell number of $5x10^5$ per mouse was yielded. For further experiments, $1x10^5$ cells/well were plated in RPMI-1640/5 % FCS. After 4 h the medium and not attached cells were removed to get pure macrophage cultures and replaced with fresh medium, according to Zhang et al. [194].

3.3.3 Primary mouse peritoneal macrophages

Cells were freshly isolated from C57BL/6J mice by peritoneal lavage, as described by Ray et al. [195]. After isolation, the number of cells was determined using a Neubauer counting chamber according to the manual. A regular isolation yielded $1.5x10^6$ cells per mouse. The cells were plated for experiments with a density of $2.0x10^5$ cells/well.

3.4 Methods

3.4.1 Cell culture

RAW 264.7 murine MΦ were cultivated in high glucose (4.5 g/l) DMEM (PAA) which contained 10 % heat inactivated FCS and 1.0 % penicilin/streptamycin-mix.

Isolated alveolar MΦ cells were cultivated in RPMI-1640 (PAA) + 5 % heat inactivated FCS and 1 % penicilin/streptamycin-mix.

Isolated peritoneal MΦ were cultivated in high glucose (4.5 g/l) DMEM, containing 10 % heat inactivated FCS and 1 % penicillin/streptomycin-mix.

All cells types were incubated at 37°C, 5.0 % CO_2 and 95.0 % humidity. All cell culture procedures were done under sterile conditions. All solutions were preheated at 37°C before use, if not specified elsewhere.

3.4.2 Methylthiazole tetrazolium (MTT) assay

Methylthiazole tetrazolium (MTT) is a yellowish powder. In living cells, mitochondrial dehydrogenases convert MTT into a dark blue coloured water-insoluble MTT-formazan product.

Before use, MTT was dissolved in DMSO for a 5.0 mg/ml stock solution. For cell viability determination, 20 µl of the stock solution were added into the culture medium of each sample, after the indicated treatment time and incubated for another 20 min at 37°C. Thereafter, the medium was discarded and the blue insoluble MTT-formazan was dissolved in 100 µl DMSO. The extinction of each sample was measured at 570 nm with a Dias microplate reader (Dynatech Laboratories). Each sample was measured in triplicates and each experiment was repeated at least three times. Changes in extinction were normalized against the untreated control. To calculate the percentage of cell viability, the following formulawas used: A_{570} (treated cell)/A_{570} (non-treated cells) x 100.

3.4.3 Cytotoxicity assay

To quantify cytotoxic effects, the Cytotoxicity detection Kit^{plus} (Roche) was used. This colourimetric test is based on the release of lactat dehydrogenase from damaged cells into cell culture medium. Cytotoxicity quantification was performed according to the manufacturer's protocol. Absorbance was detected at a wavelength of 490 nm.

3.4.4 Enzyme-linked Immunosorbent assay (ELISA)

TNFα levels were measured in the supernatant of cultured cells by using the ELISA BD OptEIA mouse TNFα Elisa set (BD Biosciences) according to the manufacturer's protocol. The absorbance was detected at 450 nm and a reference wavelength at 570 nm

3.4.5 Western blot analysis

Cell harvest

The medium was withdrawn and the cells were washed once with PBS. Thereafter, cells were washed once with cold EDTA (0.5 M)/PBS solution followed by incubation with Accutase (PAA) at 37°C, 5 % CO_2 for 8-10 min. Cells were collected with 5 ml PBS and centrifuged at 900 rpm, 5 min. at RT. The supernatant was discarded and the pellet was resuspended in 1 ml PBS. After a second centrifugation at 4000 rpm, 5 min. RT, the supernatant was discarded and the cell pellet was frozen for further processing at -80 °C.

Cell homogenisation and subcellular fractionation by differential centrifugation

Homogenisation of RAW264.7 cells was performed by cell membrane disruption, using a Potter S homogenator (B Braun). Thawed Cells were resuspended in 100 µl of homogenisation buffer (HB), 0.25 M sucrose and 5 mM MOPS, pH 7.4. For 10 ml, 1.0 mM EDTA, 0.1 % ethanol, 0.2 mM DTT, 1.0 mM aminocaproic acid and 100 µl Protease Inhibitor Mix M (Serva) were added before use. The cells were homogenised for 180 s at 1000 rpm. Complete homogenisation was controlled by trypan blue staining of the cell sample and visualised by light microscopy.

The homogenate was centrifuged at 100 g, 15 min at +4.0°C using a Sorvall Evolution centrifuge (Sorvall). The supernatant (U1) was withdrawn and collected in a 500 µl Eppendorftube (Eppendorf). The pellet was resuspended in 100 µl HB and homogenised 180 s at 1,000 rpm. This homogenate was centrifuged 15 min at 100 g. The supernatant (U2) was

withdrawn and mixed with U1. Forty µl of U1+U2 was frozen in liquid nitrogen. The pellet was resuspended in 40 µl HB and frozen in liquid nitrogen.

Supernatant U1+U2 was centrifuged at 1,950 g, 15 min. if not indicated otherwise. The supernatant (U3) was withdrawn and collected in a 500 µl Eppendorf tube. The pellet was resuspended in 100 µl HB and centrifuged at 1,950 g, 15 min at +4.0 °C. The supernatant (U4) was withdrawn and mixed with U3. Forty µl of U3+4 was frozen in liquid nitrogen. The pellet was resuspended in 40 µl HB and frozen in liquid nitrogen.

Supernatant U3+4 was centrifuged at 23,500 g, 15 min. The supernatant (U5) was withdrawn and collected in a 500 µl Eppendorf tube. The pellet was resuspended in 100 µl HB and centrifuged at 23,500 g, 15 min. The supernatant (U6) was withdrawn and mixed with U5. Forty µl of U5+6 were frozen in liquid nitrogen. The pellet was resuspended in 40 µl HB and frozen in liquid nitrogen. This pellet contains mainly peroxisomes, as well as light mitochondria, lysosomes and microsomes. For further western blot analysis of peroxiomal proteins, this fraction was used.

All solutions and supernatants were kept on ice during homogenisation and peroxisome enrichment. All centrifugation steps were performed at +4 °C. For long-time storage, the samples were stored at -80 °C.

Protein determination according to Bradford

According to Bradford et al. [196], BSA was used as standard for protein determination in increasing concentrations (1.0 µg/ml, 2.5 µg/ml, 5.0 µg/ml, 10.0 µg/ml, 15.0 µg/ml and 25.0 µg/ml). The HB alone was used as blank. Before determination, 1.0 µl of the sample was diluted in 124 µl ddH_2O and mixed with 125 µl Bradford reagent. For protein measurement, the mixed solution was incubated 10 min at RT. The protein concentration was determined using the Smartspec™ 3000 spectrophotometer (BioRad)

Gel preparation

For protein resolving, a 12 % SDS-Page Gel was prepared using the Mini-PROTEAN 3 Cell (Bio-Rad), if not stated otherwise. Assembly of the gel chambers was according to the manual. After assembling, the chamber was filled with 70 % ethanol to remove all contaminations and check for sealing, the ethanol was discarded afterwards. The resolving gel was prepared according to the protocol (see Tab. 11) and filled into the chamber. To create an even surface, the resolving gel was overlaid with 70 % ethanol. The stacking gel was prepared during the polymerisation of the resolving gel, according to the protocol (see Tab. 11). Immediately after addition of the stacking gel the spacer were placed.

Sample preparation

After protein determination, equal amounts of protein from each sample (7-30 µg) were mixed with 1x SDS sample buffer (Laemmli buffer). For protein denaturation, samples were heated 8 min at 95 °C, quickly chilled on ice and spinned down.

Separation of proteins

The prepared protein samples were filled each into one well of the gel chamber. The Precision Plus™ protein standards, dual colour (BioRad) and Precision Plus™ protein standards, unstained (BioRad) were mixed and used separately to determine protein size. The passage of the protein samples through the gel was done under a constant voltage of 200 V for 1 h.

Protein transfer

Before use, the Protean® filter paper (BioRad) was equilibrated in NuPAGE transfer buffer (Invitrogen). The used PVDF-membrane had to be wetted in 70 % ethanol and equilibrated in transfer buffer before use. One sheet of the equilibrated filter was placed in the Trans-Blot SD, semidry transfer cell (Bio-Rad). Then the wetted PVDF-membrane was placed on top of the filter paper (avoiding bubbles, rough side face up). The resolving gel was cut off from the stacking gel and placed upon the PVDF-membrane. A second filter paper was placed on top. Settings were C=constant at 1.8 mA/cm² for 1 h at RT.

Protein detection

Unspecific bindings were blocked by incubating the PVDF-membrane in 10 % milk/TBST for 1 h at RT. Protein specific primary antibodies were diluted in 5 % milk/TBST and incubated overnight (O/N) at +4 °C. Thereafter, membranes were washed 3x15 min in TBST at RT on a shaker. The membrane was incubated at RT for 1 h with a secondary antibody (1:30,000 in TBST). During this time the secondary antibody, conjugated with alkaline phosphatase, binds to the primary antibody. After another 4x10 min washing in TBST at RT on shaker, the membrane was incubated with Immun Star™ AP substrate (BioRad) for 2 min at RT. The chemoluminescence was detected by BioMax MR (Kodak) with indicated exposure times. The x-ray film was developed in Dental READYMATIC developer (Kodak) for 2 min at RT, short wash in H_2O and fixed in Dental READYMATIC fixer (Kodak) for 10 min at RT. Final washing in H_2O at RT for 10 min.

3.4.6 RT-PCR

Isolation of total mRNA

Total mRNA of RAW264.7 as well as alveolar and peritoneal MΦ was isolated using the RNeasy Mini Kit (Qiagen). Cells were lysed in 350 µl RLT (lysis buffer) and homogenised by repeated suction and squirting (>15x) through a 19 gauge needle. RNA extraction was done according to the manufacturer's protocol. The RNA was eluted with RNase free water and stored at -80°C. Quality and quantity control was performed by optical density measurement using the SmartspecTM 3000 spectrophotometer (BioRad). RNA integrity was determined by 1 % agarose gel electrophoresis, visualising the 28s, 18s and 5s ribosomal RNA bands.

Agarose gel electrophoresis

RNA samples were mixed with 5x RNA loading buffer (4.0 µl sample RNA + 1.0 µl RNA loading buffer). To degenerate the sample RNA, the mixture was heated at 65 °C for 5 min. The samples were immediately chilled on ice afterwards and were loaded on a 1 % agarose gel. Separation was performed at 90 V for 30 min.

Synthesis of cDNA

To remove DNA contaminations from the total RNA preparation, a DNase-I digestion was performed. One microgram of RNA sample was added to the DNase-1 digestion mix. The mixture was incubated for 15 min at RT. The digestion process was stopped by adding 1.0 µl 25 mM EDTA solution and subsequent incubation for 10 min at 65 °C.

Tab. 21: DNase-1 digestion mix

Reagent	Quantity
RNA sample	1.0 µl
10x DNas-1 reaction buffer	1.0 µl
DNase I, amplification grade, 1U/µl	1.0 µl
RNase free water	to 10.0 µl

cDNA preparation

Total RNA was transcribed into cDNA according to the protocol below

Tab. 22 Oligo(dT) primer mix

Reagent	Quantity
Oligo(dT)12-18 (500 µg/ml) primer	1.0 µl
RNA sample (1.0 µg)	~ 4.0-8.0 µl
dNTP mixture (10 mM each)	1.0 µl
Sterile distilled water	to 12.0 µl

For oligo(dT) primer annealing, the mixture was heated 5 min at 65°C and afterwards directly chilled on ice. To this mixture 4.0 µl 5x first strand buffer, 2.0 µl 0.1 M DTT and 1.0 µl RNaseOUT™ (40 U/µl) was added, mixed and incubated for 2 min at 42°C. To induce cDNA transcription, 1.0 µl of SuperScript™ II Reverse Transcriptase (200 U) was added and the whole mixture was incubated for 1 h at 42 °C. The reaction was stopped by heating it up to 70°C for 15 min. After transcription, cDNA was stored for PCR at -20°C. All heating steps were performed in a TRIO-thermoblock (Biometra).

RT-PCR reverse transcription polymerase chain reaction

To analyse the abundance of specific mRNA within RAW264.7 or primary peritoneal/alveolar MΦ, we performed RT-PCR as a method to evaluate corresponding gene expression. 28s rRNA or Gnb2l were used as housekeeping genes for loading control. As negative control, we ran a "H_2O" lane in parallel, were sample cDNA was replaced by water The RT-PCR master mix was prepared according to Tab. 23.

Tab. 23: RT-PCR master mix

Reagent	Quantity
cDNA sample (1.0 µg)	0.7-1.2 µl (depending on cDNA concentration)
10x PCR buffer	1.0 µl
10 mM dNTPs	2.5 µl
Forward primer (10.0 pmol/µl)	1.0 µl
Reverse primer (10.0 pmol/µl)	1.0 µl
Taq DNA polymerase (5 U/µl)	0.2 µl
Nuclease free water	to 25.0 µl
Total PCR volume	25.0 µl

The PCR reaction was performed in a BioRad iCycler, using the protocol in Tab. 24. The annealing temperature depends on the used primer pair (see Tab. 14)

Tab. 24: RT-PCR cycling protocol

repeats	process	Time [s]	Temperature [°C]
1x	denaturation	360	94.0
35x	denaturation	30	94.0
	annealing	30	55.0-65.0
	elongation	30	72
1x	elongation	360	72

Analysis of RT-PCR products

After RT-PCR, samples were mixed with 2.0 µl 5x loading buffer, which contains the dye bromphenol blue. To analyse the RT-PCR products 10.0 µl of each sample were loaded on a 2.0 % agarose gel (+ 0.5 % ethidium bromide). Separation was performed at 120 V for 45 min. The PCR products were visualized by UV illumination of the gel using the Gel-Doc 2000, gel documentation system (Bio-Rad). For semi quantitative interpretation of the data, intensity values of the samples were normalized against the values of 28s rRNA.

3.4.7 Immunofluorescence

RAW264.7 or primary mouse MΦ were grown on 12 mm cover slips for immunofluorescence staining. Cells were fixed with 4.0 % PFA/PBS (pH 7.4) for 20 min at RT. For permeabilisation, cells were incubated in Triton X100 (0.01 % in PBS) for 10 min at RT. Aldehyde groups and other unspecific epitopes were blocked by incubating the cells in 0.1 % glycin, 5 min at RT to avoid unspecific staining. After each step, cells were washed with PBS 15 min at RT. For primary antibody staining, cells were incubated with corresponding primary antibodies O/N at +4°C (for dilutions see Tab. 17). After incubation, the cells were washed 4x 10 min with PBS at RT. Primary antibody binding was visualised by incubating corresponding secondary antibody (see Tab. 18) for 2 h at RT. After incubation, the cells were washed 4x 10 min with PBS at RT. Nuclei were counterstained with TOTO-3 iodide and DAPI (for dilutions see Tab. 19) 10 min at RT. After incubation, cell were washed 1x with PBS 10 min at RT. Cover slips were mounted in a 3:1 mix of Mowiol 4-88 and N-propylgalate to prevent bleaching of the dye. Cellular staining was analysed with a Leica DMRD fluorescence microscope (Leica).

3.4.8 Preparation of oxLDL

For preparation of oxLDL, isolated LDL from human blood plasma was used. Before oxLDL preparation, a dialysis tube was activated by shortly boiling it in 5 mM EDTA in a microwave, followed by two times boiling in ddH_2O. The tube was sealed afterwards on one side and a 1:1 dilution of LDL/PBS was inserted. The tube was sealed completely and incubated in PBS two times for 3 h at RT. The tube was transferred to 50 µM $CuSO_4$ and incubated O/N at RT. The $CuSO_4$ was neutralised with 50 µM EDTA for 1 h at RT. The oxidized LDL was sterile filtered and was stable for up to 14 days at +4°C. A small oxLDL sample was used for protein determination.

An oxLDL sample was subjected to gel electrophoresis, using a 1.0 % agarose gel, with BSA as negative control, for oxidation control. The samples were stained with coomassi blue 1 h at RT after separation, 45 min at 80 V. Thereafter, the gel was discoloured in ddH_2O overnight at RT.

4. Results

At the beginning of this project, very little was known about the biology of peroxisomes in MΦ; except for morphological data from our group [1]. Nearly all published data in the literature on peroxisomal metabolism were based on investigations using liver [60, 61, 185, 197-199] or kidney [56, 200] and for studies on peroxisomal biogenesis most research groups focused on fibroblasts or yeasts [201-205]. However, it was already known from previous work from our group and others, that peroxisomes are versatile organelles, changing their morphology and enzyme composition according to environmental and metabolic needs [206-210]. Therefore, peroxisomes in macrophages might also adapt their peroxisomal compartment according to their activation state during inflammatory processes. However, no knowledge was available on peroxisome isolation in macrophages. Thus, all the techniques for isolating and staining of peroxisomes in macrophages had to be established within the experimental work of this thesis.

In consequence, the Result section is subdivided into five parts:

1. Transfer and establishing of protocols for MΦ experiments. Isolation and cultivation of primary and RAW264.7 MΦ, followed by staining for and isolation of peroxisomes from these cell types

2. + 3. Effect of LPS or oxLDL on the inflammatory response and the peroxisomal compartment of the murine RAW264.7 MΦ cell line.

4. + 5. Effect of LPS on the inflammatory response and the peroxisomal compartment of murine primary MΦ with WT or Pex11α KO phenotype.

4.1. Transfer and establishing protocols for MΦ experiments

Up to now the effect of pro-inflammatory stimuli on the peroxisomal compartment of myeloid cells has not been investigated. Therefore, all techniques regarding the exploration of the peroxisomal compartment had to be adjusted from hepatocytes to the isolation and enrichment of peroxisomes in MΦ. Consequently, the first experiments were designed to transfer established protocols of hepatic peroxisome enrichment to the model organism of this thesis, the murine MΦ cell line RAW264.7.

4.1.1 Effect of cell sample freezing on enrichment of peroxisomal proteins

According to the protocol for peroxisome enrichment and purification from rat liver of Völkl et al. [198] the use of freshly isolated liver cell samples for homogenization was recommended. However, it was noted that the homogenisation of RAW cells was not complete and a large amount of cells pelleted at 100 g and were lost for further centrifugation steps as shown by Western blot analysis using antibodies against peroxisomal proteins. Even after careful rehomogenisation of the 100 g pellet, cells were still lost in the first pellet. Since it was suggested from the literature that freezing and thawing of cells can lead to improved homogenisation, we tested out whether one freeze/thaw cycle would affect the peroxisome enrichment after centrifugation in comparison to enrichment of peroxisomes from freshly harvested cells (see *Material and Methods,* p.49).

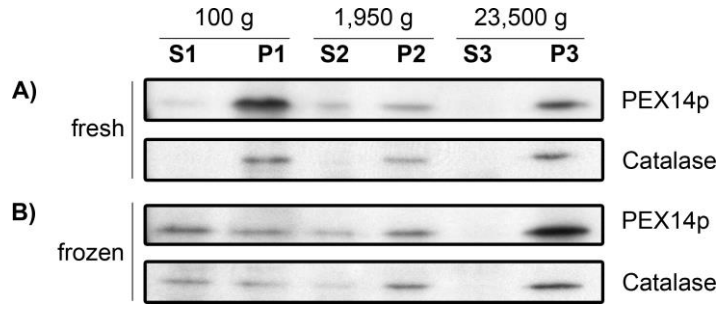

Fig. 10 Summary plates of Western blot analyses of cellular fractions from fresh or frozen RAW264.7 MΦ.
Cell homogenates of A) freshly harvested (fresh) or B) over-night at -80°C frozen cells (frozen) were fractionated by repeated centrifugation steps with increasing velocities (100 g, 1,950 g, 23,500 g). After each centrifugation step, each sample of supernatant (S1, S2 or S3) and pellet (P1, P2 or P3) was frozen in liquid nitrogen for Western blot analysis. 10 µg protein of each fraction was separated on 12 % SDS-polyacrylamide gels and subjected to immunoblot analysis with appropriate antibodies. The picture shows a representative result of n=3 experiments.

In fresh RAW cell samples most of the investigated proteins (PEX14p and catalasewere located in the pellet P1 (Fig. 10A). In contrast, the investigated proteins in frozen cell samples were equally distributed between P1 and S1, suggesting a higher yield of free organelles. Indeed, Western blots of the frozen RAW264.7 cell samples revealed that most of the peroxisomes are mainly enriched in the 23,500 g pellet and no catalase protein was released from the peroxisomal matrix into the supernatant S3, suggesting that a very good and smooth isolation protocol for the mechanical sensitive organelle "peroxisome" has been established. Although a few large peroxisomes sediment in the pellet of heavy mitochondria (P2), most of the small and medium sized peroxisomes were recovered within the expected fraction (P3), which will further be called "enriched peroxisomal fraction".

After 23,500 g centrifugation, the Western blot bands for PEX14p and catalase in P3 from the frozen cell sample had the highest specific protein abundance in comparison to fresh cell sample. These findings indicated that one freeze/thaw cycle of RAW264.7 cell samples before homogenisation is beneficial for the homogenisation procedure and the peroxisome enrichment and detection of peroxisomal proteins in Western blot analysis.

4.1.2 Influence of different centrifugation velocities on peroxisome enrichment

The classical protocol for peroxisome enrichment suggested a velocity of 1,950 g for the second differential centrifugation step to separate peroxisomes from larger mitochondria [198]. As stated above, this protocol is related to the enrichment of peroxisomes from rat liver hepatocytes in which peroxisomes are larger than in MΦ [1, 211]. To optimise the protocol for RAW264.7 mouse MΦ and to take the difference between peroxisomes size in RAW264.7 and hepatocytes (smaller/larger, lighter/heavier or lower/higher density) into account, different velocities (1,950 g, 5,000 g and 10,000 g) for the second centrifugation step were tested to determine its effect on organelle separation (mitochondria/peroxisomes) and on peroxisomal enrichment.

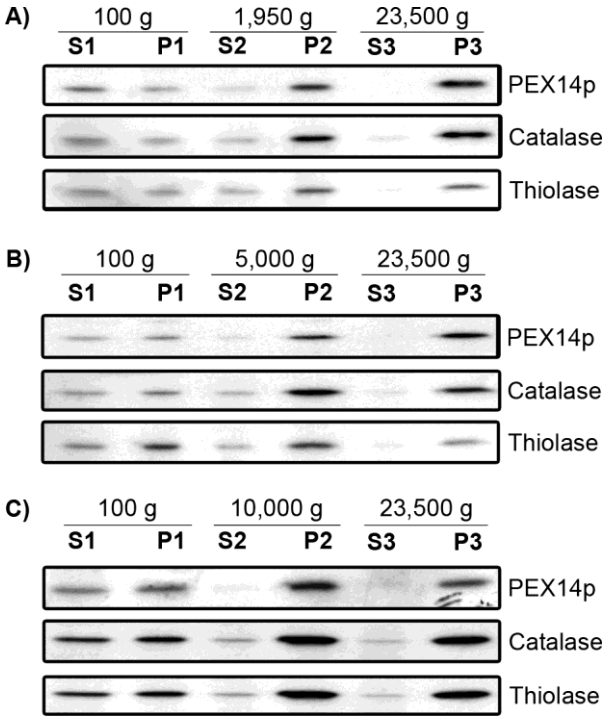

Fig. 11 Summary of Western blot analyses of cellular fractions of RAW264.7 after centrifugation at different velocities during the second centrifugation step.
Cell homogenates of frozen cells (over-night at -80°C) were fractionated by differential centrifugation with increasing velocities: 100 g for all samples (A-C), (A) 1,950 g (B) 5,000 g or (C) 10,000 g, followed by centrifugation at 23,500 g for all samples (A-C). After each centrifugation a sample of supernatant (S) and pellet (P) was frozen in liquid nitrogen for Western blot analysis. 10 µg protein of each fraction was separated on 12 % SDS-polyacrylamide gels and subjected to immunoblot analysis with appropriate antibodies. The picture shows a representative result of n=3 experiments.

Comparing supernatants and pellets after the distinct second centrifugation steps, a shift of the protein bands from the pellet P3 into pellet P2 of all investigated proteins (see Fig. 11) was noted, especially at higher velocities (5,000 g and 10,000 g). For PEX14p, this shift was most prominent. The protein bands of the P3 preparations (23,500 g) became less intense after higher velocities in the second differential centrifugation step (P2) (Fig. 11 B, C). This indicates that despite their different size peroxisomes in RAW264.7 do not behave differently from peroxisomes in rat hepatocytes regarding their centrifugation characteristics. Indeed, there was no improvement of peroxisome enrichment in P3 after centrifugation with velocities higher than 1,950 g in the second differentiation step.

To conclude, we were not able to improve the separation of peroxisomes originating from RAW264.7 mouse MΦ with higher velocities than 1,950 g in the second differential centrifugation step. According to these results, for all following peroxisome isolations, except for the use of frozen cells for the homogenization procedure, the original enrichment protocol was applied as previously reported by Völkl et al. for rat liver peroxisomes [198].

4.1.3 Effect of serum containing versus serum free medium on LPS or TPA induced mRNA expression of pro-inflammatory marker genes

It is known that the peroxisomal compartment reacts very sensitive on changes in the metabolic state of cells, such as starvation or changes in medium composition [212-214]. Moreover, it was reported, that the MΦ response to inflammatory stimuli changes in the presence or absence of FCS in the medium [215]. Due to these reasons, the mRNA expression of the inflammatory marker genes COX-2 and iNOS was compared in different medium conditions and in response to different pro-inflammatory stimuli. Since in many of the LPS-experiments with MΦ time points between 6 h and 24 h were used, the same treatment periods were used to test the effects of medium differences. RAW264.7 MΦ were incubated for indicated periods in DMEM with or without 10 % FCS and the inflammatory response was induced by stimulation with 1.0 µg/ml or 0.5 µM TPA respectively.

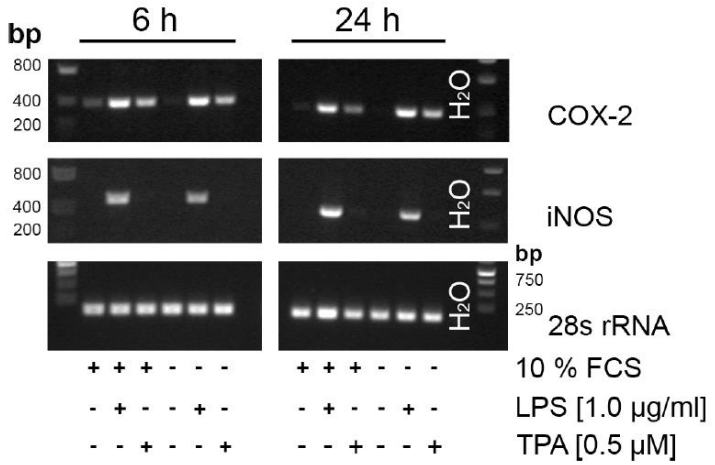

Fig. 12 mRNA expression of pro-inflammatory marker genes in different medium conditions induced by distinct inflammatory stimuli.
RAW264.7 cells were cultivated in DMEM medium with or without 10 % FCS. Cells were treated for indicated time periods with 1.0 µg/ml LPS or 0.5 µM TPA. The inflammatory response induced by LPS or TPA was analyzed by RT-PCR of pro-inflammatory marker genes COX-2 and iNOS. Samples were separated on 2.0 % agarose gels by gel electrophoresis, 45 min at 90 V. Equal sample loading was confirmed by 28S rRNA. The picture shows a representative result of n=3 experiments.

According to these findings, a robust induction of expression of COX-2 mRNA after LPS treatment in FCS-containing and FCS-free media was noted. COX-2 mRNA steady state levels were slightly higher in serum containing medium. It is noteworthy, that iNOS induction after LPS simulation was even higher under Serum conditions. Moreover, an increase of iNOS expression was observed at later time points. TPA treatment did induce a lower effect on COX-2 mRNA expression. Furthermore, TPA did induce a slight iNOS mRNA increase. Due to these results, all following experiments with RAW264.7 cells were performed in 10 %

FCS-containing medium to prevent long-term starvation effects on the peroxisomal compartment. Moreover, LPS was used in the following experiments as pro-inflammatory stimulus because this set up showed the most prominent pro-inflammatory response.

4.1.4 Confirmation of LPS induced activation of RAW264.7 cells by CD68

LPS is a known inducer of the pro-inflammatory response and its usage in different cell culture model systems is well described. As a positive control and a marker for RAW264.7 activation in Western blot analysis, we used an antibody against CD68. It was described that CD68 protein expression is increased during the inflammatory response of MΦ [216]. The function of CD68 is not yet discovered in total. However, it is a member of the lysosomal/endosomal-associated membrane glycoprotein (LAMP-) family and also a member of the scavenger receptor family [217]. Members of this family are typically related to clearance of cellular debris and are related to promotion of phagocytosis [218]. RAW 264.7 cells were treated with 1.0 µg/ml LPS (see material and methods) for different time points (6 h and 24 h) to investigate the effects of LPS on the activation of the MΦ response to the pro-inflammatory response of stimuli.

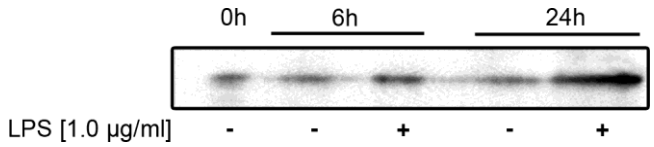

Fig. 13 LPS mediated CD68 induction after activation of RAW264.7 cells.
After incubation with 1.0 µg/ml LPS for indicated periods, 10 µg protein of RAW264.7 cell homogenate samples were separated on 12 % SDS-polyacrylamide gels and subjected to immunoblot analysis with an anti-CD68-antibody

In untreated cells a fine band of the CD68 protein was visible at all time points (Fig. 13), which did not change over time. After LPS-treatment, an increased CD68 protein abundance was noted, with highest induction after 24 h (Fig. 13). Due to the results of this and the previous chapter, it was concluded that in RAW264.7 cells a pro-inflammatory response was initiated after LPS treatment. Because the highest CD68 protein expression was observed at 24 h and peroxisomal half-life has been described to be nearly three days, incubation times of 24 h or longer were used for further experiments.

4.1.5 Effect of LPS on mRNA expression of pro-inflammatory genes in RAW264.7 cells at later time points

As a positive control, demonstrating the LPS induced long-term effect on MΦ, the mRNA expressions of the COX-2, iNOS and the TNFα gene were analysed by RT-PCR after 24 h, 48 h and 72 h LPS stimulation of RAW264.7 cells.

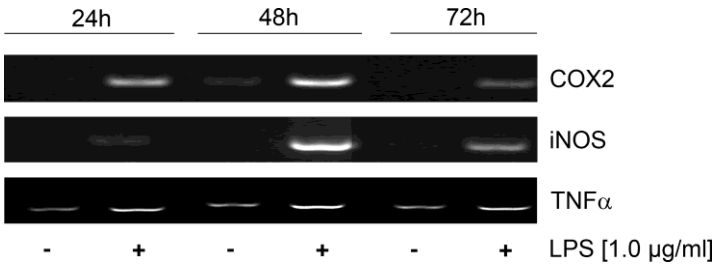

Fig. 14 mRNA expressions of LPS-responsive genes after elongated treatment periods.
RAW264.7 cells were incubated for indicated periods with or without 1.0 µg/ml LPS. After isolation of total mRNA, RT-PCRs with appropriate primer pairs were conducted. Equal amounts of the PCR products of each sample were separated in 2.0 % agarose gels. The figure shows a representative result of n=3 experiments.

A marked induction of COX-2 and iNOS mRNA expressions was noted in comparison to the less intense TNFα increase at all time points after treatment with 1.0 µg/ml LPS. The expression levels reached a clear peak at 48 h and decreased thereafter (Fig. 14). In comparison to the COX-2 mRNA expression, iNOS showed a later and stronger increase in LPS treated RAW264.7 cells. In untreated RAW264.7 a continuous expression of TNFα mRNA on a low level was noted, which did not change during the duration of the experiment. LPS treatment increased the TNFα mRNA expression at the indicated time points less pronounced, reaching its peak also at 48 h.

In conclusion, a robust pro-inflammatory response of RAW264.7 cells after treatment with 1.0 µg/ml LPS at later time points was noted, reaching its peak of gene activation after 48 h. Therefore, in all following experiments these time points were used to analyse changes of genes for peroxisomal proteins induced by the pro-inflammatory response in RAW264.7 cells.

4.1.6 Experiments with primary murine wild type MΦ

To analyse whether the effects of LPS treatment on the peroxisomal compartment and dependent gene expression are RAW264.7 cell line specific artefacts, alveolar and peritoneal MΦ were isolated from WT C57/BL6 mice and incubated with or without 1.0 µg/ml LPS. As a read out, the before mentioned pro-inflammatory marker genes were analysed by RT-PCR.

4.1.6.1 Purity of the isolated murine WT alveolar and peritoneal macrophages

After alveolar MΦ isolation according to the protocol of Zhang et al. [194] or peritoneal MΦ based on the one of Ray et al. [195], the purity of the isolated adherent cells was revealed by immunofluorescence staining for CD68. As described earlier, this marker protein is present in all MΦ and indicates phagocytic activity. In Fig. 15 A (next page), it is clearly visible that nearly all stained nuclei of adherent cells derived from alveolar lavage preparations are surrounded by CD68 positive immunostaining. The same is true for peritoneal MΦ, originating from peritoneal cavity lavage (Fig. 15 B). This indicates that the vast majority of the adherent cells are MΦ. Only a negligible part of the adherent cells are of different cellular origin. Approximately $1.5x10^6$ peritoneal MΦ in comparison to $5x10^5$ alveolar MΦ were isolated per adult mouse. Therefore, for all following experiments mainly peritoneal MΦ were used.

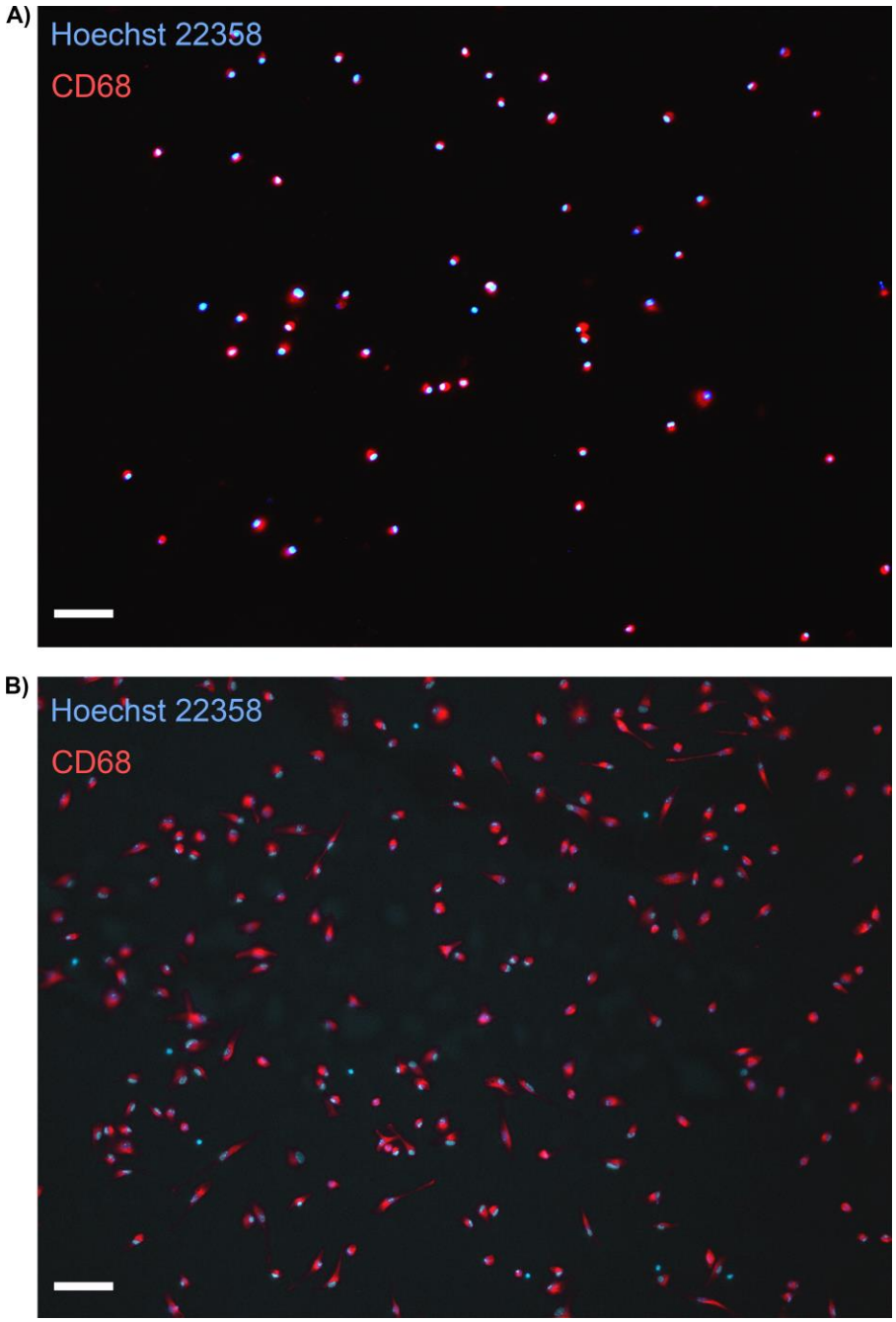

Fig. 15 CD68 immunofluorescence staining of isolated murine A) alveolar and B) peritoneal MΦ:
After isolation, A) murine alveolar and B) peritoneal MΦ were plated and cultured for 24 h to adhere. After washing non adherent cells were removed and the primary cells were fixed with 4 % paraformaldehyde fixative. Macrophages were detected with the anti-CD68 antibody. Nuclear counterstaining was done with Hoechst 22358. The bars represent 100 µm.

4.1.6.2 LPS experiments to visualise primary MΦ activaion

In order to compare the pro-inflammatory response of peritoneal WT MΦ after 1.0 µg/ml LPS treatment in serum-containing medium to the reaction of RAW264.7 cells, RT-PCR analyses for the corresponding pro-inflammatory marker genes (COX-2, iNOS and TNFα) as for RAW264.7MΦ were performed.

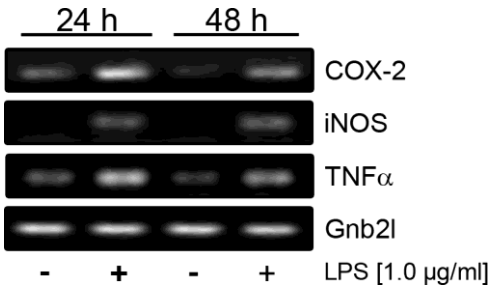

Fig. 16 Effect of LPS on mRNA expression of COX-2, iNOS and TNFα in peritoneal WT MΦ.
Isolated murine peritoneal WT MΦ were incubated for indicated periods with or without 1.0 µg/ml LPS. After total mRNA isolation, RT-PCRs with appropriate primer pairs were conducted with 1.0 µl of each DNA sample. Equal amounts of the PCR products of each sample were separated in 2.0 % agarose gels. Loading control was against the product of the primer pairs of the house keeping gene Gnb2l. The figure depicts representative results of n=3 experiments.

Fig. 16 shows, that the isolated unstimulated peritoneal MΦ exhibited already a basal expression of COX-2 and TNFα mRNAs at both time points, with lower levels at 48 h compared to 24h. In contrast, iNOS expression was undetectable in the absence of LPS. After LPS treatment strong increases of COX-2, iNOS and TNFα mRNA expression levels were observed at both time points. These results indicate, that isolated peritoneal MΦ show a strong pro-inflammatory response to LPS treatment. In contrast to RAW264.7 cells, isolated peritoneal MΦ showed a stronger increase of TNFα mRNA expression after LPS treatment and an earlier peak of mRNA expression for all pro-inflammatory marker genes. However, the basic mRNA expression pattern of investigated inflammatory maker genes in isolated peritoneal MΦ and RAW264.7MΦ is comparable.

4.2. Effect of LPS or oxLDL treatment on the peroxisomal compartment of RAW264.7 and primary mouse MΦ

4.2.1 Effect of LPS on mRNA expression of genes encoding peroxisomal proteins *

After establishing optimal conditions and time points for the detection of inflammatory response in RAW264.7, the influence of LPS treatment on the mRNA expression levels of different marker genes for peroxisomes ("peroxisomal genes") were analysed by RT-PCR. In order to visualise the alterations on peroxisomal functions, the mRNAs for genes encoding catalase (*Cat*, ROS degradation), thiolase A (*Acaa1*, peroxisomal β-oxidation), ABCD3 (*Abcd3*, fatty acid transport and PEX11α (*Pex11α*, peroxisomal proliferation) and PEX13 (*Pex13*, peroxisomal matrix protein import) were analysed. Moreover, PLP-1 mRNA was analyzed, encoding a protein binding to PEX11α and involved in peroxisomal and mitochondrial division. Prolonged LPS incubation times were used to analyse the changes during the resolution phase of an acute inflammation.

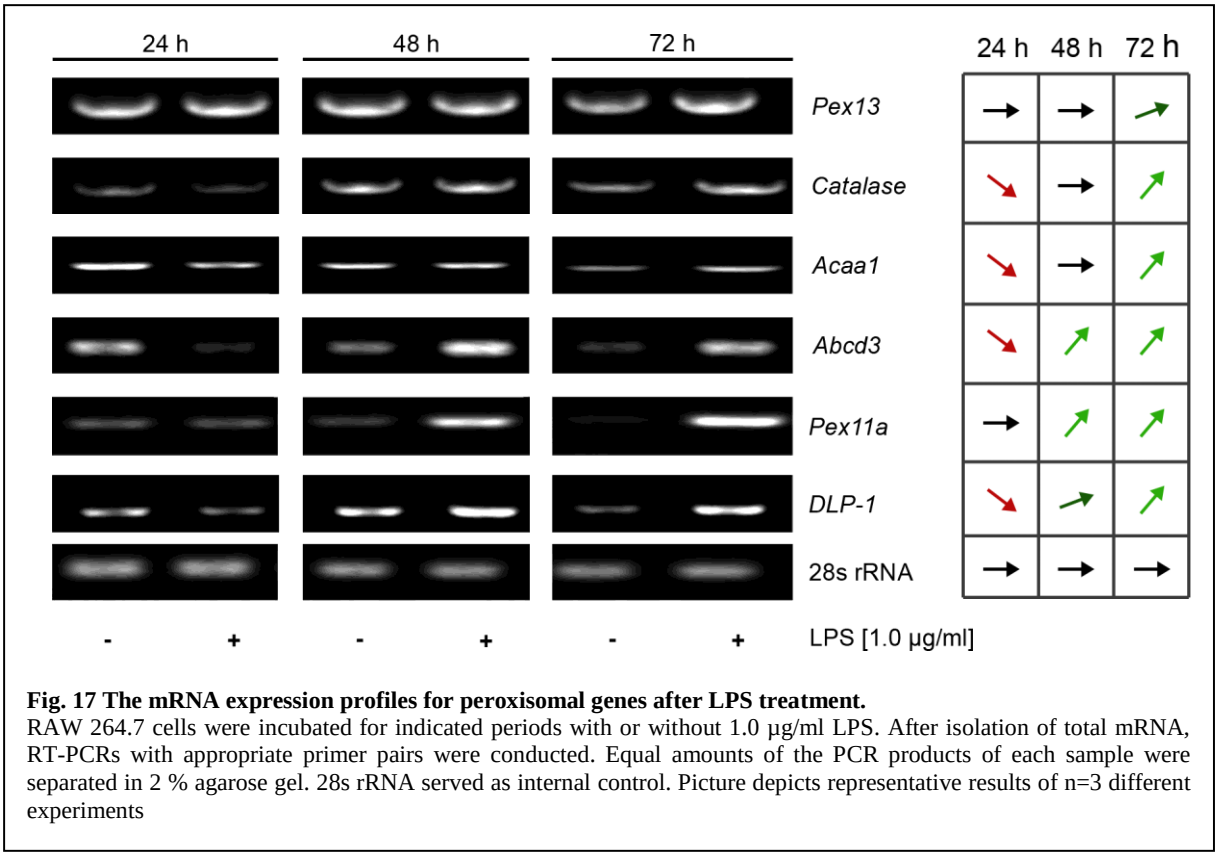

Fig. 17 The mRNA expression profiles for peroxisomal genes after LPS treatment.
RAW 264.7 cells were incubated for indicated periods with or without 1.0 µg/ml LPS. After isolation of total mRNA, RT-PCRs with appropriate primer pairs were conducted. Equal amounts of the PCR products of each sample were separated in 2 % agarose gel. 28s rRNA served as internal control. Picture depicts representative results of n=3 different experiments

* After submission of this thesis, I was informed that the results from the biphasic reaction of the peroxisomes induced by LPS stimulation could not be reproduced by another investigator. Respective reasons are unclear and should be clarified in further investigations.

Overall, clear effects of LPS treatment on the expression of most genes encoding proteins involved in peroxisome metabolism and proliferation were noted. After 24 h LPS treatment, the expression of *Pex11α* and *Pex13* mRNAs did not change (Fig. 17) while the mRNA levels for all other investigated genes were decreased compared to untreated controls. After 48 h LPS treatment the mRNA expressions for *Pex11α, Abcd3* and *Dlp-1*-mRNAs were increased compared to untreated controls, whereas *Pex13*, *Cat* and *Acaa1* mRNA levels in treated cell samples were equal to the expression levels of untreated cells. After 72 h incubation with LPS, expression levels of all investigated mRNAs were higher than in untreated controls.

Since *Pex11α* and *Dlp-1* are both genes involved in peroxisomal proliferation, this was a first hint that peroxisomes might divide during the late phase of the LPS induced inflammatory response. At later time points (72 h) peroxisomal gene expression was increased compared to control values.

4.2.2 Effect of LPS treatment on expression of peroxisomal genes in WT murine peritoneal MΦ

Isolated WT murine peritoneal MΦ were treated with or without 1.0 µg/ml LPS (serum-containing conditions) and subjected to RT-PCR analysis after total mRNA isolation. Since from primary MΦ only a limited amount of cDNA could be obtained, RT-PCR for *Pex11α*, *Cat*, and *Acaa1* was performed. Alterations of *Pex11α, Cat* and *Acaa1* mRNA expressions are presented in Fig. 18.

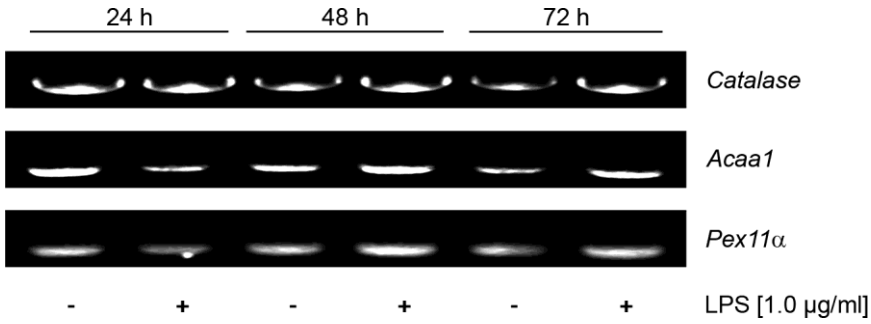

Fig. 18 mRNA expression profile for peroxisomal genes in peritoneal MΦ after LPS treatment.
Isolated murine peritoneal WT MΦ were incubated for indicated periods with or without 1.0 µg/ml LPS. After mRNA isolation, RT-PCRs with appropriate primer pairs were conducted. Equal amounts of the PCR products of each sample were separated in 2.0% agarose gels. The picture depicts representative result of n=3 experiments.

LPS treatment for 24 h of WT peritoneal MΦ led to reduced *Pex11α* and *Acaa1* mRNA levels whereas *Cat* was only slightly changed. After 48 h incubation, the expression levels of all investigated genes were higher in treated in comparison to untreated cells. This effect was also visible after 72 h incubation.

Comparing these results with the ones of RAW264.7, it is evident, that the mRNA expression pattern of RAW264.7 (Fig. 17) and WT peritoneal mouse MΦ (Fig. 18) after LPS stimulation is comparable, although it is not as pronounced in WT peritoneal mouse MΦ.

Indeed, peritoneal MΦ should not be sensitive against LPS, since LPS might originate from the physiological bacterial colonization of the colon. In summary, the results indicate that a common basic behavioural pattern of the mRNA expression for genes of peroxisomal proteins is found in these types of MΦ.

4.2.3 Effect of LPS on peroxisomal protein abundance

Western blot analyses of LPS treated or untreated RAW264.7 MΦ was performed to analyse whether mRNA expressions correlated well with the corresponding peroxisomal protein abundances.

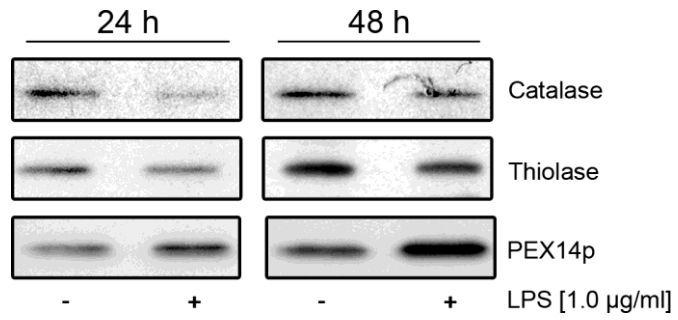

Fig. 19 Summary of Western blot analyses of LPS treatment of RAW264.7 MΦ and its effect on peroxisomal protein abundance. RAW 264.7 were incubated for indicated periods with or without 1.0 µg/ml LPS. Protein samples of whole cell homogenates (5.0 µg) were separated on a 12 % SDS-polyacrylamide gel and subjected to immunoblot analyses with appropriate antibodies. Representative pictures of n=3 different experiments are depicted.

According to the results of the Western blot analyses (see Fig. 19) a strong decrease in catalase as well as thiolase protein abundance in RAW264.7MΦ after 24 h LPS treatment was noted. In contrast, PEX14p protein expression was increased after 24 h incubation with LPS. After 48 h the catalase protein almost recovered to control levels. Thiolase was less reduced in comparison to 24 h. Interestingly, the protein abundance for PEX14p was further increased after 48 h LPS treatment, indicating eventually a relative change in the content of surface membrane proteins to peroxisomal matrix proteins, suggesting a difference in peroxisomal structure.

4.2.4 Effect of LPS on peroxisome morphology and numerical abundance

As shown in RT-PCR and Western Blot analyses, LPS exerts a great impact on peroxisomal mRNA expression and protein abundance. To visualise the morphological changes within the peroxisomal compartment during LPS treatment, immunofluorescence staining of RAW264.7 cells after 24 h and 48 h LPS [1.0 µg/ml] incubation periods were prepared. Antibodies against the peroxisomal membrane protein PEX14p and the peroxisomal matrix protein catalase were used to analyse differences in organelle number and organelle morphology.

After 24 h LPS incubation, RAW264.7 cells were increased in size and shape compared to untreated controls. Untreated RAW264.7 cells exhibited a more monocytic phenotype, whereas LPS-treated cells resembled activated MΦ. Moreover, peroxisome number in LPS treated cells increased in staining for both, PEX14 as well as catalase, compared to untreated control samples (see Fig. 20 A+B, E+F). After 48 h LPS treatment, additional structural changes appeared in cell morphology of treated RAW264.7 cells with stretching out and flattening and exhibition of filopodia and large vacuoles. These changes were accompanied by a tremendous increase in peroxisome number. Whereas the peroxisomes were spread out through the cytoplasm with some aggregates of organelles near the nucleus after 24 h incubation, most of these organelles exhibited a more perinuclear distribution and formed large clusters after 48 h LPS treatment. Moreover, several peroxisomes were located in close neighbourhood to vacuoles, leading to spherical arrangements of many individual organelles within the cytoplasm (see Fig. 20 C+D, G+H). This pattern was observed in both preparations, for PEX14p as well as catalase.

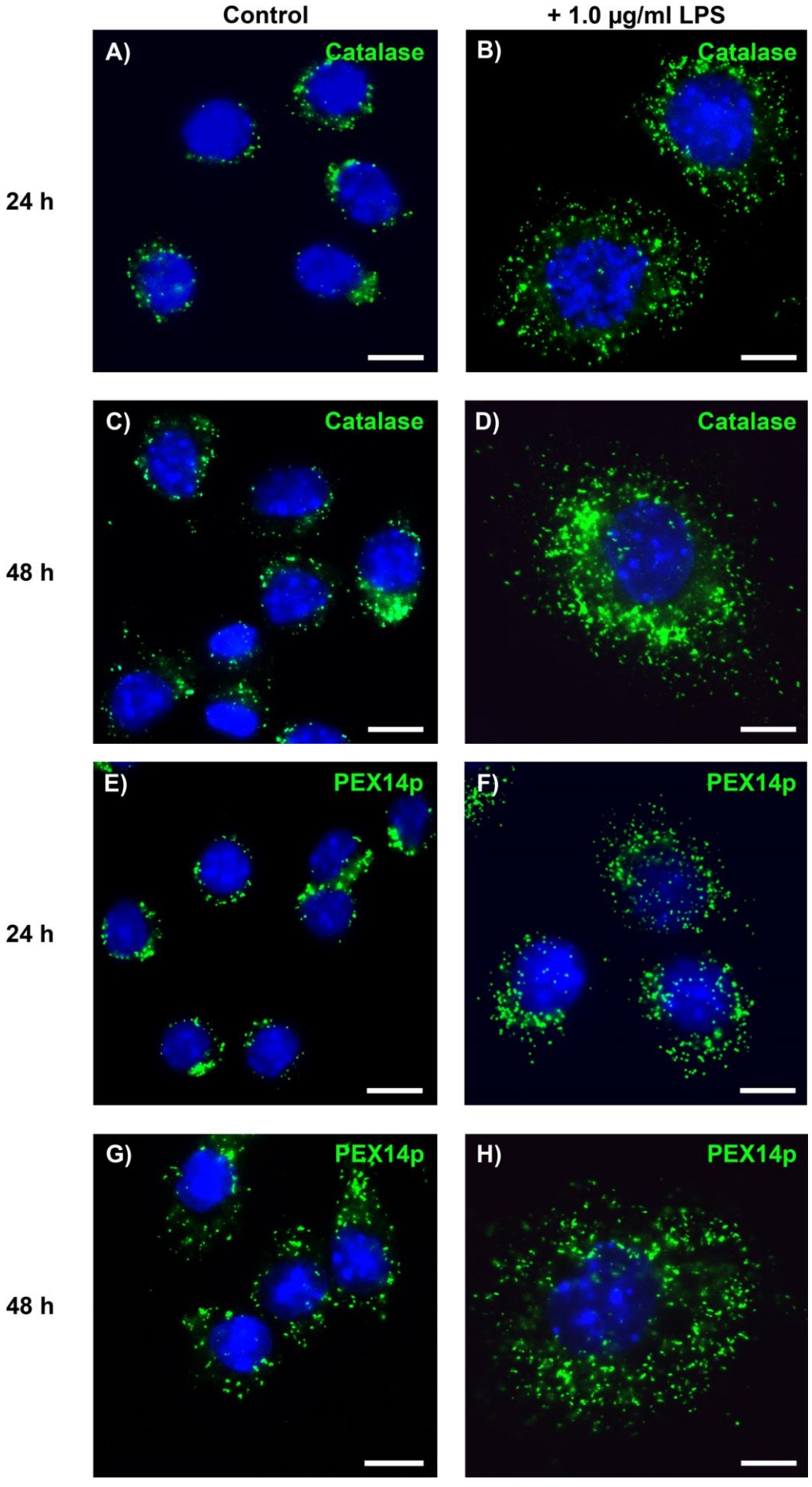
Control
+ 1.0 µg/ml LPS
24 h
48 h
24 h
48 h
A)
Catalase
B)
Catalase
C)
Catalase
D)
Catalase
E)
PEX14p
F)
PEX14p
G)
PEX14p
H)
PEX14p

Fig. 20 Immunofluorescence stainings of RAW264.7 cells for peroxisomal proteins.
Stainings of RAW264.7 cells for catalase (A-D) or PEX14p (E-H) (green). Cells were incubated for 24 h (A+B, E+F) or 48 h (C+D, G+H) with 1.0 µg/ml LPS (B+D, F+H) or without (A+C, E+G). Pictures show representative immunofluorescence micrographs of 3 different experiments. Nuclei were counterstained with Hoechst 22358 (blue). Bars represent 20 µm.

Peroxisomes in each individual cell were counted (30-50 cells/sample) to quantify the peroxisomal changes. Indeed, already after 24 h LPS treatment, peroxisome number doubled in catalase and PEX14p stained cells compared to untreated controls (see Fig. 21). After 48 h LPS treatment, the peroxisome number increased seven fold in comparison to untreated control samples. Calculations using the two sided unpaired students`s t-test revealed that the increase of peroxisome number after 48 h was highly significant compared to corresponding untreated controls.

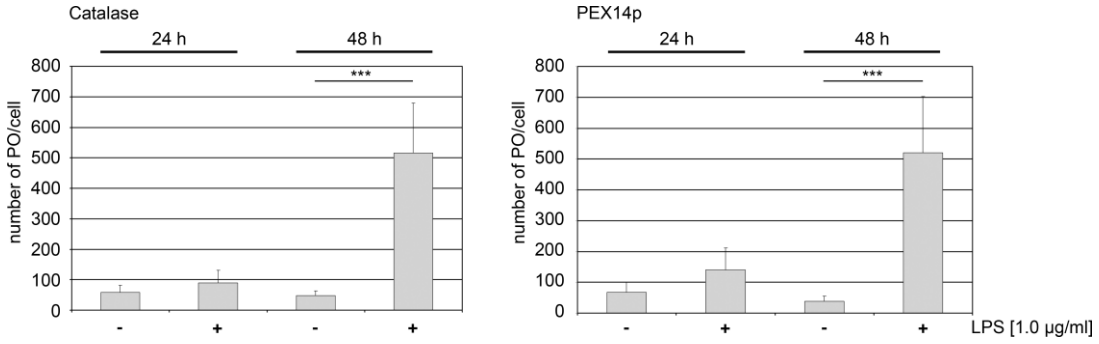

Fig. 21 Peroxisome abundance in RAW264.7.
Cells were fixed with 4 % paraformaldehyde after indicated periods of incubation with or without LPS [1.0 µg/ml]. Peroxisomes were counted in cells in which individual peroxisomes could be identified. Cells with clusters, where individual organelles could not be resolved were not taken into consideration. 30-50 cells per experiment and treatment (n = 3) were analysed. Software aided counting with the "imageJ" software of catalase or PEX14p labelled particles per individual cell. Bars represent the mean number of peroxisomes/cell +/- standard deviations. *** = $p < 0.001$ Student`s t-test.

4.3 Treatment of RAW264.7 cells with proatherogenic oxidized LDL particles in comparison to LPS

Atherosclerosis is a chronic inflammatory disease of the arterial wall, in which MΦ are activated in the sub-endothelial intima by oxidized LDL particles (oxLDL) [189]. To compare the effects of different types of MΦ activation on the peroxisomal compartment, RAW 264.7 cells were incubated with different concentrations of oxLDL. Effects of the oxLDL treatment were compared with the effects after LPS treatment.

4.3.1 Long-term effect of oxLDL or LPS on mRNA expression of inflammation-related marker genes

Since peroxisomes contain different enzymes which are involved in ROS-degradation and β-oxidation of a large variety of complex lipids, it was hypothesised, that peroxisomes in MΦ play an important role during formation of foam cells and progression of oxLDL driven inflammatory changes of the arterial intima during atherosclerotic processes (for a review see [189]). To compare the effects of oxLDL and LPS on MΦ activation and peroxisomal alterations, RAW264.7 cells were incubated with distinct concentrations of oxLDL (12.5 µg/ml, 25 µg/ml and 50 µg/ml) in comparison to 1.0 µg/ml LPS for 24 h and 48 h in serum containing medium. The mRNA expressions of the different pro-inflammatory marker genes (COX-2, iNOS, TNFα and HO-1) were analysed by RT-PCR.

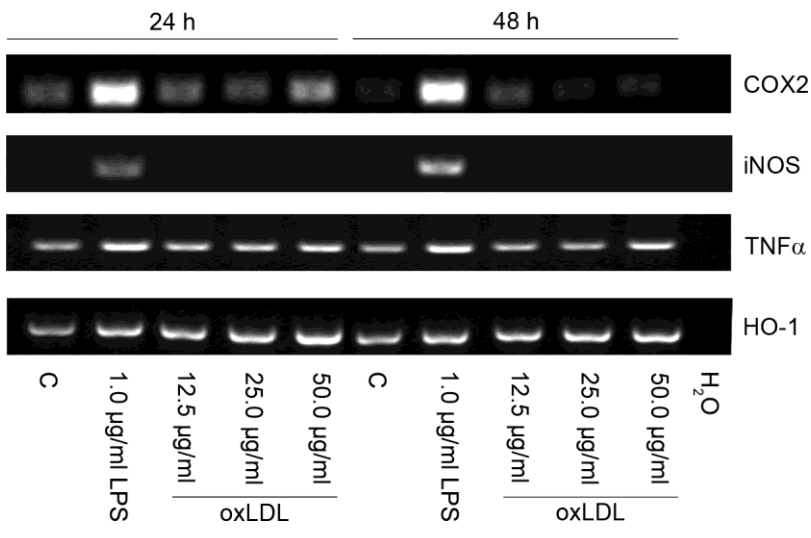

Fig. 22 mRNA expression of pro inflammotry genes after LPS or oxLDL treatment. RAW 264.7 cells were incubated for indicated periods with 1.0 µg/ml LPS or increasing concentrations of oxLDL (12.5 µg/ml, 25.0 µg/ml, 50.0 µg/ml). After isolation of mRNA, RT-PCR with appropriate primer pairs was conducted. Equal amounts of the PCR products of each sample were separated in 2.0 % agarose gel. Representative picture of n=3 different experiments.

In comparison to the robust increase of mRNA expressions of all investigated pro-inflammatory genes after 24 h and 48 h LPS treatment (Fig. 22), incubation of RAW264.7 with oxLDL induced only a marked increase of COX-2 after 24 h and TNFα after both incubation periods. This effect was only visible at the highest oxLDL concentration (50.0 µg/ml). OxLDL incubation exerted hardly any effect on iNOS mRNA expression (Fig. 22).
In contrast to pro-inflammatory genes, all concentrations of oxLDL induced a clear increase of the HO-1 mRNA, a gene known to be up regulated during MΦ activation with different stimuli [222]. Moreover, levels of HO-1 and TNFα mRNAs increased with increasing oxLDL concentrations. According to these results, a concentration of 50.0 µg/ml oxLDL was used for RAW264.7 activation in further experiments.

4.3.2 Effects of oxLDL in comparison to LPS on peroxisomal protein abundance

After determine the working concentration of 50.0 µg/ml oxLDL, RAW264.7 cells were incubated for 24 h or 48 h with this concentration. To compare the effects of oxLDL with the effects of LPS on the protein expression of peroxisomal proteins, the cells were incubated with 1.0 µg/ml LPS for indicated time periods. Western blot analyses were performed using antibodies against catalase, thiolase, ABCD3 as well as PEX13p and PEX14p to determine protein abundance of peroxisomal proteins.

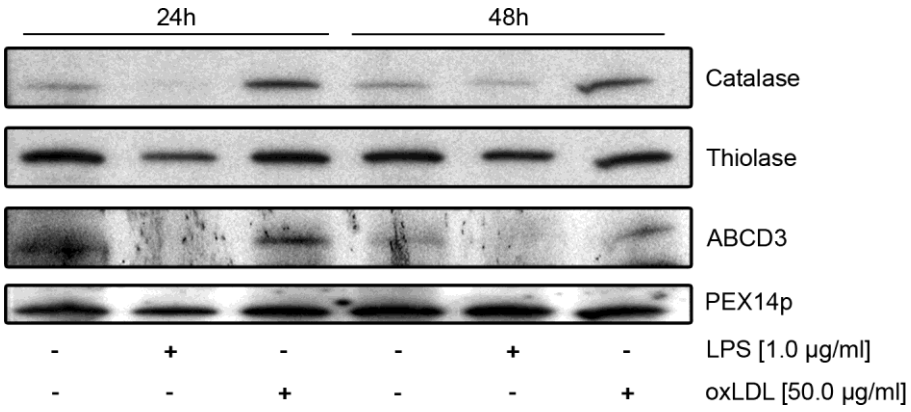

Fig. 23 Summary of Western blot analyses of the effects of oxLDL or LPS on peroxisomal protein abundance. RAW264.7 cells were incubated for indicated periods with or without 50.0 µg/ml oxLDL or 1.0 µg/ml LPS. Cell homogenates of frozen cell samples were fractionated. 5.0 µg protein each of the enriched peroxisome fractions P3 were separated on 12 % SDS-polyacrylamide gels and subjected to Western blot analyses with appropriate antibodies. Representative picture of n=3 different experiments are depicted.

In comparison to the control sample, incubation of RAW264.7 with 50.0 µg/ml oxLDL for 24 h or 48 h respectively, led to a clearly visible increase of catalase protein level (Fig. 23) in

contrast to the strong decrease in the LPS treated samples. Whereas all protein levels of thiolase seemed to be unchanged at both time points after oxLDL treatment (Fig. 23). Similarly, the protein levels of the fatty acid transporter ABCD3 was hardly altered after 24 h, whereas it was slightly increased after 48 h oxLDL treatment. In contrast, thiolase and ABCD3 proteins were clearly decreased after LPS treatment. PEX14p does not seem to be affected by oxLDL and might be increased slightly only after 24 h oxLDL treatment.

According to these results, oxLDL induces a different response on mRNA level of pro-inflammatory genes than LPS and an opposite effect on peroxisomal metabolic marker proteins.

4.4 Effects of TLR-4-, NFκB- and TNFR- inhibitors on the LPS-induced alterations of the peroxisomal compartment

Inhibitors against critical elements of the LPS signal transduction were used to investigate the underlying signalling pathway, since incubation of RAW264.7 with LPS led to changes in peroxisomal mRNA expression and protein abundance as well as induces peroxisome proliferation. The first step in the pro-inflammatory LPS response is the recognition of LPS by its receptor TLR-4. CLI-095 (blocking the binding of LPS with TLR-4) was used to inhibit LPS recognition. Celastrol was applied to inhibit the NFκB-mediated signal transduction. Finally, to exclude the possibility of autocrine TNFα activation, the TNFα-R inhibitor SPD-304 was used.

4.4.1 MTT-test: Effect of CLI-095, celastrol and SPD-304 on cell viability

An initial experiment with the above mentioned inhibitors revealed, that the concentrations of celastrol and SPD-304 which were suggested by the manufacturer, were toxic for RAW264.7 at the time points of our interest (24 h, 48 h, 72 h). up to then, most experiments performed with these inhibitors used time periods up to 12 h. Therefore, the concentrations had to be reduced to a non-toxic level for longer incubation periods. To determine the maximum working concentration for each inhibitor, RAW264.7 cells were incubated for 24 h with increasing concentrations of the appropriate inhibitor as indicated in Fig. 24. The effects of the used inhibitors on cell viability were measured via the MTT-assay as described in *Material and Methods*, p .45.

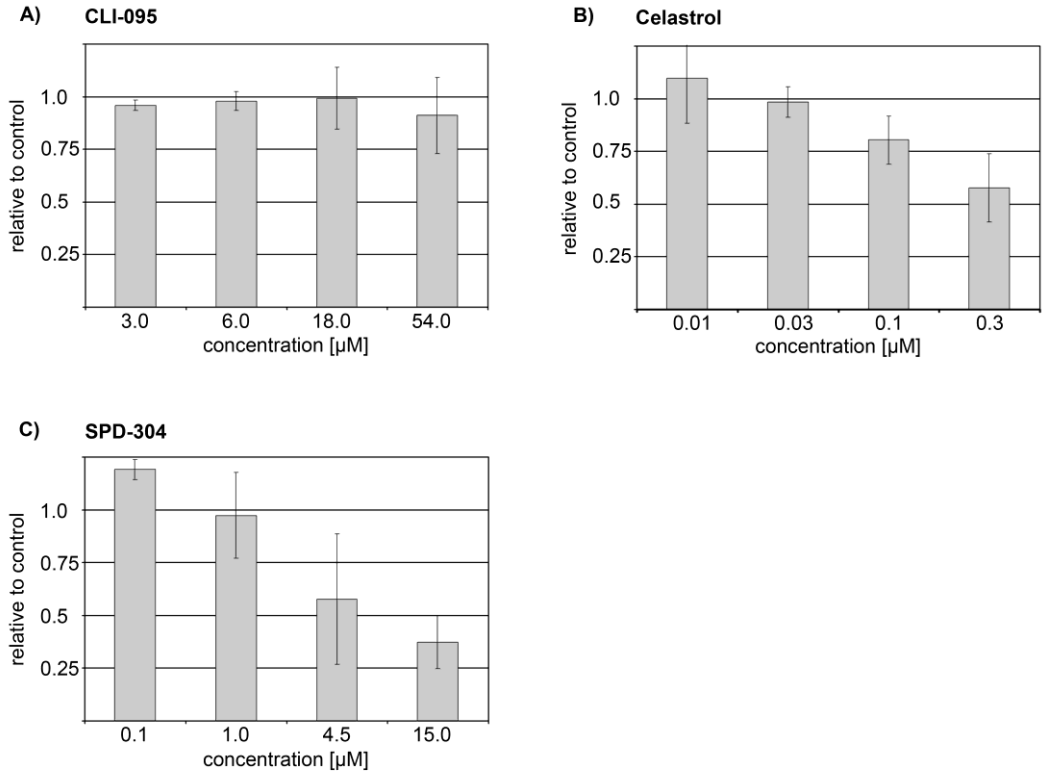

Fig. 24 Effect of inhibitors of inflammatory signalling pathways on cell viability.
RAW264.7 cells were incubated for 24 h with indicated concentrations of respective inhibitors. Viability of control =1. Mean values of n=3 independent experiments are depicted. Error bars = S.D.

According to these results, CLI-095 can be used at concentrations up to 18 µM without any negative effects on cell viability (see Fig. 24 A). The proposed working concentration of the company for celastrol was 2.5 – 10.0 µM. Although much lower concentrations were used (see Fig. 24 B), a dose dependent increase in cell toxicity at these concentrations was observed. According to these results, we used a celastrol concentration of 0.03 µM in all following experiments. The incubation of RAW264.7 with SPD-304 showed a dose dependent increase in cell toxicity (Fig. 24 C) represented by a decrease in cell viability. For all further experiments, a SPD-304 concentration of 1.0 µM was used. According to the results of the toxicity tests, lower concentrations of celastrol (0.03 µM) and SPD-304 (1.0 µM) than recommended from the manufacturer were used, wherefore their inhibitory potency on the NFκB and TNFα signalling pathways might not be complete.

4.4.2 Effects of inhibitors on mRNA expression on pro-inflammatory marker genes

RAW264.7 cells were incubated with or without 1.0 µg/ml LPS or coincubated for 24 h with or without 1.0 µg/ml LPS and CLI-095 [18.0 µM], celastrol [0.03 µM] or SPD-034 [1.0 µM], respectively. The inhibition of LPS-induced gene expression by the distinct inhibitors was analysed by RT-PCR for the pro-inflammatory maker genes COX-2 or iNOS, respectively.

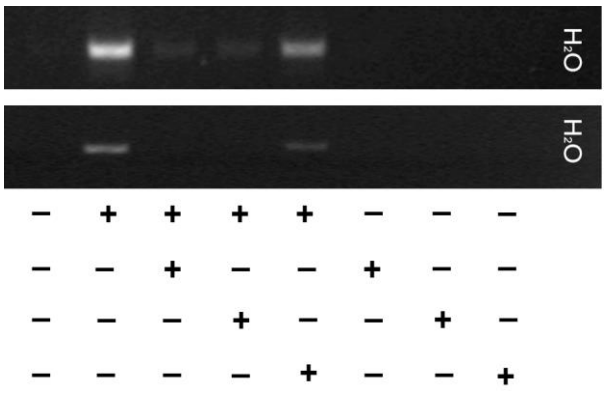

Fig. 25 Effects of CLI-095, celastrol or SPD-034 on the mRNA expression of COX-2 or iNOS after LPS treatment. RAW264.7 cell were treated with or without 1.0 µg/ml LPS. Coincubation with CLI-095 [18.0 µM], Celastrol [0.03 µM] or SPD-034 [1.0 µM] for 24 h. RT-PCR was performed with corresponding primer pairs. Equal amounts of the PCR product were separated on 2.0 % agarose gels. Figure represents the result of n = 3 experiments.

As seen before (see Fig. 14), treatment of RAW264.7 cells with LPS led to increased COX-2 and iNOS mRNA expressions (Fig. 25). Coincubation of the cells with LPS and CLI-095 or celastrol blocked COX-2 mRNA expression nearly completely, only faint bands were detectable in comparison to the "LPS only" treated sample. The expression of iNOS mRNA was completely inhibited. The effect of SPD-034 conicubation was less pronounced compared to CLI-095 and celastrol, although clear reduction of COX-2 and iNOS mRNA expression was noted. The incubation of RAW264.7 cells with the inhibitors alone induced no mRNA expression of COX-2 or iNOS.

According to these results, TLR-4 and NFκB signalling was convincingly blocked during LPS incubation. It is not suprising, that the coincubation of SPD-034 did not completely block of COX-2 or iNOS mRNA expression after LPS treatment, since it the initial induction of COX-2 and iNOS is not primarily mediated by TNFα but rather by TLR-4/NFκB activation.

4.4.3 Effect of inhibitors of pro-inflammatory signalling pathways on levels of peroxisomal proteins

RAW264.7 cells were incubated with or without 1.0 µg/ml LPS for 24 h, 48 h and 72 h. Additionally, RAW264.7 cells were coincubated with 1.0 µg/ml LPS and either 18.0 µM CLI-095 or 0.03 µM celastrol or 1.0 µM SPD-304. After preparation of whole cell lysates, equal amounts of proteins from each sample were used to perform Western blot analyses.

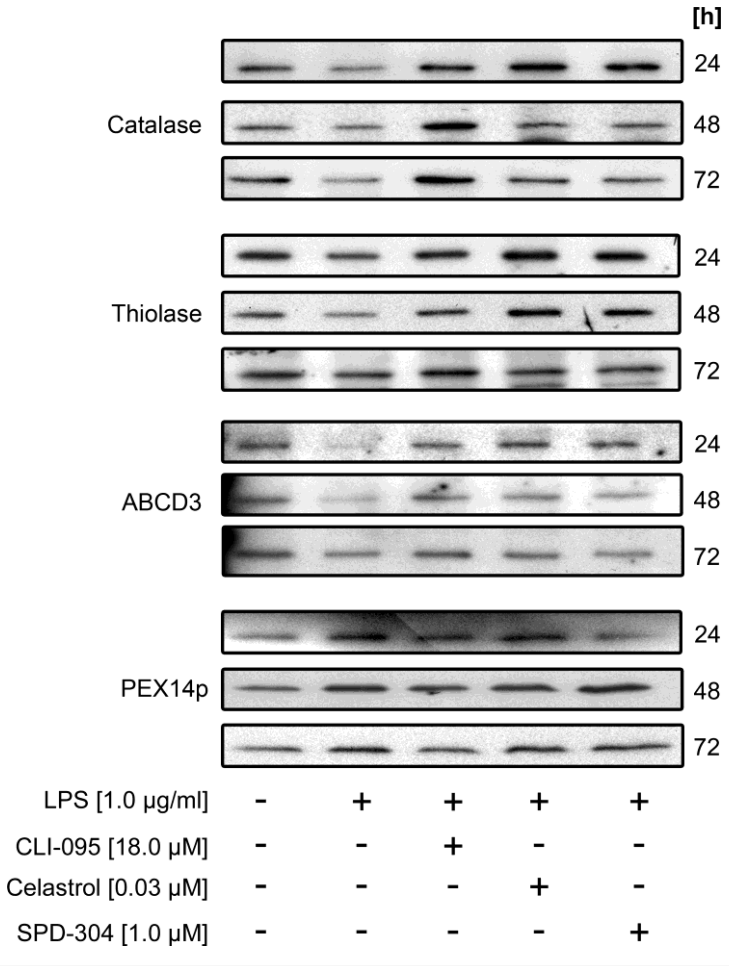

Fig. 26 Summary of Western blot analyses of the effects of pro-inflammatory pathway inhibitors on LPS induced changes of the peroxisomal compartment.
RAW 264.7 cells were incubated for indicated periods with or without 1.0 µg/ml LPS. Additionally, coincubation of 1.0 µg/ml LPS and CLI-095 (18.0 µM), Celastrol (0.03 µM) or SPD-034 (1.0 µM) was performed. 10 µg protein of each whole cell lysate was separated on 12 % SDS-polyacrylamide gels and subjected to immunoblot analysis with appropriate antibodies. Representative pictures of n=3 different experiments.

As expected from previous experiments, incubation of RAW264.7 with LPS induced a decrease in protein levels of catalase, thiolase and ABCD3 at all investigated time points (Fig. 26 A-C). In contrast, PEX14p was increased after LPS treatment at all time points (Fig. 26 D). Coincubation of CLI-095 with LPS prevented the reduction of catalase, thiolase and ABCD3 at all investigated time points reliably (see Fig. 26 A-C). The protein levels of thiolase and ABCD3 after LPS+CLI-095 treatment were even higher as the corresponding controls (Fig. 26 C, D). Interestingly, highest levels of catalase and thiolase proteins were obtained

especially after 24 h LPS+CLI-095 treatment. (Fig. 26 A). A similar effect was also noted by coincubation of LPS/celastrol and LPS/SPD-304 after 24 h. The PEX14p levels in LPS+CLI-095 treated cells were equal to the ones of the untreated control at all time points (Fig. 26 D). Inhibitory effects of celastrol and SPD-304 were also detectable, especially after 24 h incubation but were less pronounced at 48 h and 72 h (Fig. 26 A-D). After 48 h and 72 h celastrol and SPD-304 also prevented LPS induced catalase reductions, brought them back to control levels (Fig. 26 A). Celastrol and SPD-304 did also prevent the LPS induced thiolase reductions, but seemed to increase thiolase levels above the ones of the untreated controls at 24 h and 48 h (Fig. 26 B). After 72 h the thiolase levels in celastrol+LPS and SPD-304+LPS samples did not seem to be fully recovered in comparison to control levels (Fig. 26 B). Comparable effects were observed also for ABCD3. After 24 h, celastrol and SPD-304 prevented the LPS mediated ABCD3 reductions (Fig. 26 C). In contrast after 48 h and 72 h the inhibitory effects of both chemicals were not as strong as the one for CLI-095. Moreover, CLI-095 prevented the LPS mediated increases of PEX14p at all time points (Fig. 26 D), but Celastrol and SPD-304 were not able to prevent this effect.

In conclusion, the results indicate that all inhibitors were able to block the LPS mediated alterations of the investigated peroxisomal proteins. The effect of CLI-095 was strongest and most constant during all time points, whereas celastrol and SPD-304 exhibited their strongest effects only at 24 h.

4.5 Effect of a Pex11α KO on the inflammatory response of primary mouse MΦ

The observations regarding the effect of LPS on the peroxisomal compartment, especially the high induction of Pex11α gene expression, led to the question, whether the knockout of the Pex11α gene would affect the inflammatory response of MΦ. For these experiments bonemarrow-derieved macrophages (BMDM) isolated from Pex11α KO mice, that were generated and characterized by our group before, were used [212].

4.5.1 Effect of LPS on the peroxisomal compartment in BMDM of WT and *PEX11α* KO mice

To transfer the results obtained from RAW264.7 cells to primary MΦ similar experiments as mentioned before were performed with BMDMs from WT animals. To analyse the effects of a Pex11αKO on the LPS-response, BMDM from Pex11αKO mice were processed in parallel.

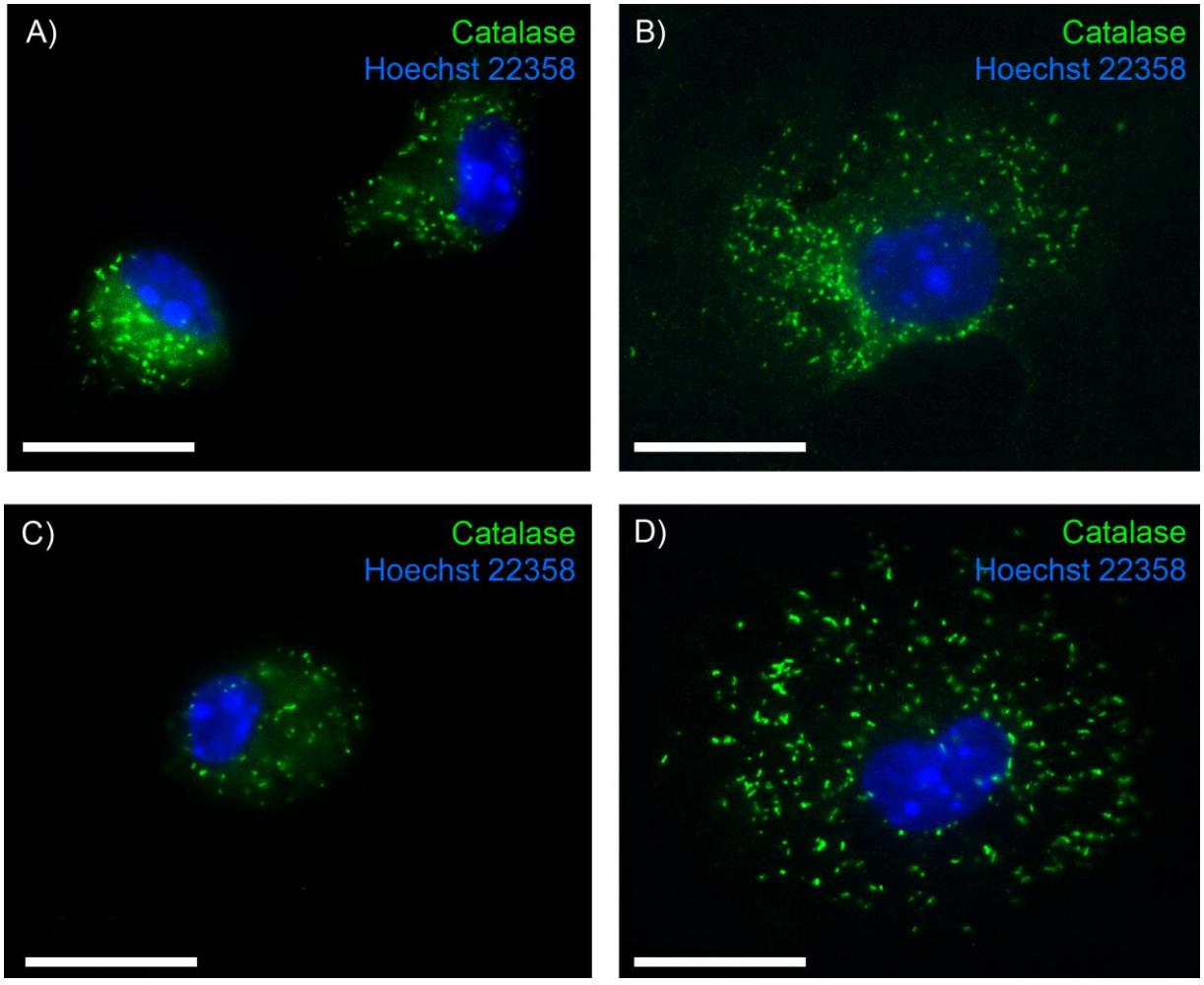

Fig. 27 Influence of LPS on the peroxisomal compartment of WT and Pex11α KO MΦ.
Isolated BMDM from WT and PEX11α KO mice were plated on glass cover slips and treated for 24 h with or without 1.0 µg/ml LPS. Primary antibody was directed against catalase protein. Nuclear counterstaining by Hoechst22358. Untreated A) WT and C) Pex11α KO MΦ. Peroxisomes in treated WT MΦ B) seem to be smaller, are present at a higher numerical abundance and exhibited a higher clustering than peroxisomes of LPS treated Pex11α KO MΦ D). The bars represent 10µm.

Structural changes of the peroxisomal compartment were analysed by catalase immunoflourescence staining of LPS-treated and -untreated WT or Pex11α KO BMDM.

Despite the preincubation of BMDM for differentiation with M-CSF conditioned medium (DMEM) for a period of 5 days effects of M-CSF on the peroxisomal compartment would rather be expected at much earlier time-points, e.g. 24 h, as described also for other growth factors [223]. Peroxisomes in WT BMDM exhibited the typical spherical to rod shaped morphology present also in RAW264.7 cells under regular culture conditions.

In BMDM isolated from Pex11α KO mice, peroxisomes appeared slightly larger, less numerous as well as more spherical in comparison to peroxisomes in WT BMDM. The peroxisomes in the WT cells were small, round to rod-shaped and exhibited a high numerical abundance and formed large clusters in the perinuclear region. Moreover, several "beads on a string" structures were noted, suggesting peroxisomal fission. This phenotype was comparable to the one observed in LPS treated RAW264.7 MΦ.

In contrast, the peroxisomes in LPS-treated Pex11α KO MΦ appeared to be enlarged, exhibited a lower numerical abundance and formed smaller perinuclear clusters than their WT counterparts. Additionally, many "beads on a string" structures were present. Two cell biological processes might explain these phenomenons: 1) The elongated peroxisomes could either be stuck in the fission process or 2) the transport of already divided peroxisomes via binding to elements of the cytoskeleton could be impaired.

In summary, LPS treatment seemed to induce peroxisomal fission and proliferation, which is impaired by the KO of the Pex11α gene. Moreover, during this experiment, another major difference between WT and Pex11αKO BMDM was noted. After LPS treatment, more dead cells were observed in the medium of Pex11αKO BMDM than in the medium of their WT counterparts. Therefore, cell survival after LPS treatment of WT compared to Pex11α MΦ was analysed, using a LDH release-based cytotoxicity kit (Roche).

4.5.2 Effect of LPS on cell death or survival

The LDH release based cytotoxicity test (Roche) was used to quantify the effect of LPS treatment on cell-survival and -damage. The LDH-release values were photometrical quantified and the cell survival was calculated according to the formula given by the manufacturers. The calculated values are depicted in Fig. 28.

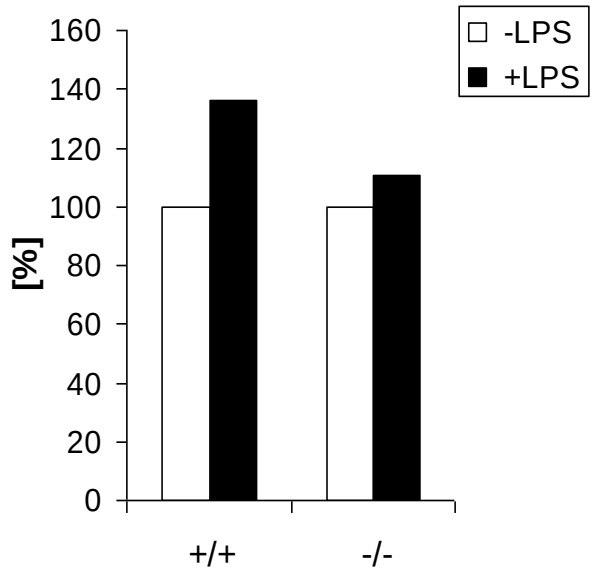

Fig. 28 Effect of LPS treatment on cell survival of WT (+/+) and Pex11α KO (-/-) BMDM.
Isolated BMDM from WT or Pex11α KO animals were treated with or without 1.0 µg/ml LPS for 24 h. Thereafter 100 µl of the medium was removed and LDH assay were performed. The values of the untreated WT or KO cells were set to 100 %. KO MΦ show an impaired gain of survival after LPS treatment.

According to these results, the treatment of WT cells (+/+) led to an increased survival of LPS treated cells compared to untreated controls (Fig. 28). In contrast the Pex11α KO MΦ showed no increase in cell survival after LPS treatment. The values of untreated WT and Pex11α KO MΦ were at the same level.

The increase of cell survival could be related to the activation of pro-survival signalling pathways like MAP kinases, such as p38, or Akt (also known as PKB) after LPS treatment [224]. Another possibility would be a changed activation of pro-apoptotic signalling pathways. Therefore, markers for activation of pro-apoptotic pathways were analysed.

4.4.3 Bad expression in LPS treated WT and *PEX11α* KO MΦ

The first step was to check mRNA levels of Bad, a pro-apoptotic member of the Bcl family, which is involved in intrinsic induction of apoptosis in which a mitochondrial permeability transition pore (MPTP) is formed. Thereafter, cytochrome c is released from the mitochondria, inducing caspase-3 activation. During intrinsic apoptosis, Bad is involved in the formation of the MPTP.

Due to material restrictions (missing specific antibody) only RT-PCR analysis of Bad mRNA expression but no Western blots could be performed.

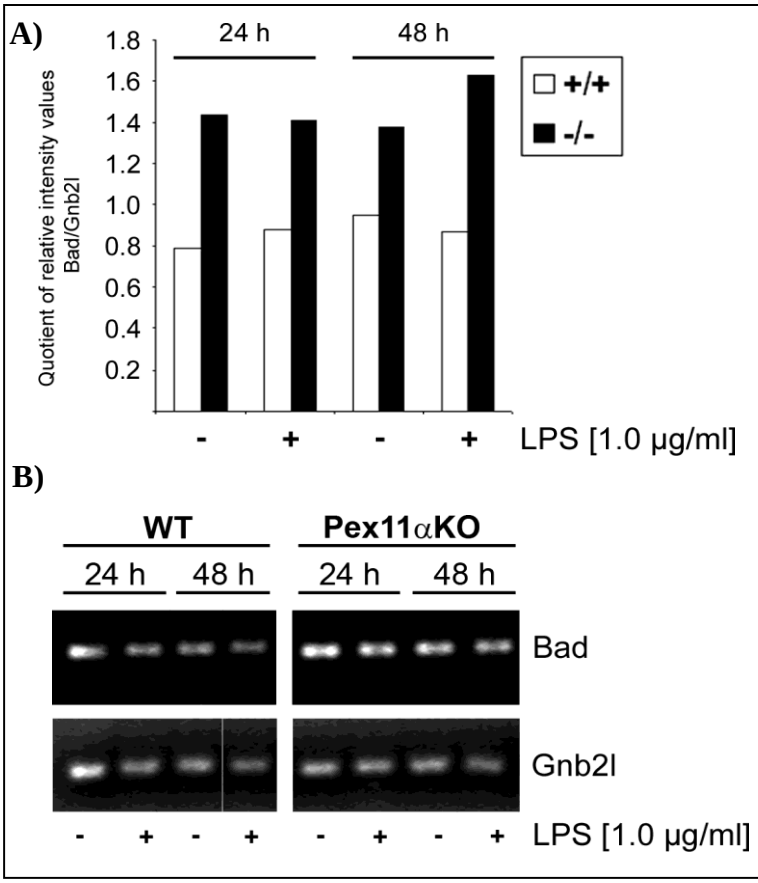

Fig. 29 A) Quantification of relative mRNA values for Bad.
Intensity values for Bad mRNA of different samples were divided by the appropriate values for Gnb2l, a marker gene that has been shown in the literature not to be altered by LPS treatment.

B) Bad mRNA expression in WT and Pex11α KO BMDM after LPS treatment.
Isolated murine BMDM from WT and KO animals were incubated for indicated periods with or without 1.0 µg/ml LPS. After mRNA isolation, RT-PCRs with primer pairs against Bad and Gnb2l as loading control were performed. Equal amounts of the PCR product of each sample were separated in 4.0 % agarose gels. Figure 28 B shows representative result of n=3 experiments.

Indeed, Bad mRNA expressions were increased in Pex11α KO MΦ compared to WT cells at 24 h and 48 h (Fig. 29 B), suggesting the activation of pro-apoptotic pathways in Pex11α KO MΦ. This effect was visible by comparing untreated WT and Pex11α KO cells. Bad mRNA expression was quantified in relation to the one of Gnb2l, a house keeping gene which was reported not to be altered after LPS treatment (Fig. 29 A). LPS-treatment did not exert a strong effect on Bad expression in WT and Pex11α KO MΦ, when values were calculated in relation to Gnb2l. Higher general Bad expression levels in Pex11α KO BMDM might be one

of the reasons, why Pex11α KO MΦ cultures exhibit a higher cell death rate after LPS treatment compared to WT MΦ cultures.

4.5.4 Caspase-3 cleavage in LPS treated WT and *PEX11α* KO MΦ

Activation of Bad occurs during intrinsic apoptosis pathway, whereas downstream lies the activation of the executioner caspase-3. Cleavage of procaspase-3 is a direct marker for caspase-3 activation. Western blot analysis of LPS treated WT and Pex11α KO MΦ was performed to analyse whether elevated levels of activated caspase-3 are present in Pex11α KO MΦ. An antibody against both parts of cleaved caspase-3 was used.

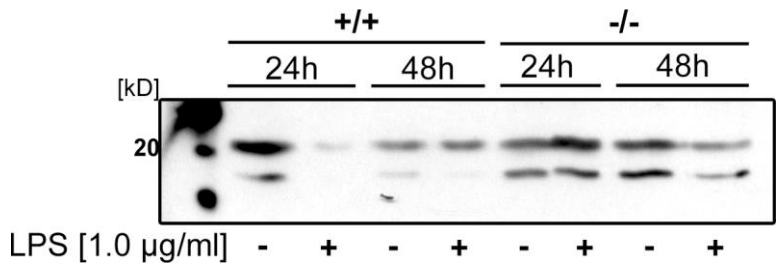

Fig. 30 Summary of Western blot analyses of Effect of LPS treatment on Caspase-3 cleavage in WT and Pex11α KO BMDM.
Isolated BMDM from WT or Pex11α KO animals were incubated for indicated periods with or without 1.0 µg/ml LPS. 4 µg protein each of whole cell lysate sample was separated on 15 % SDS-polyacrylamide gels and subjected to immunoblot analysis with an antibody against cleaved caspase-3. Representative picture of n=3 different experiments. These preliminary experiments should be validated in macrophages of a higher number of animals.

According to the results of the Western blot analysis (Fig. 30), a decrease of cleaved caspase-3 in WT cells after 24 h due to LPS treatment is visible, which is not maintained after 48 h. The reduced amount of activated cleaved caspase-3 protein might explain the increased cell survival of WT BMDM after LPS treatment, as shown before. In contrast, the level of cleaved caspase-3 in Pex11α KO MΦ seems to be increased after 24 h LPS treatment, which could explain the increased cell death. This effect is not present after 48 h LPS treatment. Long-term LPS treatment rather seems to have opposite effects on Pex11α KO BMDM.

4.5.5 Effect of LPS on the mRNA expression of pro-inflammatory marker genes of WT and *PEX11α* KO BMDM

The Pex11α gene knock out exerts a tremendous effect on peroxisome morphology and cell survival after LPS treatment. The mRNA expression levels of inflammatory marker genes were analysed (COX-2, iNOS) in total RNA samples of WT and Pex11α KO BMDM after 48 h LPS treatment [1.0 µg/ml] to answer the question, whether the Pex11α KO has an influence on the pro-inflammatory response after LPS treatment. Furthermore, isolated BMDM from male and female donor mice were cultivated separately to investigate gender specific effects on the expression of COX-2 or iNOS after LPS treatment.

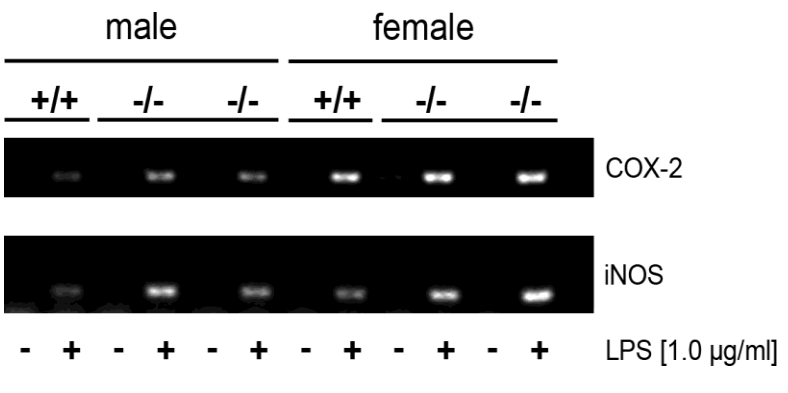

Fig. 31 mRNA expressions of pro-inflammatory genes in murine primary BMDM after LPS treatment.
Isolated murine WT or Pex11α KO BMDM were incubated for 48 h with or without 1.0 µg/ml LPS. After mRNA isolation, RT-PCRs with appropriate primer pairs were performed. Equal amounts of the PCR products of each sample were separated in 4.0 % agarose gel. Image shows representative result of n=3 experiments. These preliminary experiments should be validated in macrophages of a higher number of animals.

According to the PCR analyses the deficiency of the Pex11α gene exerted a clear impact on the expression levels of pro-inflammatory marker genes (see Fig. 31). Expression levels of COX-2 as well as of iNOS mRNAs are clearly increased in Pex11αKO BMDM compared to WT cells. Furthermore BMDM of female mice exhibited higher expression levels of COX-2 and iNOS mRNAs under untreated and after LPS treated conditions compared to their male counterparts.

5. Discussion

Peroxisomes are ubiquitous organelles, however every organ and cell type investigated so far contains a very unique configuration of this organelle [211, 225]. Composition of membrane and matrix proteins differ between peroxisomes of different cell types, representing the wide spectrum of tasks peroxisomes fulfil. Most of the information on peroxisome morphology and physiology has been generated in liver, kidney or brain of rat, mouse or fibroblasts of human subjects or patients with peroxisomal diseases [4, 211, 226-231]. Although there are reports linking inflammatory processes to changed peroxisomal activity in various organs, especially in the brain, little is known about the effect of inflammatory processes on the peroxisomal compartment within one of the key cell types of the innate immunity, the monocyte/macrophage (MΦ) [1, 232].

According to the different parts in the results section of this dissertation, the discussion is also structured in four different parts.

1) During the experimental work of this thesis protocols for peroxisome isolation have been transferred and established to investigate the peroxisomal compartment in MΦ. After establishing all necessary methods, the influence of inflammatory mediators on the peroxisomal compartment has been investigated.

2) The results of this dissertation reveal a strong influence of MΦ activation on peroxisomal gene expression as well as peroxisomal protein abundance, indicating a possible role of the metabolism of this organelle in inflammation regulation.

3) The next set of experiments aimed at discovering the responsible signalling pathways, using pharmacological inhibitors against key factors of inflammatory signalling (TNF-R, NFκB and TLR-4).

4) Since a strong response of the Pex11α gene was found in different phases of the inflammatory response, isolated MΦ originating from *Pex11α* gene knock out mice were used to investigate the influence of the gene knock out on the pro-inflammatory response in these cells, including the late resolution phase of the inflammatory reaction [212].

5.1 Transfer and establishing protocols for MΦ

In order to investigate the effect of pro-inflammatory stimuli on the peroxisomal compartment of macrophages, methods for peroxisome enrichment in the liver had to be adapted and established for the isolation of these organelles in macrophages in our laboratory.

The isolation of peroxisomes from whole cell lysate is a very useful tool to investigate the protein composition of peroxisomes. The transfer of the isolation protocol from the original publication from Völkl and Fahimi to MΦ was the first step in investigating the peroxisomal compartment in this cell type [198]. In contrast to this study wherein whole rat liver homogenates were subjected to cell fractionation, cell lysates from murine RAW264.7 MΦ were used in this dissertation. The cell line RAW264.7 has advantages compared to isolated MΦ and is a well characterised immortal cell line. Cultivation can easily be performed continuously without the sacrifice of donor mice for alveolar or peritoneal MΦ isolation. Moreover, the cell number of harvested RAW264.7 cells is much higher than from isolated alveolar or peritoneal MΦ, allowing resource intensive experiments, such as subcellular fractionation by differential centrifugation and subsequent Western blot analyses. However, a well-known drawback of cell lines is a possible loss or alteration of functions due to long-term cultivation, which might lead to mutations. Because of these reasons, additional experiments with isolated MΦ from mice were performed, to compare the results between the RAW264.7 cell line and primary MΦ of different origins (e.g. BMDMs, peritoneal or alveolar MΦ) to exclude the possibility that the results represent cell line specific artefacts.

In the publications referring to peroxisome enrichment from distinct tissues the use of fresh samples was recommended, since peroxisomes are very sensitive organelles [198, 199, 233, 234]. However, in this thesis could be shown, that the use of a regular Elvehjem Potter or even a Dounce homogenizer for homogenisation of cell culture samples from RAW264.7 cells is not advisable. RAW264.7 cells are small cells and only a very low volume of sample was available (100 µl) in comparison to the tissue samples used for the homogenisation procedure described in the literature (~20 ml for rat liver). By using the regular Potter-Elvehjem homogenizer for the small volumes of MΦ cell cultures, a large part of the sample was lost, because the plasma membrane of the MΦ was not completely opened and the non-broken cells pelleted down in the first centrifugation step. A careful literature analysis revealed that multiple cycles of freezing and thawing of the cell cultures, followed by shearing the cell samples through a 22 gauge needle were performed for MΦ. However, these protocols, aimed at the isolation of other organelle types from MΦ [235–238]. Since

peroxisomes are very fragile organelles, from which matrix proteins leak out easily, the adaption of the original protocol to the isolation of these organelles in MΦ had to be performed carefully. The results of this thesis indicate that one freeze/thaw cycle of the RAW264.7 cell samples before homogenisation with a Potter-Elvehjem homogenizer improves the peroxisomal enrichment by differential centrifugation compared to using fresh cell samples (p. 54) as well as preserves the integrity of peroxisomes and prevents matrix protein leakage out of these organelles. Another beneficial aspect of this method was the easier handling of the cell samples, because many cell culture samples could be stored at -80°C and pooled if necessary after the harvest until peroxisome enrichment and further protein analyses were performed.

Another critical factor for peroxisome enrichment was the application of the correct centrifugation velocity for the separation of distinct organelles. For peroxisome isolation from rat hepatocytes a velocity of 1,950 g was recommended according to Völkl et al. [198] to separate peroxisomes from larger mitochondria. Since peroxisomes differ in morphology and protein composition between distinct organs of different species [1, 185, 227, 239-244], the effect of different velocities in the second step of the differential centrifugation procedure was investigated in RAW264.7 (p. 56). The results indicate that peroxisome enrichment is not improved using velocities higher than 1,950 g, wherefore for all subsequent experiments a centrifugation velocity of 1,950 g at the second centrifugation step was used.

5.2 Effect of pro-inflammatory stimuli on RAW264.7 MΦ and primary mouse MΦ

5.2.1 Selection of the model system

In order to create a robust inflammatory response in RAW264.7 MΦ, we compared two different pro-inflammatory stimuli, LPS and TPA. Both stimuli have been used regularly for studying pro-inflammatory activation of different MΦ cell lines and primary MΦ in the literature [245-250]. By using these two stimuli distinct pathways of MΦ can be investigated.

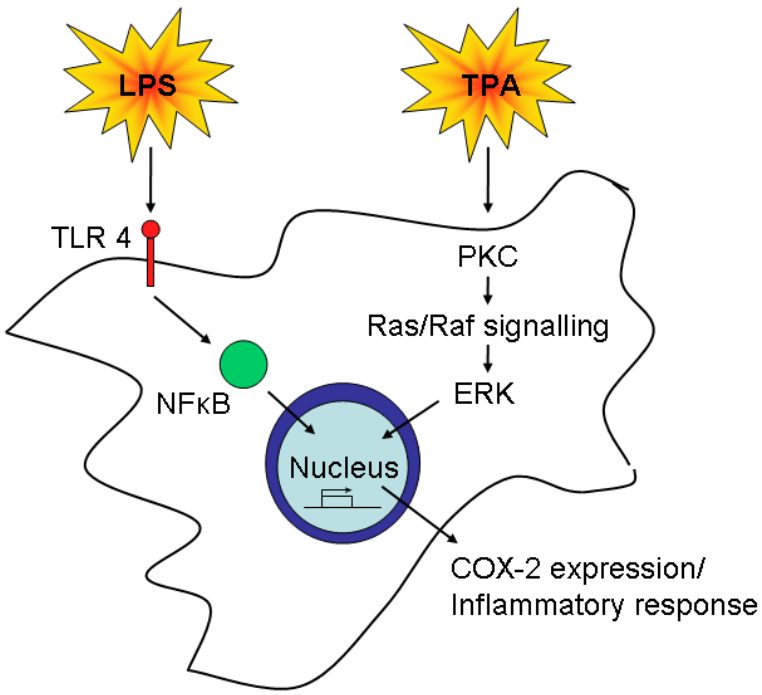

Fig. 32 Schematic overview of LPS and TPA induced macrophage activation.
LPS induced MΦ activation is mediated via TLR 4 signalling. After LPS binding NFκB is released from IκB, translocates into the nucleus and induces the expression of pro-inflammatory genes, such as COX-2. TPA mimics the PKC product diacylglycerol, activating Ras/Raf signalling and induces COX-2 expression via ERK.

Since TPA mimics PKC-signalling downstream of diacylglycerol, this stimulus might be useful for further studies with Pex gene KO mice, in which the lipid components of the plasma membrane might be disturbed. Moreover, it has been described that phorbolesters may lead to peroxisome proliferation [251].

In addition to these two stimuli, the effect of serum withdrawal on the inflammatory response was analysed. Most protocols suggested the use of serum withdrawal before stimulation of MΦ [252, 253]. However, serum starvation is a very important factor influencing peroxisome metabolism. It is well known that the peroxisomal compartment changes in response to altered nutritional conditions (e.g. starvation and growth factors) [20, 212, 254-256]. Severe differences were noted in fact in this thesis when MΦ were stimulated under serum or serum-free conditions. Interestingly, the results indicate that LPS induces the most pronounced pro-inflammatory response in RAW264.7 cells when incubated in serum containing medium (p. 58) and provide the first clear-cut evidence that indeed serum should be used to generate the strongest pro-inflammatory response. The incubation in serum containing medium does prevent starvation induced effects on the peroxisomal compartment during the inflammatory response, especially during long-term incubation (>24 h), after which MΦ die by apoptosis under serum-free conditions (data not shown). For long-term experiments, e.g. to study the resolution of inflammation, serum addition is therefore a necessary requirement.

5.2.2 Induction of the inflammatory response in RAW264.7 and primary mouse MΦ

The most critical step in investigating the effect of a pro-inflammatory stimulus on the peroxisomal compartment of MΦ is to quantify the activation of MΦ by investigating the activation cascade of known pro-inflammatory enzymes. In the literature the reaction cascade of macrophage cell lines as well as primary MΦ to LPS incubation regarding the expression of inflammatory marker genes, such as iNOS, COX-2 and TNFα, has been well described. However, these include only short incubation periods up to 24 h [245, 257-260]. Unfortunately, before the beginning of this thesis only scarce information was available on extended LPS incubation periods up to 72 h [261]. It was necessary to document protein alterations in the peroxisomal compartment after LPS treatment for time periods up to 72 h, because the half-life of peroxisome protein turn-over is approximately 3 days [242].

The first experiments were performed to confirm a reliable induction of an inflammatory response in long term LPS incubation periods up to 72 h in RAW264.7. From the literature, it is known that the incubation of RAW264.7 cells with LPS leads to an increased expression of the differentiation and activation marker protein CD68 [262]. CD68 is present at the surface of the MΦ plasma membrane as well as in endosomal membranes and it is thought to be involved in phagocytic processes. The results of this thesis (p. 59) showed indeed a clear

increase of CD68 protein abundance after LPS incubation, a positive confirmation that the RAW264.7 cells reacted appropriately to the LPS stimulation. Additionally, the effect of LPS on the mRNA induction of the pro-inflammatory marker genes COX-2, iNOS and TNFα in RAW264.7 MΦ was analysed [263-267]. Moreover, the expression of HO-1, an anti-inflammatory protein, was investigated, which is known to be up-regulated by ROS produced during LPS stimulation [222].

The steady state expression levels of corresponding mRNAs of RAW264.7 and primary MΦ after LPS treatment at different incubation periods exhibited distinct patterns (p. 60). Compared to the increase of COX-2 and iNOS expression, induction of the TNFα gene mRNA was less pronounced in RAW264.7 cells. The reason for this might be the different way of activation of the appropriate COX-2 or iNOS and TNFα genes by distinct single stimuli [268]. These results on RAW264.7 MΦ correspond very well to data from the literature on LPS stimulation and the expression of CD68 and mRNA expression levels of inflammatory mediators iNOS, COX-2 and TNFα [269].

Overall, the results on RAW264.7 cells show that a pro-inflammatory response to LPS treatment occurs, suggesting that this cell line is a suitable model organism for investigating the effects of LPS on pro-inflammatory reactions. Therefore, RAW264.7 MΦ seem to be well suited to study the alterations of the peroxisomal compartment therein.

Parallel to the experiments with RAW264.7 MΦ, a similar set of experiments was performed using isolated peritoneal MΦ. The experiment confirmed that nearly all cultivated cells were CD68 positive (>98 %, p.62). However, due to the low cell number yield after isolation of primary peritoneal MΦ these cells were used for RNA isolation and no Western blot analysis could be performed.

Peritoneal MΦ exhibited a strong increase of COX-2 and iNOS mRNA expression after 24 h and 48 h LPS treatment (p. 63). These results are in line with findings in the literature but it has to be mentioned that LPS incubation periods used in these publications were usually ≤ 24 h and differ from the LPS incubation periods in this thesis (> 24 h)[270]. In comparison to RAW264.7 MΦ, peritoneal MΦ show a stronger reaction regarding TNFα mRNA expression after LPS treatment. Apparently, there are differences in pro-inflammatory signalling between primary murine MΦ and the RAW264.7 cell line. Indeed, Rouzer et al. showed, that the RAW264.7 MΦ are not able to autoregulate TNFα release via the prostaglandin dependent pathway [271]. These differences must be taken into account, when the effects of LPS on the peroxisomal compartment of both cell types are discussed. However,

the results of this thesis show, that both cell types exhibited a strong inflammatory response to LPS at given time points, which allowed for the investigation of the effects of LPS treatment on the peroxisomal compartment in the RAW264.7 MΦ cell line (especially also to analyse protein values) as well as in peritoneal WT MΦ (for analyses on RNA level) at prolonged incubation periods.

5.2.3 Effect of oxLDL on the peroxisomal compartment of RAW264.7

Macrophage activation does not only occur after LPS-stimulation, but also by incubation with oxidized LDL particles. Therefore, the reaction of the peroxisomal compartment of RAW264.7 after oxLDL treatment was investigated. Physiologically, LDL is a complex mixture of protein and different types of lipids [272], that are oxidized under pathological conditions. It is well known that during pathogenesis of atherosclerosis low density lipoproteins (LDL) are trapped in the intima and are subject to oxidative modification, leading to the formation of oxidized LDL (oxLDL). The intimal oxLDL particles initiate an inflammatory response in epithelial cells leading to the attraction of blood monocytes to the site of LDL oxidation. The attracted monocytes invade the vessel wall, differentiate to macrophages and start to phagocytose the oxLDL in order to abolish the initial cause for inflammation. However, the overload of macrophages with oxLDL leads to foam cell formation, MΦ cell death and progression and chronification of the pro-inflammatory response (for a review of the processes leading to atherosclerosis see [189]).

Recognition of oxLDL and the underlying signalling pathways leading to the inflammatory responses have been well studied [273, 274]. However, the role of peroxisomes during these processes is not known. Since peroxisomes contain enzymes involved in ROS protection, e.g. catalase, as well as enzymes for bioactive lipid degradation, especially prostaglandin and leukotrien degradation, it is likely that oxLDL has an impact on the peroxisomal compartment of macrophages during the initiation and progression of atherosclerosis. Indeed, the oxidized lipid fraction of oxLDL activates PPARγ signalling in macrophages [275] and many peroxisomal genes contain PPREs in their corresponding promoter regions [225]. According to these considerations, the hypothesis for this thesis was generated that peroxisomes might play an important role in degradation of oxLDL in MΦ.

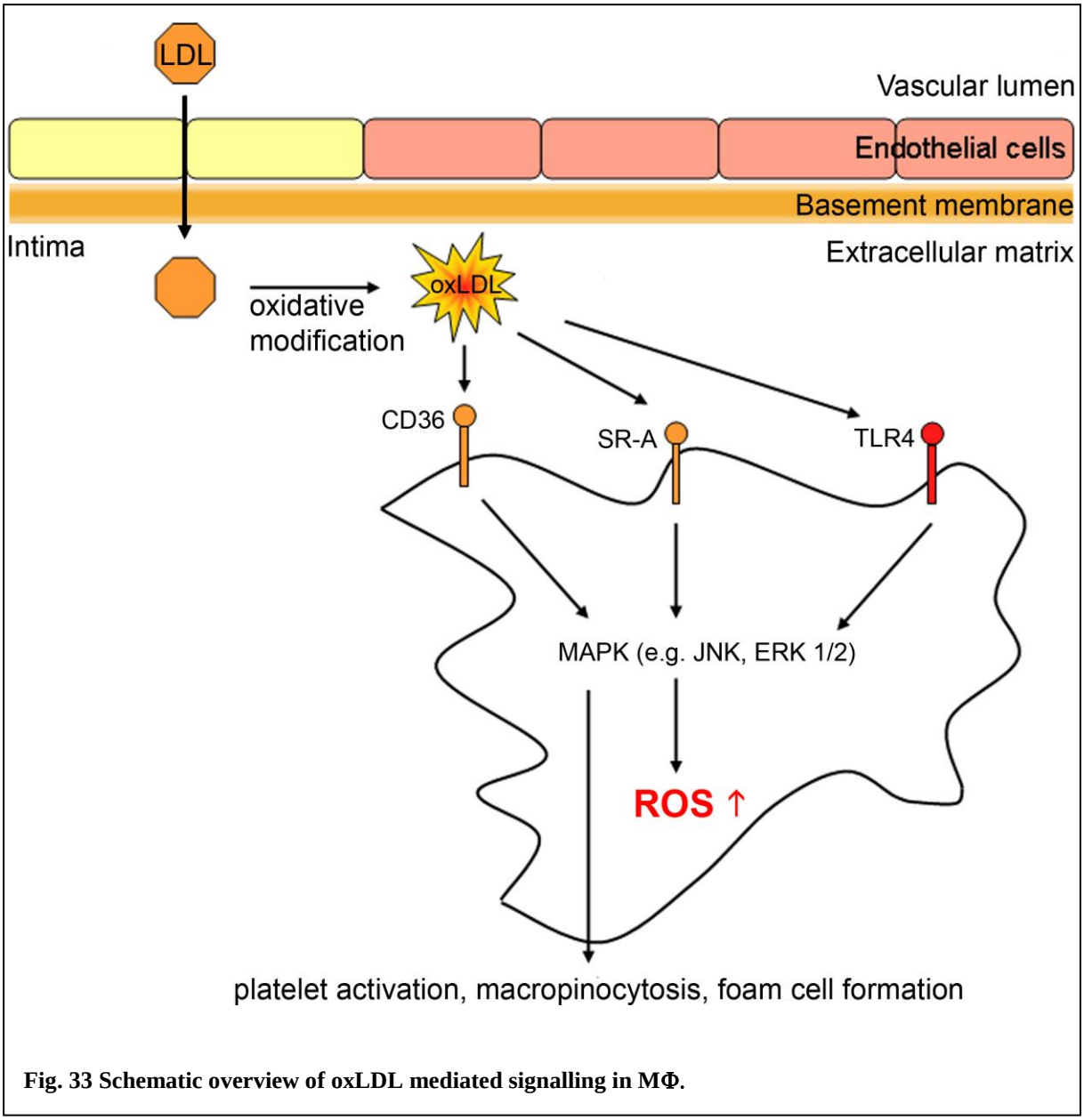

Fig. 33 Schematic overview of oxLDL mediated signalling in MΦ.

The different effects of LPS and oxLDL stimulation on the inflammatory response and the peroxisomal compartment of RAW264.7 cells might be explained by the different signalling pathways induced by these stimuli (p.70, p71). As described above, LPS recognition is mediated by TLR-4 and subsequently by NFκB signalling [276], whereas oxLDL is mainly recognised by a different set of receptors, such as scavenger receptor A (SR-A, =CD204) and CD36 [277, 278]. It is noteworthy, that Ohnishi et al. reported recently about the interference of SR-A and TLR-4 signalling, in a competitive manner which could explain the opposite effects of LPS and oxLDL on the peroxisomal compartment of MΦ [279]. However, in other publications it was described, that oxLDL could bind to TLR-4 [280], leading to an induction

of the inflammatory response [281]. Interestingly, Stewart et al. showed that CD36 initiates TLR-4/TLR-6 heterodimer formation after oxLDL recognition [282].

It is known that PPARγ also influences TLR4 signalling (reviewed in [283]). Moreover, the lipid fraction of oxLDL effects PPAR signalling, more precisely PPARα and PPARγ. Despite that the effect of oxLDL on PPAR signalling in MΦ has been studied no information was available on oxLDL effect on the peroxisomal compartment [284]. This thesis provides the first direct evidences that the peroxisomal compartment is affected by oxLDL treatment. The effect of PPARα signalling on the peroxisomal gene expression of β-oxidation enzymes and the overall compartment has been well described for other cell types and organ systems revealing also a strong cell type specific differences [212, 285]. Taken together, it is most likely that oxLDL incubation of MΦ indeed leads to PPAR mediated changes in the peroxisomal compartment of MΦ. The exact mechanisms of these processes, however, have to be clarified in future experiments

Although, these oxLDL results are very remarkable, it has to be mentioned that working with oxLDL has several drawbacks. LDL has to be isolated from donor blood samples in high amounts and has to be oxidised to oxLDL subsequently. Problems are therefore the supply with donor blood samples and the unpredictable composition of the generated oxLDL due to non-standardised oxidation events happening during the regular procedure of oxLDL preparation. LPS on the other hand is a well-defined single molecule, easy to order in high purity and to work with. Additionally, LPS incubation of RAW264.7 led to a much more pronounced induction of a pro-inflammatory response. Therefore, it was decided to prioritise LPS-experiments and to analyse the influence of LPS on the peroxisomal compartment of MΦ in detail. The effect of oxLDL on the peroxisomal compartment of MΦ will be investigated in future studies, which certainly will provide valuable information about the role of peroxisomes in MΦ during the molecular pathogenesis of atherosclerosis.

5.3 Peroxisomes in Macrophages

Although the organelle “peroxisome” itself was described for the first time more than 50 years ago [3], very little is known about its physiological role in cells of the immune system. Khan et al. described the influence of LPS on the peroxisome function in rat liver and emphasized only on a role of Kupffer cell released TNFα influencing especially peroxisomal β-oxidation [185, 186]. Since peroxisomes harbour many antioxidative enzymes and are involved in plasmalogen biosynthesis as well as the degradation of a variety of signalling and

bioactive lipid mediators, it can be hypothesised that peroxisome metabolism is involved in the regulation of the inflammatory response by influencing ROS level and metabolising lipid based pro- as well as anti-inflammatory mediators.

Karnati and Baumgart-Vogt discovered the presence of an abundant peroxisomal compartment in alveolar MΦ and described the role of peroxisomes during the physiological functions of this cell type [1, 286]. Moreover, during the experimental work of this thesis Dixit et al. discovered very recently that peroxisomes are involved in antiviral defence indicating an important role of peroxisomes in the innate immune response [287].

5.3.1 Effect of LPS on the peroxisomal compartment of RAW264.7 MΦ and primary mouse MΦ

After the confirmation of the LPS-induced pro-inflammatory response in RAW264.7 MΦ and primary mouse MΦ, the effect of LPS treatment on the peroxisomal compartment in these cell types was investigated. LPS effects on catalase and PPARα were described in the literature in rat liver by Beier et al. [288]. Furthermore, Contreras et al. reported a reduced β-oxidation activity in rat liver after LPS treatment [186]. From the same lab, Khan and colleagues showed that deletion of Kupffer cells from rat liver normalized the situation in the liver after LPS treatment [185], linking the observed LPS mediated effects on liver peroxisomes partly to the cytokine release (e.g. TNFα) of liver specific MΦ, the Kupffer cells. Moreover, Paintila et al. described the effects of LPS on peroxisomal proteins involved in myelin synthesis in the developing murine brain revealing that LPS and TNFα led to impaired peroxisomal β-oxidation and elevated ROS generation via inhibition of PPARα signalling [289]. Ahlemeyer et al., colleagues from our group, reported about the destructive effect of elevated ROS levels after Pex11β gene KO on peroxisome and mitochondrial function, leading to apoptosis of neurons [72]. It is likely that LPS induced reduction of peroxisomal β-oxidation is 1) a cell type specific phenomenon depending on the abundance of TLR4 as well as corresponding signalling pathways and 2) is further enhanced by the release of pro-inflammatory cytokines (e.g. TNFα) which varies in individual cell types. However, the question how and when inflammatory processes lead to impairment or reconstitution of peroxisomal function is still not answerd.

In this thesis it was revealed that in RAW264.7 MΦ genes of peroxisomal proteins involved in ROS degradation (catalase), β-oxidation (thiolase, ABCD3) and peroxisomal proliferation (DLP-1, Pex11α) are strongly influenced by the LPS incubation (p. 64). Comparing these results with the results of the primary peritoneal MΦ, alterations in the peroxisomal

compartment of peritoneal MΦ are not as pronounced as in RAW264.7 MΦ (p. 65). Nevertheless, a similar pattern of mRNA alterations was observed in both cell types. These differences might be related to the different origins of the cells. RAW264.7 is an immortalised cell line for long time cultivation while primary MΦ were freshly isolated (from lung, peritoneal cavity or differentiated from bone marrow derived stem cells).

In contrast to the observed decrease of peroxisomal β-oxidation enzyme mRNA expression, the gene for peroxisomal biogenesis protein Pex14 exhibited the same mRNA expression level in LPS treated and untreated cells and its corresponding protein PEX14p was increased after LPS treatment. Additionally, increased Pex11α and DLP-1 mRNA expression after LPS treatment at later time points (> 24 h) was observed. Unfortunately Western blot analysis for Pex11 proteins were not possible although several different antibodies from the group of Steve Gould (John Hopkins University, Baltimore, USA) as well as from different companies have been tested in this thesis. No antibody against Pex11 proteins gave reliable results and the commercial available antibodies described as "working well" recognized non-specific proteins at a similar kD range, shown by Ahlemayer et. al. in supplementary materials [72]. Therefore, only the functional effect of LPS on Pex11α- and DLP-1-mediated peroxisome alterations and proliferation were determined indirectly by immunofluorescence staining of RAW264.7 MΦ using an anti Pex14p antibody, providing excellent staining for MΦ peroxisomes (p. 68) [1]. As revealed by the immunofluorescence stainings, the peroxisome number was indeed increased after LPS treatment (p. 65), which is in line with the increased expression of Pex11α and DLP-1 mRNA after prolonged LPS incubation periods. These results suggest that LPS treatment leads to peroxisome proliferation, because both genes encode proteins involved in peroxisomal fission [212, 239, 255]. It is likely that after an initial reduction of metabolic active peroxisomal proteins in the early stage of the pro-inflammatory response leading the accumulation of PPARγ activating substrates, peroxisomes proliferate and reconstitute their protein composition at the late inflammation stage, involved in the resolution phase of the acute inflammatory processes.

This would also imply that a dysfunction of Pex11αp or peroxisomal metabolic pathways would lead to a delay of the resolution or to a chronification of inflammatory processes. Indeed, significant alterations of pro-inflammatory reactions were found in Pex11α KO animals as discussed in chapter 5.4.

5.3.2 Effect of pharmacological inhibitors on the inflammatory response and the peroxisomal compartment in RAW264.7

The results discussed above led to the hypothesis that LPS-dependent signalling pathways lead to the influence on the gene activity and expression of peroxisomal matrix proteins and alterations observed on peroxisomal fission via the TLR-4/NFκB followed by TNFα release and subsequent TNF-R dependent signalling. Beier et al. have already shown in rat liver, that TNF-α influences PPARα mediated peroxisome metabolism [288]. In line with the results of this thesis, Contreras et al. have suggested that LPS dependent cytokine release might be responsible for impaired peroxisomal β-oxidation in rat liver, implicating also an autocrine stimulation of the liver specific MΦ, the Kupffer cells via TNFα [186]. To test this hypothesis, we used pharmacological inhibitors against TLR-4, NFκB and TNF-R (see Fig. 34). The TNF-R inhibitor was included because TNFα is one of the most important inflammatory cytokine released during the inflammatory response of MΦ.

The initial experiment determined the working concentrations for the pharmacological inhibitors (p 74): CLI-095 against the TLR-4 receptor, celastrol against NFκB and SPD-034 against TNF-R. Indeed, it was noted that the recommended working concentrations by the corresponding manufacturer of celastrol and SPD-034 for short incubation periods were highly toxic to the RAW264.7 cells at prolonged incubation periods up to 72 h. CLI-095 could be used at the proposed concentration of 18.0 µM without inducing a cytotoxic effect. In contrast, celastrol and SPD-034 showed a dose dependent increase in cytotoxicity. These effects might be related to the extended incubation times up to 72 h. Since NFκB-activation is also involved in pathways related to cell survival [290], a prolonged inhibition of this pathway might lead to increased cell death. The reason for toxicity of SPD-034 is less clear. Non-toxic concentrations were applied for further experiments, bearing in mind that lower concentrations of celastrol and SPD-034 might also influence their inhibitory capacities on appropriate signalling pathways.

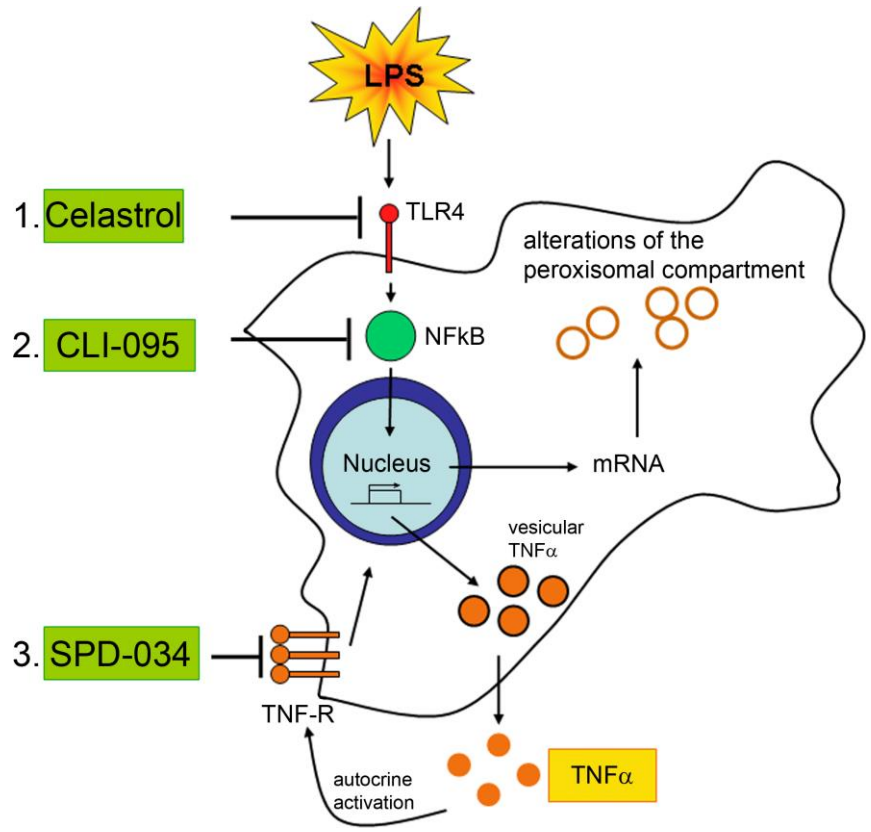

Fig. 34 Schematic overview of the LPS induced pro-inflammatory signalling cascade in MΦ and corresponding inhibitors.
(1.) First step of LPS induced MΦ activation is LPS/TLR4 binding. CLI-095 inhibits LPS/TLR4 binding. (2.) The most critical step in MΦ is the release of NFκB from IκB and its translocation into the nucleus. NFκB release is inhibited by celastrol. (3.) LPS signalling leads to the release of vesicular TNFα into the interstitium, acting as autocrine and paracrine messenger. The binding of TNFα with its receptor TNF-R is inhibited by SPD-034.

The inhibitory capacities of the compounds and the effects of their conincubation with LPS were determined by COX-2 or iNOS mRNA expression analyses which revealed strong inhibitory capacities for all compounds. The inhibitors abolished (CLI-095, Celastrol) or reduced (SPD-034) COX-2 and iNOS mRNA expression after LPS treatment (p. 75).

These results indicated that there was a direct effect of LPS on the abundance of peroxisomal proteins during the TLR-4 and NFκB mediated inflammatory response. Moreover, it could be shown, that also the TNFα release was in an auto-/paracrine manner involved in mediating the effects in peroxisomal gene expression levels and protein abundance alterations (p. 76). As described above, it is well known, that inflammatory processes do also influence PPAR signalling [283], which is directly linked to peroxisomal gene expression and metabolism [5]. According to these reports, PPARα is reduced during inflammation [80], whereas PPARγ is increased [82]. Future studies are necessary to clarify the role of PPAR mediated regulatory

mechanisms on alterations of individual peroxisomal enzymes and peroxisome proliferation and the activation of the NFκB and TNFα signalling pathways. It is most likely, that at least some of the effects on the peroxisomal compartment are mediated by distinct PPARs in the MΦ. It is plausible that changed PPARα and PPARγ signalling during the inflammatory response have an impact on the peroxisomal compartment. However, the effect of the inhibitors on peroxisomal protein abundance could also be interpreted that peroxisomal genes might be directly regulated by NFκB mediated signalling. This would have a strong impact on the role of peroxisomes during inflammatory processes. Because peroxisomes contain enzymes involved in the degradation of pro-inflammatory mediators, e.g. eicosanoids, peroxisomes could play an important role during the resolution phase of inflammation by degrading these pro-inflammatory mediators.

5.4 Effect of PEX11α KO on the inflammatory response of primary mouse MΦ

As described in chapter 5.3, LPS exhibited significant effects on the peroxisomal compartment of MΦ. In addition to metabolic changes, the induction of PEX11α mRNA expression was very prominent, which is in line with the increased number of peroxisomes induced in later phase of LPS treatment. To gain insights on the effects of a Pex11α dysfunction on the inflammatory response, primary MΦ isolated from Pex11α KO mice with a C57Bl/6J background were analysed.

Pex11α KO mice are the only knockout mice with a general peroxisomal biogenesis defect that survive until adulthood [212], wherefore MΦ isolation from these adult knock out animals was indeed possible. In contrast to Pex11α KO animals, KO mice with other peroxisomal biogenesis defects die during the first days of life [72]. Even KO mice of the Pex11β gene, encoding a protein of the same family, possess a severe phenotype, leading to death immediately after birth.

Peroxisomes in MΦ of PEX11α KO mice were larger and less numerous compared to the WT MΦ (p. 79). This is in line with previously published data in fibroblasts, neurons and hepatoma cells in mouse liver that reported about a role of PEX11α in peroxisomal proliferation or altered peroxisomal fission due to changes in nutritional factors [21, 212, 239]. Pex11α KO MΦ showed an increase of apoptotic/necrotic cell death after LPS treatment, which was quantified with a LDH-assay (p. 81). The results of these experiments suggest that the disruption of the Pex11α gene does influence the general cell survival of MΦ under LPS-induced stress conditions. Interestingly, alterations of mitochondrial cristae have been reported from our group in the liver of Pex11α KO mice [212] and it is known, that high levels of oxidative stress can induce the intrinsic apoptosis pathway via mitochondrial cytochrom c release [295-297]. Therefore, Western blot analyses of Pex11α deficient BMDM, using an antibody against both cleaved forms of activated caspase-3 were performed (p. 83), which revealed an increase of caspase-3 activation in LPS treated PEX11α KO MΦ compared to WT MΦ, corroborating the microscopical results [298, 299]. Moreover, the mRNA level for Bad, a marker of intrinsic apoptosis via the mitochondrial pathway [300], was elevated in PEX11α KO MΦ, further supporting these results (p. 82).

Apparently PEX11α KO MΦ are more susceptible to intrinsic cell death than WT MΦ under LPS induced stress. The source of this stress is among other things oxidative stress after TLR-4 mediated oxidative burst [301, 302].

Interestingly, mRNA-expression levels of the pro-inflammatory marker genes COX-2 and iNOS were highly elevated after LPS-treatment in Pex11α KO MΦ in comparison to corresponding levels of LPS-stimulated WT MΦ. This suggests that the Pex11α KO affects the LPS-response in MΦ. Moreover, sex specific differences were observed in the reaction of Pex11α KO MΦ originating from male or female KO mice to LPS stimulation. Female animals exhibited higher values in both, untreated and LPS-treated conditions than Pex11α KO MΦ from male mice, regarding the mRNA expression levels of COX-2 or iNOS (p. 84). Indeed, it has been reported that sex specific differences have a strong impact on the function of the mammalian innate immune system [303]. Furthermore, recently Rettew et al. have shown in mouse that testosterone led to a decrease in TLR-4 expression in mouse MΦ [304]. In the same line of evidence Rettew and his coworkers could show, that estrogens regulate the TLR-4 expression on MΦ in an *in vivo* mouse model [305].

However, how the Pex11α gene deficiency influences the TLR-4 signalling cascade, leading to changed COX-2 and iNOS levels is not clear. The KO of Pex11α could have an impact on the degradation of signalling lipid mediators (e.g. arachidonic acid), leading to an increased pro-inflammatory response and a higher and prolonged ROS level induced bythe levated level of pro-inflammatory eicosanoids (prostaglandins and leukotriens), strongly affecting the resolution phase of the inflammatory processes.

According to these results, peroxisomes might play an important role in the metabolic regulation of macrophage activity.

6. Conclusion and outlook

In this thesis the peroxisomal compartment in the murine macrophage cell line RAW264.7 and in murine primary macrophages has been characterised. The results of this dissertation provide first evidences for an important role of peroxisomes in innate immunity of macrophages during their reaction against the pro-inflammatory stimulus LPS. Interestingly, opposite effects were noted on the peroxisomal compartment by treatment with oxLDL. Moreover, major alterations were noted at pro-inflammatory reactions in MΦ with PEX11α defect. Pex11α induction and peroxisome proliferation and reconstitution of peroxisomal enzyme levels occur in the late phase (≥ 48 h) of LPS-stimulation. Taken together the results of this thesis suggest that peroxisomes are involved in the regulation of the pro-inflammatory response and the resolution of inflammatory processes. The observed processes could play an important regulatory role during chronic inflammatory diseases such as atherosclerosis, Alzheimer's disease or liver cirrhosis. This might be related to impaired peroxisome function on several levels: 1) impaired ROS defence leads to increased oxidative stress and prolonged inflammatory processes. 2) disturbed detoxification of xenobiotics and changed metabolism of anti-inflammatory signalling molecules (e.g. prostaglandins).

To gain a deeper understanding of the role of peroxisomes during the inflammatory process of MΦ, further studies have to be performed. Life cell imagine of tagged peroxisomes in MΦ will reveal the kinetics of peroxisome proliferation during MΦ activation. Chip based gene expression experiments (microarray analysis) will give an overview of the gene expression pattern under peroxisome KO conditions and will provide valuable information about the expected corresponding protein expression. These studies could be combined with si/sh RNA experiments in macrophage cell lines, to analyse the influence of other peroxisomal gene knock outs on the inflammatory response of MΦ. Future *in vivo* experiments with the Pex11α mouse model will clarify, whether peroxisomes are essential organelles in the innate immune defence against bacterial infections and if Pex11α animals are more prone to severe septic shock. Indeed the Pex11α KO mouse model also provides an ideal tool to study the consequences of peroxisome disturbances on signalling pathways of distinct cell types of the innate immune system and will open new perspectives regarding the resolution phase and chronification of inflammatory processes.

7. Summary

Macrophages are, as part of the innate immune system, at the first line of defense against invading pathogens and intrinsic inflammatory factors. Although it is known that macrophages contain peroxisomes which fulfill important functions in cell metabolism, e.g. ROS degradation or lipid metabolism, before the beginning of this thesis, nothing was known about the role of peroxisomes in macrophages.

In this thesis, all methods available were established to study peroxisomes in macrophages. Pro-inflammatory reactions were induced by LPS or oxidized LDL. Moreover, LPS-mediated effects on macrophages were characterized under conditions of peroxisomal dysfunction.

Establishment of an optimal protocol for subcellular fractionation by differential centrifugation for the isolation of enriched peroxisomal fractions revealed that freezing of the macrophage cell samples was beneficial for the homogenization procedure and necessary for the best peroxisome recovery. Only these enriched peroxisome fractions enable the study of less abundant peroxisomal metabolic proteins, such as the peroxisomal thiolase. Moreover, during the establishment of an optimal protocol for long term LPS treatment, it was noted, that serum addition to the incubation medium was essential for macrophage long-term survival. Serum-free incubation, as generally used in the literature, exerted negative effects on cell survival and the peroxisomal compartment.

After LPS treatment, RT-PCR and Western blot analyses as well as immunoflourescence studies with antibodies against POL proteins revealed tremendous changes in the peroxisomal compartment and related genes. Up to 24 h β-oxidation enzymes, the H_2O_2 degrading catalase as well as the peroxisomal biogenesis protein *PEX11α* were strongly reduced. In contrast, the *PEX13* gene was hardly influenced and *PEX14* not altered at all. Since Pex14p was not changed, an antibody against this protein was used as an ideal marker to identify peroxisomes after LPS treatment. Immunofluorescence-based studies on peroxisome morphology revealed a significant increase in numerical abundance of peroxisomes after long-term LPS incubation (> 48 h). Moreover, increased *PEX11α* induction preceded the peroxisomal proliferation and the protein levels of catalase as well as β-oxidation enzymes were almost reconstituted at late incubation times. This suggests an important role of peroxisomal metabolism in the resolution of inflammatory processes in macrophages. Furthermore, the underlying signaling pathway was investigated with specific inhibitors against TLR-4, NFκB and TNF-$R_{1/2}$. The results

revealed that the peroxisomal response was mediated by the TLR-4/NFκB pathway, as well as the TNF-R pathway in the early phase of LPS-treatment.

Incubation of macrophages with oxidized LDL (oxLDL) induced opposite effects on the peroxisomal compartment of macrophages, increasing protein levels of catalase and thiolase. This suggests that the peroxisomal compartment in macrophages is activated during clearing of oxidized lipids and would lead to cell protection against oxLDL-mediated lipotoxicity and oxidative stress, possibly preventing or retarding foam cell formation during the development of atherosclerosis.

Finally, experiments focused on LPS-induced effects under peroxisomal dysfunction conditions in primary macrophages of *Pex11α* knockout mice, since this gene was severely affected in distinct phases of LPS-treatment. Indeed increased macrophage cell death and activation of caspase-3 was observed, accompanied by increase of Bad mRNA expression, suggesting an activation of the intrinsic mitochondrial apoptosis pathway. Moreover, sex-specific differences in expression of pro-inflammatory marker genes were noted under steady-state conditions as well as under LPS-stimulation, revealing a stronger reaction of macrophages isolated from female mice.

Taken together, the results of this thesis indicate that peroxisomes are abundant in macrophages and fulfill important metabolic tasks during macrophage activation by distinct pro-inflammatory stimuli. As shown in *Pex11α* gene KO experiments, peroxisomal dysfunction severely alters pro-inflammatory mediators and might lead to prolongation or chronification of inflammatory processes. In this respect, peroxisomal metabolic pathways play an important role for the protection of macrophages against cell death during activation and anti-pathogenic response and the resolution of inflammatory processes. Since the observed effects seemed to be part of a general defense mechanism in MΦ, it is likely, that peroxisomes play also a role in a variety of chronic inflammatory diseases, such as liver cirrhosis, neuro-degenerative diseases like Alzheimer's disease or atherosclerosis.

8. Zusammenfassung

Makrophagen stehen als Teil der angeborenen Immunabwehr an vorderster Front der körpereigenen Verteidigung gegen eindringende Pathogene und intrinische inflammatorische Faktoren. Obwohl bekannt ist, dass Makrophagen Peroxisomen enthalten, die wichtige Funktionen im Zellmetabolismus ausführen, z.B. ROS-Abbau oder Lipid β-Oxidation, war zu Beginn dieser Dissertation keine Fakten über die Rolle von Peroxisomen in Makrophagen bekannt.

In der vorliegenden Arbeit wurden alle Methoden etabliert, um Peroxisomen in Makrophagen zu untersuchen. Die Aktivierung der Makrophagen wurde durch Inkubation mit LPS bzw. mit oxLDL ausgelöst. Darüber hinaus wurden LPS-induzierte Effekte in Makrophagen mit defekten Peroxisomen untersucht.

Die Etablierung eines optimalem Protokolls zur subzellularen Fraktionierung und Isolierung einer angereicherten Peroxisomenfraktion mit Hilfe von differentieller Zentrifugation erbrachte, dass Einfrieren der Zellproben bessere Ergebnisse bei der Homogenisierung lieferte und notwendig war, um eine ideale Anreicherung der Peroxisomen zu erzielen. Nur durch die Verwendung der angereicherten Peroxisomenfraktion konnten auch peroxisomale Enzyme analysiert werden, die nur in geringer Menge exprimiert werden, wie z.B. die peroxisomale Thiolase. Während der Etablierung eines optimalen Protokolls zur Langzeitinkubation der Makrophagen mit LPS zeigte sich, dass die Zugabe von Serum ins Inkubationsmedium essentiell notwendig war, um das Überleben der Zellen zu sichern. Des weiteren beeinträchtigte die Verwendung von serumfreiem Medium, wie sie in der Literatur angegeben wird, die Peroxisomenaktivität.

RT-PCR und Western Blot-Analysen sowie Immunofluoreszenz-Studien erbrachten tiefgreifende Veränderungen des peroxisomalen Kompartments nach LPS Behandlung. Nach 24 h wurde die Genexpression von β-Oxidationsenzymen, der H_2O_2 abbauende Katalase und des peroxisomalen Biogeneseproteins *PEX11α* drastisch reduziert. Dagegen war die Expression des *PEX13* Gens kaum und die des *PEX14* nicht beeinflusst. Da die LPS Behandlung *PEX14* nicht beeinträchtigte, wurde ein Antikörper gegen Pex14p als idealer Marker zum Nachweis der Peroxisomen nach LPS-Behandlung verwendet. Versuche - basierend auf Immunofluoreszenzfärbungen von peroxisomalen Proteinen zum Nachweis des Organells - ergaben, dass sich die Peroxisomenanzahl nach Langzeitbehandlung mit LPS (≥48 h) signifikant vermehrte. Zudem ging der Peroxisomenproliferation ein Anstieg der

Pex11α-Genexpression voraus und die Proteinspiegel von peroxisomalen β-Oxidationsenzymen und Katalase wurden weitgehend wiederhergestellt. Diese Ergebnisse weisen auf eine Rolle des peroxisomalen Metabolismus in der Auflösung inflammatorischer Prozesse in Makrophagen hin. Weiterführend wurden die zugrunde liegenden Signalwege untersucht. Verwendet wurden spezifische Inhibitoren gegen TLR-4, NFκB sowie TNF-R. Die Ergebnisse zeigten, dass die peroxisomale Reaktion auf die LPS-Behandlung durch den TLR-4/NFκB Signalweg sowie durch TNF-R, insbesondere in frühen Zeitpunkten, vermittelt wurden.

Die Behandlung von Makrohagen mit oxidiertem LDL (oxLDL) zeigte entgegengesetzte Effekte wie die LPS-Behandlung. Eine Western Blot-Analyse erbrachte erhöhte Proteinmengen an Katalase sowie Thiolase. Dies könnte ein Hinweis darauf sein, dass das peroxisomale Kompartment in Makrophagen während der Beseitigung von intimalem oxLDL aktiviert wird. Damit könnte der Schutz von Makrophagen vor Lipotoxizität und oxidativen Stress verbunden sein, um die Schaumzellbildung zu verhindern

Zuletzt konzentrierten sich die Versuche auf den Einfluss einer peroxisomalen Dysfunktion auf die LPS indizierte Makrophagenaktivierung. Dazu wurden Makrophagen aus *PEX11α* KO Mäusen isoliert, da sich gezeigt hatte, dass die *PEX11α*-Expression stark von der LPS-Behandlung beeinflusst wird. Tatsächlich wurden in *PEX11α* KO Makrophagen ein erhöhter Zelltod und die Aktivierung von Caspase-3 beobachtet, verbunden mit einer erhöhten Bad mRNA-Expression in KO-Makrophagen, was darauf hindeutet, dass der intrisiche mitochondriale Apoptoseweg vermehrt induziert ist. Des Weiteren traten geschlechtsspezifische Unterschiede in der Reaktion auf LPS-Behandlung auf, was sich durch eine stärkeren Expression pro-inflammatorischer Marker in Makrophagen von weiblichen *PEX11α* KO Mäusen äußerte.

Zusammenfassend läßt sich feststellen, dass Peroxisomen in Makrophagen stark ausgeprägt vorkommen und dort wichtige Funktionen während der Aktivierung von Makrophagen durch verschiedene Stimuli wahrnehmen. Wie durch Versuche an *PEX11α*-KO-Mäusen gezeigt wurde, verändert die peroxisomale Dysfunktion gravierend die Expression pro-inflammatorischer Marker und könnte zur Verlängerung oder zur Chronifizierung inflammatorischer Prozesse führen. Daher erfüllt der peroxisomale Metabolismus wichtige Funktionen im Schutz von Makrophagen vor frühzeitigem Zelltod während ihrer Aktivierung und der Pathogenabwehr. Der hier beobachtete Effekt könnte Teil eines generellen Schutzmechanismus in Makrophagen sein. Daher ist es wahrscheinlich, dass Peroxisomen

ebenfalls bei chronischen Entzündungskrankheiten wie Leberzirrhose, neurodegenerativer Erkrankungen, z.B. Alzheier, oder Atherosklerose, eine Rolle spielen.

9. Abbreviations

Temperatue

°C	Grad Celsius

Time

h	hour
m	minute
s	second

Weight

g	gram
mg	milli gram
µg	micro gram

Volume

l	liter
ml	milliliter
µl	microliter

Other

BSA	bovine serum albumin
Cox-2	cyclooxygenase-2
ddH_2O	double deionised water
DMEM	Dulbeccos modified Eagle`s medium
EDTA	ethylenediaminetetraacetic acid
ERK	extracellular signal-regulated kinase
FCS	fetal calf serum
GAPDH	glyceraldehydes-3-phosphate dehydrogenase
HB	homogenization buffer
IκB	inhibitor of NF-κB
JNK	c-jun N-terminal kinase
LPS	lipopolysaccharide

MΦ	macrophage
MAPKs	mitogen activated protein kinases
MTT	3-(4,5-Dimethylthiazol-2-yl)-2,5-diphenyltetrazolium bromide
NF-κB	nuclear factor-κB
NO	nitric oxide
PBS	phosphate buffered saline
PMA	phorbol myristate acetate
ROS	reactive oxygen species
RT	room temperature
RPMI-1640	Roswell Park Memorial Institut 1640
SDS	sodium dodecyl sulfate
SDS-PAGE	sodium dodecyl sulfate polyacrylamide gel electrophoresis
TBS	tris buffered saline
TLR	toll-like receptor
TNFα	tumour necrosis factor-α
TPA	2-O-tetradecanoylphorbol-13-acetate

10. List of tables

11. List of figures

All graphics base on own designs, if not stated otherwise

12. References

1. Karnati, S. and E. Baumgart-Vogt, *Peroxisomes in mouse and human lung: their involvement in pulmonary lipid metabolism.* Histochem Cell Biol, 2008. **130**(4): p. 719-40.
2. Rhodin, J., *Correlation of ultrastructural organization and function in normal and experimentally changed proximal convoluted tubule cells in the mouse kidney*, in *Aktiebolaget Godvil.* 1954 Karolinska Institute: Stockholm.
3. De Duve, C. and P. Baudhuin, *Peroxisomes (microbodies and related particles).* Physiol Rev, 1966. **46**(2): p. 323-57.
4. Gould S.J., V.D., Raymond G.V., *The peroxisome biogenesis disorders.* 8th ed. The metabolic and molecular bases of inherited disease, ed. B.A.L. Scriver C.R., Sly W.S. Vall D. Vol. 2. 2001, New York: McGraw-Hill.
5. Reddy, J.K. and G.P. Mannaerts, *Peroxisomal lipid metabolism.* Annu Rev Nutr, 1994. **14**: p. 343-70.
6. Duhita, N., et al., *The origin of peroxisomes: The possibility of an actinobacterial symbiosis.* Gene, 2010. **450**(1-2): p. 18-24.
7. Ma, C., G. Agrawal, and S. Subramani, *Peroxisome assembly: matrix and membrane protein biogenesis.* J Cell Biol, 2011. **193**(1): p. 7-16.
8. Islinger, M., M.J. Cardoso, and M. Schrader, *Be different--the diversity of peroxisomes in the animal kingdom.* Biochim Biophys Acta. **1803**(8): p. 881-97.
9. Beier, K. and H.D. Fahimi, *Environmental pollution by common chemicals and peroxisome proliferation: efficient detection by cytochemistry and automatic image analysis.* Prog Histochem Cytochem, 1991. **23**(1-4): p. 150-63.
10. Schluter, A., et al., *PeroxisomeDB 2.0: an integrative view of the global peroxisomal metabolome.* Nucleic Acids Res. **38**(Database issue): p. D800-5.
11. Girzalsky, W., H.W. Platta, and R. Erdmann, *Protein transport across the peroxisomal membrane.* Biol Chem, 2009. **390**(8): p. 745-51.
12. Grou, C.P., et al., *The peroxisomal protein import machinery--a case report of transient ubiquitination with a new flavor.* Cell Mol Life Sci, 2009. **66**(2): p. 254-62.
13. Brocard, C. and A. Hartig, *Peroxisome targeting signal 1: is it really a simple tripeptide?* Biochim Biophys Acta, 2006. **1763**(12): p. 1565-73.
14. Girzalsky, W., D. Saffian, and R. Erdmann, *Peroxisomal protein translocation.* Biochim Biophys Acta. **1803**(6): p. 724-31.
15. Lazarow, P.B., *The import receptor Pex7p and the PTS2 targeting sequence.* Biochim Biophys Acta, 2006. **1763**(12): p. 1599-604.
16. Kunau, W.H., *Peroxisomes: the extended shuttle to the peroxisome matrix.* Curr Biol, 2001. **11**(16): p. R659-62.
17. Schliebs, W. and W.H. Kunau, *PTS2 co-receptors: diverse proteins with common features.* Biochim Biophys Acta, 2006. **1763**(12): p. 1605-12.
18. Platta, H.W. and R. Erdmann, *Peroxisomal dynamics.* Trends Cell Biol, 2007. **17**(10): p. 474-84.
19. Thieringer, H., et al., *Modeling human peroxisome biogenesis disorders in the nematode Caenorhabditis elegans.* J Cell Sci, 2003. **116**(Pt 9): p. 1797-804.
20. Erdmann, R. and G. Blobel, *Giant peroxisomes in oleic acid-induced Saccharomyces cerevisiae lacking the peroxisomal membrane protein Pmp27p.* J Cell Biol, 1995. **128**(4): p. 509-23.
21. Thoms, S. and R. Erdmann, *Dynamin-related proteins and Pex11 proteins in peroxisome division and proliferation.* FEBS J, 2005. **272**(20): p. 5169-81.

22. Knoblach, B. and R.A. Rachubinski, *Phosphorylation-dependent activation of peroxisome proliferator protein PEX11 controls peroxisome abundance.* J Biol Chem. **285**(9): p. 6670-80.
23. Gandre-Babbe, S. and A.M. van der Bliek, *The novel tail-anchored membrane protein Mff controls mitochondrial and peroxisomal fission in mammalian cells.* Mol Biol Cell, 2008. **19**(6): p. 2402-12.
24. Camoes, F., et al., *Organelle dynamics and dysfunction: A closer link between peroxisomes and mitochondria.* J Inherit Metab Dis, 2009. **32**(2): p. 163-80.
25. Delille, H.K., R. Alves, and M. Schrader, *Biogenesis of peroxisomes and mitochondria: linked by division.* Histochem Cell Biol, 2009. **131**(4): p. 441-6.
26. Kaur, N. and J. Hu, *Dynamics of peroxisome abundance: a tale of division and proliferation.* Curr Opin Plant Biol, 2009. **12**(6): p. 781-8.
27. Nagotu, S., M. Veenhuis, and I.J. van der Klei, *Divide et impera: the dictum of peroxisomes.* Traffic. **11**(2): p. 175-84.
28. Mannaerts, G.P., P.P. Van Veldhoven, and M. Casteels, *Peroxisomal lipid degradation via beta- and alpha-oxidation in mammals.* Cell Biochem Biophys, 2000. **32 Spring**: p. 73-87.
29. Biardi, L. and S.K. Krisans, *Compartmentalization of cholesterol biosynthesis. Conversion of mevalonate to farnesyl diphosphate occurs in the peroxisomes.* J Biol Chem, 1996. **271**(3): p. 1784-8.
30. Hajra, A.K. and J.E. Bishop, *Glycerolipid biosynthesis in peroxisomes via the acyl dihydroxyacetone phosphate pathway.* Ann N Y Acad Sci, 1982. **386**: p. 170-82.
31. Mannaerts, G.P. and P.P. Van Veldhoven, *Metabolic pathways in mammalian peroxisomes.* Biochimie, 1993. **75**(3-4): p. 147-58.
32. Breidenbach, R.W. and H. Beevers, *Association of the glyoxylate cycle enzymes in a novel subcellular particle from castor bean endosperm.* Biochem Biophys Res Commun, 1967. **27**(4): p. 462-9.
33. Muller, W.H., et al., *Localization of the pathway of the penicillin biosynthesis in Penicillium chrysogenum.* EMBO J, 1991. **10**(2): p. 489-95.
34. Titorenko, V.I. and R.A. Rachubinski, *The life cycle of the peroxisome.* Nat Rev Mol Cell Biol, 2001. **2**(5): p. 357-68.
35. Schrader, M. and H.D. Fahimi, *Peroxisomes and oxidative stress.* Biochim Biophys Acta, 2006. **1763**(12): p. 1755-66.
36. Hansch, R., et al., *Plant sulfite oxidase as novel producer of H2O2: combination of enzyme catalysis with a subsequent non-enzymatic reaction step.* J Biol Chem, 2006. **281**(10): p. 6884-8.
37. del Rio, L.A., et al., *Reactive oxygen species, antioxidant systems and nitric oxide in peroxisomes.* J Exp Bot, 2002. **53**(372): p. 1255-72.
38. Liu, H.M., et al., *[Analysis of fatty acids in rat liver peroxisomes].* Se Pu, 2001. **19**(5): p. 475-7.
39. Hashimoto, T., *Peroxisomal beta-oxidation enzymes.* Cell Biochem Biophys, 2000. **32 Spring**: p. 63-72.
40. Wanders, R.J., E.G. van Grunsven, and G.A. Jansen, *Lipid metabolism in peroxisomes: enzymology, functions and dysfunctions of the fatty acid alpha- and beta-oxidation systems in humans.* Biochem Soc Trans, 2000. **28**(2): p. 141-9.
41. Wanders, R.J. and H.R. Waterham, *Biochemistry of mammalian peroxisomes revisited.* Annu Rev Biochem, 2006. **75**: p. 295-332.
42. Cooper, T.G. and H. Beevers, *Beta oxidation in glyoxysomes from castor bean endosperm.* J Biol Chem, 1969. **244**(13): p. 3514-20.

43. Cooper, T.G. and H. Beevers, *Mitochondria and glyoxysomes from castor bean endosperm. Enzyme constitutents and catalytic capacity.* J Biol Chem, 1969. **244**(13): p. 3507-13.
44. Hashimoto, T., *Individual peroxisomal beta-oxidation enzymes.* Ann N Y Acad Sci, 1982. **386**: p. 5-12.
45. Lazarow, P.B., et al., *Identification of beta-oxidation enzymes among peroxisomal polypeptides. Increase in Coomassie blue-stainable protein after clofibrate treatment.* FEBS Lett, 1982. **150**(2): p. 307-10.
46. Kunau, W.H., et al., *Comparative enzymology of beta-oxidation.* Biochem Soc Trans, 1988. **16**(3): p. 418-20.
47. Poirier, Y., et al., *Peroxisomal beta-oxidation--a metabolic pathway with multiple functions.* Biochim Biophys Acta, 2006. **1763**(12): p. 1413-26.
48. Uchida, Y., et al., *Purification and properties of rat liver peroxisomal very-long-chain acyl-CoA synthetase.* J Biochem, 1996. **119**(3): p. 565-71.
49. Uchiyama, A., et al., *Molecular cloning of cDNA encoding rat very long-chain acyl-CoA synthetase.* J Biol Chem, 1996. **271**(48): p. 30360-5.
50. Schaffer, J.E. and H.F. Lodish, *Expression cloning and characterization of a novel adipocyte long chain fatty acid transport protein.* Cell, 1994. **79**(3): p. 427-36.
51. Lombard-Platet, G., et al., *A close relative of the adrenoleukodystrophy (ALD) gene codes for a peroxisomal protein with a specific expression pattern.* Proc Natl Acad Sci U S A, 1996. **93**(3): p. 1265-9.
52. Netik, A., et al., *Adrenoleukodystrophy-related protein can compensate functionally for adrenoleukodystrophy protein deficiency (X-ALD): implications for therapy.* Hum Mol Genet, 1999. **8**(5): p. 907-13.
53. Visser, W.F., et al., *Metabolite transport across the peroxisomal membrane.* Biochem J, 2007. **401**(2): p. 365-75.
54. van Roermund, C.W., et al., *The human peroxisomal ABC half transporter ALDP functions as a homodimer and accepts acyl-CoA esters.* FASEB J, 2008. **22**(12): p. 4201-8.
55. Wanders, R.J., et al., *Peroxisomes, lipid metabolism and lipotoxicity.* Biochim Biophys Acta. **1801**(3): p. 272-80.
56. Vanhove, G.F., et al., *The CoA esters of 2-methyl-branched chain fatty acids and of the bile acid intermediates di- and trihydroxycoprostanic acids are oxidized by one single peroxisomal branched chain acyl-CoA oxidase in human liver and kidney.* J Biol Chem, 1993. **268**(14): p. 10335-44.
57. Wanders, R.J., *Peroxisomes, lipid metabolism, and peroxisomal disorders.* Mol Genet Metab, 2004. **83**(1-2): p. 16-27.
58. Baes, M., et al., *Inactivation of the peroxisomal multifunctional protein-2 in mice impedes the degradation of not only 2-methyl-branched fatty acids and bile acid intermediates but also of very long chain fatty acids.* J Biol Chem, 2000. **275**(21): p. 16329-36.
59. Seedorf, U., et al., *Sterol carrier protein X is peroxisomal 3-oxoacyl coenzyme A thiolase with intrinsic sterol carrier and lipid transfer activity.* J Biol Chem, 1994. **269**(33): p. 21277-83.
60. Miyazawa, S., et al., *Properties of peroxisomal 3-ketoacyl-coA thiolase from rat liver.* J Biochem, 1981. **90**(2): p. 511-9.
61. Antonenkov, V.D., et al., *Substrate specificities of 3-oxoacyl-CoA thiolase A and sterol carrier protein 2/3-oxoacyl-CoA thiolase purified from normal rat liver peroxisomes. Sterol carrier protein 2/3-oxoacyl-CoA thiolase is involved in the metabolism of 2-methyl-branched fatty acids and bile acid intermediates.* J Biol Chem, 1997. **272**(41): p. 26023-31.

62. Jakobs, B.S. and R.J. Wanders, *Fatty acid beta-oxidation in peroxisomes and mitochondria: the first, unequivocal evidence for the involvement of carnitine in shuttling propionyl-CoA from peroxisomes to mitochondria.* Biochem Biophys Res Commun, 1995. **213**(3): p. 1035-41.
63. Wanders, R.J. and H.R. Waterham, *Peroxisomal disorders: the single peroxisomal enzyme deficiencies.* Biochim Biophys Acta, 2006. **1763**(12): p. 1707-20.
64. Watkins, P.A., A.E. Howard, and S.J. Mihalik, *Phytanic acid must be activated to phytanoyl-CoA prior to its alpha-oxidation in rat liver peroxisomes.* Biochim Biophys Acta, 1994. **1214**(3): p. 288-94.
65. Watkins, P.A., et al., *Phytanic acid activation in rat liver peroxisomes is catalyzed by long-chain acyl-CoA synthetase.* J Lipid Res, 1996. **37**(11): p. 2288-95.
66. Mihalik, S.J., A.M. Rainville, and P.A. Watkins, *Phytanic acid alpha-oxidation in rat liver peroxisomes. Production of alpha-hydroxyphytanoyl-CoA and formate is enhanced by dioxygenase cofactors.* Eur J Biochem, 1995. **232**(2): p. 545-51.
67. Croes, K., et al., *Formation of a 2-methyl-branched fatty aldehyde during peroxisomal alpha-oxidation.* FEBS Lett, 1997. **412**(3): p. 643-5.
68. Verhoeven, N.M., et al., *Resolution of the phytanic acid alpha-oxidation pathway: identification of pristanal as product of the decarboxylation of 2-hydroxyphytanoyl-CoA.* Biochem Biophys Res Commun, 1997. **237**(1): p. 33-6.
69. Foulon, V., et al., *Purification, molecular cloning, and expression of 2-hydroxyphytanoyl-CoA lyase, a peroxisomal thiamine pyrophosphate-dependent enzyme that catalyzes the carbon-carbon bond cleavage during alpha-oxidation of 3-methyl-branched fatty acids.* Proc Natl Acad Sci U S A, 1999. **96**(18): p. 10039-44.
70. Verhoeven, N.M., et al., *Involvement of microsomal fatty aldehyde dehydrogenase in the alpha-oxidation of phytanic acid.* FEBS Lett, 1998. **429**(3): p. 225-8.
71. Alberts B., J.A., Lewis J., Raff M., oberts K., Walter P., *Molecular Biology of the Cell.* 4th ed. 2002, New York: Garland Science.
72. Ahlemeyer, B., M. Gottwald, and E. Baumgart-Vogt, *Deletion of a single allele of the Pex11beta gene is sufficient to cause oxidative stress, delayed differentiation and neuronal death in mouse brain.* Dis Model Mech, 2012. **5**(1): p. 125-40.
73. Evans, R.M., *The steroid and thyroid hormone receptor superfamily.* Science, 1988. **240**(4854): p. 889-95.
74. Braissant, O., et al., *Differential expression of peroxisome proliferator-activated receptors (PPARs): tissue distribution of PPAR-alpha, -beta, and -gamma in the adult rat.* Endocrinology, 1996. **137**(1): p. 354-66.
75. Lemberger, T., et al., *PPAR tissue distribution and interactions with other hormone-signaling pathways.* Ann N Y Acad Sci, 1996. **804**: p. 231-51.
76. Heikkinen, S., J. Auwerx, and C.A. Argmann, *PPARgamma in human and mouse physiology.* Biochim Biophys Acta, 2007. **1771**(8): p. 999-1013.
77. Desvergne, B. and W. Wahli, *Peroxisome proliferator-activated receptors: nuclear control of metabolism.* Endocr Rev, 1999. **20**(5): p. 649-88.
78. Ross, J.A., A.G. Moses, and K.C. Fearon, *The anti-catabolic effects of n-3 fatty acids.* Curr Opin Clin Nutr Metab Care, 1999. **2**(3): p. 219-26.
79. Dreyer, C., et al., *Positive regulation of the peroxisomal beta-oxidation pathway by fatty acids through activation of peroxisome proliferator-activated receptors (PPAR).* Biol Cell, 1993. **77**(1): p. 67-76.
80. Reynders, V., et al., *Peroxisome proliferator-activated receptor alpha (PPAR alpha) down-regulation in cystic fibrosis lymphocytes.* Respir Res, 2006. **7**: p. 104.
81. Woerly, G., et al., *Peroxisome proliferator-activated receptors alpha and gamma down-regulate allergic inflammation and eosinophil activation.* J Exp Med, 2003. **198**(3): p. 411-21.

82. Chinetti, G., et al., *Activation of proliferator-activated receptors alpha and gamma induces apoptosis of human monocyte-derived macrophages.* J Biol Chem, 1998. **273**(40): p. 25573-80.
83. Karnovsky, M.L., *Metchnikoff in Messina: a century of studies on phagocytosis.* N Engl J Med, 1981. **304**(19): p. 1178-80.
84. Moore, M.A. and D. Metcalf, *Ontogeny of the haemopoietic system: yolk sac origin of in vivo and in vitro colony forming cells in the developing mouse embryo.* Br J Haematol, 1970. **18**(3): p. 279-96.
85. van Furth, R., et al., *[Mononuclear phagocytic system: new classification of macrophages, monocytes and of their cell line].* Bull World Health Organ, 1972. **47**(5): p. 651-8.
86. van Furth, R., et al., *The mononuclear phagocyte system: a new classification of macrophages, monocytes, and their precursor cells.* Bull World Health Organ, 1972. **46**(6): p. 845-52.
87. Henson, P.M., D.L. Bratton, and V.A. Fadok, *Apoptotic cell removal.* Curr Biol, 2001. **11**(19): p. R795-805.
88. van Furth, R., *Origin and turnover of monocytes and macrophages.* Curr Top Pathol, 1989. **79**: p. 125-50.
89. Van Furth, R., et al., *Characteristics, origin and kinetics of human and murine mononuclear phagocytoses.* Mononuclear Phagocyte. Functional Aspects, ed. R. Van Furth. 1980, the Hague: Martinus Nijhoff Publishers.
90. Meuret, G. and G. Hoffmann, *Monocyte kinetic studies in normal and disease states.* Br J Haematol, 1973. **24**(3): p. 275-85.
91. van Furth, R., *Cell kinetic and genetic aspects of macrophage activation.* Ann Inst Pasteur Immunol, 1986. **137C**(2): p. 192-7.
92. Dustin, M.L., et al., *Induction by IL 1 and interferon-gamma: tissue distribution, biochemistry, and function of a natural adherence molecule (ICAM-1).* J Immunol, 1986. **137**(1): p. 245-54.
93. Lee, C.K., et al., *Fourteen-day inhalation study in rats, using aged and diluted sidestream smoke from a reference cigarette. II. DNA adducts and alveolar macrophage cytogenetics.* Fundam Appl Toxicol, 1992. **19**(1): p. 141-6.
94. Metcalf, D., *The molecular control of cell division, differentiation commitment and maturation in haemopoietic cells.* Nature, 1989. **339**(6219): p. 27-30.
95. Metcalf, D., *Murine hematopoietic stem cells committed to macrophage/dendritic cell formation: stimulation by Flk2-ligand with enhancement by regulators using the gp130 receptor chain.* Proc Natl Acad Sci U S A, 1997. **94**(21): p. 11552-6.
96. Wiktor-Jedrzejczak, W. and S. Gordon, *Cytokine regulation of the macrophage (M phi) system studied using the colony stimulating factor-1-deficient op/op mouse.* Physiol Rev, 1996. **76**(4): p. 927-47.
97. Laskin, D.L., B. Weinberger, and J.D. Laskin, *Functional heterogeneity in liver and lung macrophages.* J Leukoc Biol, 2001. **70**(2): p. 163-70.
98. van Furth, R., *Human monocytes and cytokines.* Res Immunol, 1998. **149**(7-8): p. 719-20.
99. Muller, W.A., *New mechanisms and pathways for monocyte recruitment.* J Exp Med, 2001. **194**(9): p. F47-51.
100. *The Macrophage.* 2nd ed, ed. C.E.L. Bernard Burke. 2002, Oxford: Oxford University Press.
101. Hopkinson-Woolley, J., et al., *Macrophage recruitment during limb development and wound healing in the embryonic and foetal mouse.* J Cell Sci, 1994. **107 (Pt 5)**: p. 1159-67.

102. Lichanska, A.M. and D.A. Hume, *Origins and functions of phagocytes in the embryo.* Exp Hematol, 2000. **28**(6): p. 601-11.
103. Shapiro, S.D., et al., *Proteinases secreted by human mononuclear phagocytes.* J Rheumatol Suppl, 1991. **27**: p. 95-8.
104. Wilson, K., *Wound healing: the role of macrophages.* Nurs Crit Care, 1997. **2**(6): p. 291-6.
105. de Villiers, W.J., et al., *Macrophage phenotype in mice deficient in both macrophage-colony-stimulating factor (op) and apolipoprotein E.* Arterioscler Thromb Vasc Biol, 1998. **18**(4): p. 631-40.
106. Wang, X. and P.J. Quinn, *Lipopolysaccharide: Biosynthetic pathway and structure modification.* Prog Lipid Res. **49**(2): p. 97-107.
107. Raetz, C.R. and C. Whitfield, *Lipopolysaccharide endotoxins.* Annu Rev Biochem, 2002. **71**: p. 635-700.
108. Heinrichs, D.E., J.A. Yethon, and C. Whitfield, *Molecular basis for structural diversity in the core regions of the lipopolysaccharides of Escherichia coli and Salmonella enterica.* Mol Microbiol, 1998. **30**(2): p. 221-32.
109. Cohn, Z.A., *Activation of mononuclear phagocytes: fact, fancy, and future.* J Immunol, 1978. **121**(3): p. 813-6.
110. Hampton, M.B., A.J. Kettle, and C.C. Winterbourn, *Inside the neutrophil phagosome: oxidants, myeloperoxidase, and bacterial killing.* Blood, 1998. **92**(9): p. 3007-17.
111. Kaplan, S.S., et al., *Effect of nitric oxide on staphylococcal killing and interactive effect with superoxide.* Infect Immun, 1996. **64**(1): p. 69-76.
112. Ofek, I., et al., *Nonopsonic phagocytosis of microorganisms.* Annu Rev Microbiol, 1995. **49**: p. 239-76.
113. Stahl, P.D. and R.A. Ezekowitz, *The mannose receptor is a pattern recognition receptor involved in host defense.* Curr Opin Immunol, 1998. **10**(1): p. 50-5.
114. van der Laan, L.J., et al., *Regulation and functional involvement of macrophage scavenger receptor MARCO in clearance of bacteria in vivo.* J Immunol, 1999. **162**(2): p. 939-47.
115. Lehrer, R.I., et al., *Interaction of human defensins with Escherichia coli. Mechanism of bactericidal activity.* J Clin Invest, 1989. **84**(2): p. 553-61.
116. Sawyer, J.G., N.L. Martin, and R.E. Hancock, *Interaction of macrophage cationic proteins with the outer membrane of Pseudomonas aeruginosa.* Infect Immun, 1988. **56**(3): p. 693-8.
117. Bendtzen, K., *Interleukin 1, interleukin 6 and tumor necrosis factor in infection, inflammation and immunity.* Immunol Lett, 1988. **19**(3): p. 183-91.
118. Groopman, J.E., J.M. Molina, and D.T. Scadden, *Hematopoietic growth factors. Biology and clinical applications.* N Engl J Med, 1989. **321**(21): p. 1449-59.
119. Dinarello, C.A., *Biologic basis for interleukin-1 in disease.* Blood, 1996. **87**(6): p. 2095-147.
120. Puren, A.J., et al., *Interleukin-18 (IFNgamma-inducing factor) induces IL-8 and IL-1beta via TNFalpha production from non-CD14+ human blood mononuclear cells.* J Clin Invest, 1998. **101**(3): p. 711-21.
121. Schindler, R., et al., *Correlations and interactions in the production of interleukin-6 (IL-6), IL-1, and tumor necrosis factor (TNF) in human blood mononuclear cells: IL-6 suppresses IL-1 and TNF.* Blood, 1990. **75**(1): p. 40-7.
122. Richman-Eisenstat, J., *Cytokine soup: making sense of inflammation in cystic fibrosis.* Pediatr Pulmonol, 1996. **21**(1): p. 3-5.
123. Gordon, S., J. Todd, and Z.A. Cohn, *In vitro synthesis and secretion of lysozyme by mononuclear phagocytes.* J Exp Med, 1974. **139**(5): p. 1228-48.

124. Nathan, C.F., *Secretory products of macrophages.* J Clin Invest, 1987. **79**(2): p. 319-26.
125. Janeway, C.A., Jr. and R. Medzhitov, *Innate immune recognition.* Annu Rev Immunol, 2002. **20**: p. 197-216.
126. Takeda, K., T. Kaisho, and S. Akira, *Toll-like receptors.* Annu Rev Immunol, 2003. **21**: p. 335-76.
127. Kawai, T. and S. Akira, *The role of pattern-recognition receptors in innate immunity: update on Toll-like receptors.* Nat Immunol. **11**(5): p. 373-84.
128. Kawai, T. and S. Akira, *Signaling to NF-kappaB by Toll-like receptors.* Trends Mol Med, 2007. **13**(11): p. 460-9.
129. Akira, S., K. Takeda, and T. Kaisho, *Toll-like receptors: critical proteins linking innate and acquired immunity.* Nat Immunol, 2001. **2**(8): p. 675-80.
130. Miyake, K., *Innate immune sensing of pathogens and danger signals by cell surface Toll-like receptors.* Semin Immunol, 2007. **19**(1): p. 3-10.
131. Beutler, B., et al., *Genetic analysis of host resistance: Toll-like receptor signaling and immunity at large.* Annu Rev Immunol, 2006. **24**: p. 353-89.
132. Akira, S. and K. Takeda, *Toll-like receptor signalling.* Nat Rev Immunol, 2004. **4**(7): p. 499-511.
133. Kaisho, T. and S. Akira, *Toll-like receptor function and signaling.* J Allergy Clin Immunol, 2006. **117**(5): p. 979-87; quiz 988.
134. Carswell, E.A., et al., *An endotoxin-induced serum factor that causes necrosis of tumors.* Proc Natl Acad Sci U S A, 1975. **72**(9): p. 3666-70.
135. Mannel, D.N. and B. Echtenacher, *TNF in the inflammatory response.* Chem Immunol, 2000. **74**: p. 141-61.
136. Balkwill, F., *TNF-alpha in promotion and progression of cancer.* Cancer Metastasis Rev, 2006. **25**(3): p. 409-16.
137. Bradley, J.R., *TNF-mediated inflammatory disease.* J Pathol, 2008. **214**(2): p. 149-60.
138. Locksley, R.M., N. Killeen, and M.J. Lenardo, *The TNF and TNF receptor superfamilies: integrating mammalian biology.* Cell, 2001. **104**(4): p. 487-501.
139. Naismith, J.H. and S.R. Sprang, *Modularity in the TNF-receptor family.* Trends Biochem Sci, 1998. **23**(2): p. 74-9.
140. Banner, D.W., et al., *Crystal structure of the soluble human 55 kd TNF receptor-human TNF beta complex: implications for TNF receptor activation.* Cell, 1993. **73**(3): p. 431-45.
141. Tartaglia, L.A., et al., *A novel domain within the 55 kd TNF receptor signals cell death.* Cell, 1993. **74**(5): p. 845-53.
142. Tartaglia, L.A., et al., *Tumor necrosis factor's cytotoxic activity is signaled by the p55 TNF receptor.* Cell, 1993. **73**(2): p. 213-6.
143. Hsu, H., et al., *TNF-dependent recruitment of the protein kinase RIP to the TNF receptor-1 signaling complex.* Immunity, 1996. **4**(4): p. 387-96.
144. Hsu, H., et al., *TRADD-TRAF2 and TRADD-FADD interactions define two distinct TNF receptor 1 signal transduction pathways.* Cell, 1996. **84**(2): p. 299-308.
145. Baud, V., et al., *Signaling by proinflammatory cytokines: oligomerization of TRAF2 and TRAF6 is sufficient for JNK and IKK activation and target gene induction via an amino-terminal effector domain.* Genes Dev, 1999. **13**(10): p. 1297-308.
146. Fukushima, T., et al., *Ubiquitin-conjugating enzyme Ubc13 is a critical component of TNF receptor-associated factor (TRAF)-mediated inflammatory responses.* Proc Natl Acad Sci U S A, 2007. **104**(15): p. 6371-6.
147. Song, H.Y., et al., *Tumor necrosis factor (TNF)-mediated kinase cascades: bifurcation of nuclear factor-kappaB and c-jun N-terminal kinase (JNK/SAPK) pathways at TNF receptor-associated factor 2.* Proc Natl Acad Sci U S A, 1997. **94**(18): p. 9792-6.

148. Kirillova, I., M. Chaisson, and N. Fausto, *Tumor necrosis factor induces DNA replication in hepatic cells through nuclear factor kappaB activation.* Cell Growth Differ, 1999. **10**(12): p. 819-28.
149. Wajant, H. and P. Scheurich, *TNFR1-induced activation of the classical NFkappaB pathway.* FEBS J.
150. Varfolomeev, E.E., et al., *Targeted disruption of the mouse Caspase 8 gene ablates cell death induction by the TNF receptors, Fas/Apo1, and DR3 and is lethal prenatally.* Immunity, 1998. **9**(2): p. 267-76.
151. Sanchez, I., et al., *Caspase-8 is required for cell death induced by expanded polyglutamine repeats.* Neuron, 1999. **22**(3): p. 623-33.
152. Zhang, J., et al., *Fas-mediated apoptosis and activation-induced T-cell proliferation are defective in mice lacking FADD/Mort1.* Nature, 1998. **392**(6673): p. 296-300.
153. Yeh, W.C., et al., *FADD: essential for embryo development and signaling from some, but not all, inducers of apoptosis.* Science, 1998. **279**(5358): p. 1954-8.
154. Bodmer, J.L., et al., *TRAIL receptor-2 signals apoptosis through FADD and caspase-8.* Nat Cell Biol, 2000. **2**(4): p. 241-3.
155. Smale, S.T., *Hierarchies of NF-kappaB target-gene regulation.* Nat Immunol. **12**(8): p. 689-94.
156. Doyle, S.L. and L.A. O'Neill, *Toll-like receptors: from the discovery of NFkappaB to new insights into transcriptional regulations in innate immunity.* Biochem Pharmacol, 2006. **72**(9): p. 1102-13.
157. Shih, V.F., et al., *A single NFkappaB system for both canonical and non-canonical signaling.* Cell Res. **21**(1): p. 86-102.
158. Baeuerle, P.A., *IkappaB-NF-kappaB structures: at the interface of inflammation control.* Cell, 1998. **95**(6): p. 729-31.
159. Ghosh, S., M.J. May, and E.B. Kopp, *NF-kappa B and Rel proteins: evolutionarily conserved mediators of immune responses.* Annu Rev Immunol, 1998. **16**: p. 225-60.
160. Hoffmann, A., G. Natoli, and G. Ghosh, *Transcriptional regulation via the NF-kappaB signaling module.* Oncogene, 2006. **25**(51): p. 6706-16.
161. Hayden, M.S. and S. Ghosh, *Shared principles in NF-kappaB signaling.* Cell, 2008. **132**(3): p. 344-62.
162. Dobrzanski, P., R.P. Ryseck, and R. Bravo, *Specific inhibition of RelB/p52 transcriptional activity by the C-terminal domain of p100.* Oncogene, 1995. **10**(5): p. 1003-7.
163. Liou, H.C., et al., *The NF-kappa B p50 precursor, p105, contains an internal I kappa B-like inhibitor that preferentially inhibits p50.* EMBO J, 1992. **11**(8): p. 3003-9.
164. Carmody, R.J., et al., *Negative regulation of toll-like receptor signaling by NF-kappaB p50 ubiquitination blockade.* Science, 2007. **317**(5838): p. 675-8.
165. Haruta, H., A. Kato, and K. Todokoro, *Isolation of a novel interleukin-1-inducible nuclear protein bearing ankyrin-repeat motifs.* J Biol Chem, 2001. **276**(16): p. 12485-8.
166. Fiorini, E., et al., *Peptide-induced negative selection of thymocytes activates transcription of an NF-kappa B inhibitor.* Mol Cell, 2002. **9**(3): p. 637-48.
167. Karin, M. and Y. Ben-Neriah, *Phosphorylation meets ubiquitination: the control of NF-[kappa]B activity.* Annu Rev Immunol, 2000. **18**: p. 621-63.
168. Sato, S., et al., *Essential function for the kinase TAK1 in innate and adaptive immune responses.* Nat Immunol, 2005. **6**(11): p. 1087-95.
169. Shim, J.H., et al., *TAK1, but not TAB1 or TAB2, plays an essential role in multiple signaling pathways in vivo.* Genes Dev, 2005. **19**(22): p. 2668-81.

170. Deng, L., et al., *Activation of the IkappaB kinase complex by TRAF6 requires a dimeric ubiquitin-conjugating enzyme complex and a unique polyubiquitin chain.* Cell, 2000. **103**(2): p. 351-61.
171. Chen, F., et al., *Finding NEMO by K63-linked polyubiquitin chain.* Cell Death Differ, 2006. **13**(11): p. 1835-8.
172. Oeckinghaus, A., et al., *Malt1 ubiquitination triggers NF-kappaB signaling upon T-cell activation.* EMBO J, 2007. **26**(22): p. 4634-45.
173. Yeh, W.C., et al., *Early lethality, functional NF-kappaB activation, and increased sensitivity to TNF-induced cell death in TRAF2-deficient mice.* Immunity, 1997. **7**(5): p. 715-25.
174. Nakano, H., et al., *Targeted disruption of Traf5 gene causes defects in CD40- and CD27-mediated lymphocyte activation.* Proc Natl Acad Sci U S A, 1999. **96**(17): p. 9803-8.
175. Tada, K., et al., *Critical roles of TRAF2 and TRAF5 in tumor necrosis factor-induced NF-kappa B activation and protection from cell death.* J Biol Chem, 2001. **276**(39): p. 36530-4.
176. Wessells, J., et al., *BCL-3 and NF-kappaB p50 attenuate lipopolysaccharide-induced inflammatory responses in macrophages.* J Biol Chem, 2004. **279**(48): p. 49995-50003.
177. Tato, C.M., et al., *Opposing roles of NF-kappaB family members in the regulation of NK cell proliferation and production of IFN-gamma.* Int Immunol, 2006. **18**(4): p. 505-13.
178. Lawrence, T., et al., *IKKalpha limits macrophage NF-kappaB activation and contributes to the resolution of inflammation.* Nature, 2005. **434**(7037): p. 1138-43.
179. Li, Q., et al., *Enhanced NF-kappaB activation and cellular function in macrophages lacking IkappaB kinase 1 (IKK1).* Proc Natl Acad Sci U S A, 2005. **102**(35): p. 12425-30.
180. McGuinness, M.C. and K.D. Smith, *Cerebral inflammation in X-linked adrenoleukodystrophy.* Arch Immunol Ther Exp (Warsz), 1999. **47**(5): p. 281-7.
181. Lannuzel, A., P. Aubourg, and M. Tardieu, *Excessive production of tumour necrosis factor alpha by peripheral blood mononuclear cells in X-linked adrenoleukodystrophy.* Eur J Paediatr Neurol, 1998. **2**(1): p. 27-32.
182. Haq, E., et al., *Dysfunction of peroxisomes in twitcher mice brain: a possible mechanism of psychosine-induced disease.* Biochem Biophys Res Commun, 2006. **343**(1): p. 229-38.
183. Singh, I., et al., *Impaired peroxisomal function in the central nervous system with inflammatory disease of experimental autoimmune encephalomyelitis animals and protection by lovastatin treatment.* Brain Res, 2004. **1022**(1-2): p. 1-11.
184. Hall, D., et al., *Peroxisomal and microsomal lipid pathways associated with resistance to hepatic steatosis and reduced pro-inflammatory state.* J Biol Chem. **285**(40): p. 31011-23.
185. Khan, M., M. Contreras, and I. Singh, *Endotoxin-induced alterations of lipid and fatty acid compositions in rat liver peroxisomes.* J Endotoxin Res, 2000. **6**(1): p. 41-50.
186. Contreras, M.A., et al., *Endotoxin induces structure-function alterations of rat liver peroxisomes: Kupffer cells released factors as possible modulators.* Hepatology, 2000. **31**(2): p. 446-55.
187. Deutschland, S.B. *Anzahl der Gestorbenen nach Kapiteln der International Statistical Classification of Diseases and Related Health Problems (ICD-10).* 2008-2010; Available from: https://www.destatis.de/DE/ZahlenFakten/GesellschaftStaat/Gesundheit/Todesursachen/Tabellen/GestorbeneAnzahl.html.

188. Deutschland, S.B. *Krankheitskosten nach Krankheitsklassen und Geschlecht in Euro je Einwohner.* 2008; Available from: https://www.destatis.de/DE/ZahlenFakten/GesellschaftStaat/Gesundheit/Krankheitskosten/Tabellen/KrankheitsklassenGeschlecht.html.
189. Glass, C.K. and J.L. Witztum, *Atherosclerosis. the road ahead.* Cell, 2001. **104**(4): p. 503-16.
190. Stocker, R. and J.F. Keaney, Jr., *Role of oxidative modifications in atherosclerosis.* Physiol Rev, 2004. **84**(4): p. 1381-478.
191. Libby, P. and D.X. Zhao, *Allograft arteriosclerosis and immune-driven angiogenesis.* Circulation, 2003. **107**(9): p. 1237-9.
192. Nicholson, A.C. and D.P. Hajjar, *CD36, oxidized LDL and PPAR gamma: pathological interactions in macrophages and atherosclerosis.* Vascul Pharmacol, 2004. **41**(4-5): p. 139-46.
193. Raschke, W.C., et al., *Functional macrophage cell lines transformed by Abelson leukemia virus.* Cell, 1978. **15**(1): p. 261-7.
194. Zhang, X., R. Goncalves, and D.M. Mosser, *The isolation and characterization of murine macrophages.* Curr Protoc Immunol, 2008. **Chapter 14**: p. Unit 14 1.
195. Ray, A. and B.N. Dittel, *Isolation of mouse peritoneal cavity cells.* J Vis Exp, 2010(35).
196. Bradford, M.M., *A rapid and sensitive method for the quantitation of microgram quantities of protein utilizing the principle of protein-dye binding.* Anal Biochem, 1976. **72**: p. 248-54.
197. Dieuaide, M., et al., *Substrate stereospecificities of rat liver peroxisomal 3-hydroxyacyl-CoA dehydrogenases.* Ann N Y Acad Sci, 1996. **804**: p. 680-1.
198. Volkl, A. and H.D. Fahimi, *Isolation and characterization of peroxisomes from the liver of normal untreated rats.* Eur J Biochem, 1985. **149**(2): p. 257-65.
199. Wilcke, M. and S.E. Alexson, *Differential induction of peroxisomal populations in subcellular fractions of rat liver.* Biochim Biophys Acta, 2001. **1544**(1-2): p. 358-69.
200. Dhaunsi, G.S. and M.S. Bitar, *Antioxidants attenuate diabetes-induced activation of peroxisomal functions in the rat kidney.* J Biomed Sci, 2004. **11**(5): p. 566-70.
201. Bellu, A.R. and J.A. Kiel, *Selective degradation of peroxisomes in yeasts.* Microsc Res Tech, 2003. **61**(2): p. 161-70.
202. Sparkes, I.A. and A. Baker, *Peroxisome biogenesis and protein import in plants, animals and yeasts: enigma and variations? (Review).* Mol Membr Biol, 2002. **19**(3): p. 171-85.
203. Heikoop, J.C., et al., *Turnover of peroxisomal vesicles by autophagic proteolysis in cultured fibroblasts from Zellweger patients.* Eur J Cell Biol, 1992. **57**(2): p. 165-71.
204. Koeck, T. and K. Kremser, *L-Carnitine alters nitric oxide synthase activity in fibroblasts depending on the peroxisomal status.* Int J Biochem Cell Biol, 2003. **35**(2): p. 149-56.
205. Van Veldhoven, P.P., et al., *The deficient degradation of synthetic 2- and 3-methyl-branched fatty acids in fibroblasts from patients with peroxisomal disorders.* J Inherit Metab Dis, 1993. **16**(2): p. 381-91.
206. Antonenkov, V.D., R.T. Sormunen, and J.K. Hiltunen, *The behavior of peroxisomes in vitro: mammalian peroxisomes are osmotically sensitive particles.* Am J Physiol Cell Physiol, 2004. **287**(6): p. C1623-35.
207. Eliassen, K.A., et al., *Activity of peroxisomal enzymes, and levels of polyamines in LPA-transgenic mice on two different diets.* Lipids Health Dis, 2005. **4**: p. 23.
208. Funato, M., et al., *Aberrant peroxisome morphology in peroxisomal beta-oxidation enzyme deficiencies.* Brain Dev, 2006. **28**(5): p. 287-92.

209. Leclercq, S., et al., *Effect of dietary polyunsaturated fatty acids on the expression of peroxisomal ABC transporters.* Biochimie, 2008. **90**(10): p. 1602-7.
210. Wolf, J., W. Schliebs, and R. Erdmann, *Peroxisomes as dynamic organelles: peroxisomal matrix protein import.* FEBS J. **277**(16): p. 3268-78.
211. Baumgart, E., *Application of in situ hybridization, cytochemical and immunocytochemical techniques for the investigation of peroxisomes. A review including novel data. Robert Feulgen Prize Lecture 1997.* Histochem Cell Biol, 1997. **108**(3): p. 185-210.
212. Li, X., et al., *PEX11alpha is required for peroxisome proliferation in response to 4-phenylbutyrate but is dispensable for peroxisome proliferator-activated receptor alpha-mediated peroxisome proliferation.* Mol Cell Biol, 2002. **22**(23): p. 8226-40.
213. Schrader, M. and H.D. Fahimi, *Growth and division of peroxisomes.* Int Rev Cytol, 2006. **255**: p. 237-90.
214. Schrader, M. and S.J. Gould, *Assay and functional analysis of dynamin-like protein 1 in peroxisome division.* Methods Enzymol, 2005. **404**: p. 586-97.
215. Kato, A., et al., *Lipopolysaccharide-binding protein critically regulates lipopolysaccharide-induced IFN-beta signaling pathway in human monocytes.* J Immunol, 2004. **172**(10): p. 6185-94.
216. Pulford, K.A., et al., *Distribution of the CD68 macrophage/myeloid associated antigen.* Int Immunol, 1990. **2**(10): p. 973-80.
217. Kostich, M., A. Fire, and D.M. Fambrough, *Identification and molecular-genetic characterization of a LAMP/CD68-like protein from Caenorhabditis elegans.* J Cell Sci, 2000. **113 (Pt 14)**: p. 2595-606.
218. Song, L., C. Lee, and C. Schindler, *Deletion of the murine scavenger receptor CD68.* J Lipid Res, 2011. **52**(8): p. 1542-50.
219. Lazarow, P.B. and Y. Fujiki, *Biogenesis of peroxisomes.* Annu Rev Cell Biol, 1985. **1**: p. 489-530.
220. Orth, T., et al., *The PEROXIN11 protein family controls peroxisome proliferation in Arabidopsis.* Plant Cell, 2007. **19**(1): p. 333-50.
221. Rottensteiner, H., et al., *Conserved function of pex11p and the novel pex25p and pex27p in peroxisome biogenesis.* Mol Biol Cell, 2003. **14**(10): p. 4316-28.
222. Vijayan, V., et al., *Bruton's tyrosine kinase is required for TLR-dependent heme oxygenase-1 gene activation via Nrf2 in macrophages.* J Immunol, 2011. **187**(2): p. 817-27.
223. Bradford, B.U., *Role of peroxisomes in the swift increase in alcohol metabolism.* J Gastroenterol Hepatol, 2007. **22 Suppl 1**: p. S28-30.
224. Ardeshna, K.M., et al., *The PI3 kinase, p38 SAP kinase, and NF-kappaB signal transduction pathways are involved in the survival and maturation of lipopolysaccharide-stimulated human monocyte-derived dendritic cells.* Blood, 2000. **96**(3): p. 1039-46.
225. Baumgart, E., et al., *Detection of mRNAs encoding peroxisomal proteins by non-radioactive in situ hybridization with digoxigenin-labelled cRNAs.* Histochem Cell Biol, 1997. **108**(4-5): p. 371-9.
226. Litwin, J.A., et al., *Immunocytochemical investigation of catalase and peroxisomal lipid beta-oxidation enzymes in human hepatocellular tumors and liver cirrhosis.* Virchows Arch, 1999. **435**(5): p. 486-95.
227. Litwin, J.A., et al., *Detection of peroxisomes in human liver and kidney fixed with formalin and embedded in paraffin: the use of catalase and lipid beta-oxidation enzymes as immunocytochemical markers.* Histochem J, 1988. **20**(3): p. 165-73.

228. Litwin, J.A., et al., *Immunocytochemical demonstration of peroxisomal enzymes in human kidney biopsies.* Virchows Arch B Cell Pathol Incl Mol Pathol, 1988. **54**(4): p. 207-13.
229. Litwin, J.A. and K. Beier, *Immunogold localization of peroxisomal enzymes in Epon-embedded liver tissue. Enhancement of sensitivity by etching with ethanolic sodium hydroxide.* Histochemistry, 1988. **88**(2): p. 193-6.
230. Litwin, J.A., et al., *Immunocytochemical localization of peroxisomal enzymes in human liver biopsies.* Am J Pathol, 1987. **128**(1): p. 141-50.
231. Baes, M., et al., *A mouse model for Zellweger syndrome.* Nat Genet, 1997. **17**(1): p. 49-57.
232. Atwal, O.S., et al., *In situ heparin-induced peroxisomal reticulum and biogenesis of peroxisomes in pulmonary intravascular macrophages (PIMs) of caprine lung: an ultrastructural and cytochemical study.* Anat Rec, 2002. **266**(1): p. 69-80.
233. Graham, J.M., *Isolation of peroxisomes from tissues and cells by differential and density gradient centrifugation.* Curr Protoc Cell Biol, 2001. **Chapter 3**: p. Unit 3 5.
234. Fahimi, H.D., et al., *Zonal heterogeneity of peroxisome proliferation in rat liver.* Ann N Y Acad Sci, 1996. **804**: p. 341-61.
235. Bunce, C.M., et al., *A rapid procedure for isolating hemopoietic cell nuclei.* Anal Biochem, 1988. **175**(1): p. 67-73.
236. Hasan, Z., et al., *Isolation and characterization of the mycobacterial phagosome: segregation from the endosomal/lysosomal pathway.* Mol Microbiol, 1997. **24**(3): p. 545-53.
237. Canonico, P.G., H. Beaufay, and M. Nyssens-Jadin, *Analytical fractionation of mouse peritoneal macrophages: physical and biochemical properties of subcellular organelles from resident (unstimulated) and cultivated cells.* J Reticuloendothel Soc, 1978. **24**(2): p. 115-38.
238. Darte, C. and H. Beaufay, *Analytical subcellular fractionation of cultivated mouse resident peritoneal macrophages.* J Exp Med, 1983. **157**(4): p. 1208-28.
239. Kobayashi, S., A. Tanaka, and Y. Fujiki, *Fis1, DLP1, and Pex11p coordinately regulate peroxisome morphogenesis.* Exp Cell Res, 2007. **313**(8): p. 1675-86.
240. Laclide-Drouin, H., et al., *Effect of clofibrate on the peroxisomes of the intestine of the rat during foetal development.* Ital J Anat Embryol, 1995. **100 Suppl 1**: p. 411-7.
241. Litwin, J.A. and B. Bilinska, *Morphological heterogeneity of peroxisomes in cultured mouse Leydig cells.* Folia Histochem Cytobiol, 1995. **33**(4): p. 255-8.
242. Nenicu, A., et al., *Peroxisomes in human and mouse testis: differential expression of peroxisomal proteins in germ cells and distinct somatic cell types of the testis.* Biol Reprod, 2007. **77**(6): p. 1060-72.
243. Ribeiro, D., et al., *Peroxisome morphology in pathology.* Histol Histopathol, 2012. **27**(6): p. 661-76.
244. Roels, F., et al., *Peroxisomes during development and in distinct cell types.* Adv Exp Med Biol, 2003. **544**: p. 39-54.
245. Bjorkbacka, H., et al., *The induction of macrophage gene expression by LPS predominantly utilizes Myd88-independent signaling cascades.* Physiol Genomics, 2004. **19**(3): p. 319-30.
246. Oh, Y.C., et al., *Anti-inflammatory effect of Lycium Fruit water extract in lipopolysaccharide-stimulated RAW 264.7 macrophage cells.* Int Immunopharmacol, 2012. **13**(2): p. 181-189.
247. Deng, W.G., Y. Zhu, and K.K. Wu, *Role of p300 and PCAF in regulating cyclooxygenase-2 promoter activation by inflammatory mediators.* Blood, 2004. **103**(6): p. 2135-42.

248. Miyaura, C., et al., *An essential role of cytosolic phospholipase A2alpha in prostaglandin E2-mediated bone resorption associated with inflammation.* J Exp Med, 2003. **197**(10): p. 1303-10.
249. Kim, S.Y., et al., *Transduced PEP-1-FK506BP inhibits the inflammatory response in the Raw 264.7 cell and mouse models.* Immunobiology, 2011. **216**(7): p. 771-81.
250. Kim, D.H., et al., *Suppression of inflammatory responses by celastrol, a quinone methide triterpenoid isolated from Celastrus regelii.* Eur J Clin Invest, 2009. **39**(9): p. 819-27.
251. Bronfman, M., et al., *Peroxisome proliferators and signal transduction.* Ann N Y Acad Sci, 1996. **804**: p. 403-12.
252. Bast, A., et al., *Influence of iNOS and COX on peroxiredoxin gene expression in primary macrophages.* Free Radic Biol Med, 2010. **49**(12): p. 1881-91.
253. Zipfel, A., et al., *Release of TNF-alpha from lipopolysaccharide (LPS)-stimulated Kupffer cells in serum- and nutrient-free medium.* Inflammation, 2001. **25**(5): p. 287-92.
254. Islinger, M., et al., *Rat liver peroxisomes after fibrate treatment. A survey using quantitative mass spectrometry.* J Biol Chem, 2007. **282**(32): p. 23055-69.
255. Li, X. and S.J. Gould, *The dynamin-like GTPase DLP1 is essential for peroxisome division and is recruited to peroxisomes in part by PEX11.* J Biol Chem, 2003. **278**(19): p. 17012-20.
256. Singh, I., *Peroxisomal fatty acid oxidation and cellular redox.* Methods Enzymol, 2002. **352**: p. 361-72.
257. Lo, C.J., et al., *Cyclooxygenase 2 (COX-2) gene activation is regulated by cyclic adenosine monophosphate.* Shock, 2000. **13**(1): p. 41-5.
258. Rhee, S.H. and D. Hwang, *Murine TOLL-like receptor 4 confers lipopolysaccharide responsiveness as determined by activation of NF kappa B and expression of the inducible cyclooxygenase.* J Biol Chem, 2000. **275**(44): p. 34035-40.
259. Lee, A.K., et al., *Inhibition of lipopolysaccharide-inducible nitric oxide synthase, TNF-alpha and COX-2 expression by sauchinone effects on I-kappaBalpha phosphorylation, C/EBP and AP-1 activation.* Br J Pharmacol, 2003. **139**(1): p. 11-20.
260. Leu, T.H., et al., *Lipopolysaccharide-induced c-Src expression plays a role in nitric oxide and TNFalpha secretion in macrophages.* Mol Immunol, 2006. **43**(4): p. 308-16.
261. Haq, A.U. and R.D. Maca, *Role of IFN-gamma and alpha in IL 1 synthesis and secretion of in vitro differentiated human macrophages: a comparative study.* Immunobiology, 1986. **171**(4-5): p. 451-60.
262. Wang, S.Y., et al., *Inhibitory effect of activin A on activation of lipopolysaccharide-stimulated mouse macrophage RAW264.7 cells.* Cytokine, 2008. **42**(1): p. 85-91.
263. Martinez, J., T. Sanchez, and J.J. Moreno, *Regulation of prostaglandin E2 production by the superoxide radical and nitric oxide in mouse peritoneal macrophages.* Free Radic Res, 2000. **32**(4): p. 303-11.
264. Baek, S.H., et al., *The effects of two new antagonists of secretory PLA2 on TNF, iNOS, and COX-2 expression in activated macrophages.* Shock, 1999. **12**(6): p. 473-8.
265. Eliopoulos, A.G., et al., *Induction of COX-2 by LPS in macrophages is regulated by Tpl2-dependent CREB activation signals.* EMBO J, 2002. **21**(18): p. 4831-40.
266. Mestre, J.R., et al., *Redundancy in the signaling pathways and promoter elements regulating cyclooxygenase-2 gene expression in endotoxin-treated macrophage/monocytic cells.* J Biol Chem, 2001. **276**(6): p. 3977-82.
267. Kunkel, S.L., et al., *Prostaglandin E2 regulates macrophage-derived tumor necrosis factor gene expression.* J Biol Chem, 1988. **263**(11): p. 5380-4.
268. Chang, C.F., et al., *The lipopolysaccharide-induced pro-inflammatory response in RAW264.7 cells is attenuated by an unsaturated fatty acid-bovine serum albumin*

complex and enhanced by a saturated fatty acid-bovine serum albumin complex. Inflamm Res, 2012. **61**(2): p. 151-60.

269. Sweet, M.J. and D.A. Hume, *Endotoxin signal transduction in macrophages.* J Leukoc Biol, 1996. **60**(1): p. 8-26.
270. Lin, W., et al., *Sulforaphane suppressed LPS-induced inflammation in mouse peritoneal macrophages through Nrf2 dependent pathway.* Biochem Pharmacol, 2008. **76**(8): p. 967-73.
271. Rouzer, C.A., et al., *RAW264.7 cells lack prostaglandin-dependent autoregulation of tumor necrosis factor-alpha secretion.* J Lipid Res, 2005. **46**(5): p. 1027-37.
272. Sevanian, A., L. Asatryan, and O. Ziouzenkova, *Low density lipoprotein (LDL) modification: basic concepts and relationship to atherosclerosis.* Blood Purif, 1999. **17**(2-3): p. 66-78.
273. Harb, D., et al., *The role of the scavenger receptor CD36 in regulating mononuclear phagocyte trafficking to atherosclerotic lesions and vascular inflammation.* Cardiovasc Res, 2009. **83**(1): p. 42-51.
274. Zmijewski, J.W., et al., *Cell signalling by oxidized lipids and the role of reactive oxygen species in the endothelium.* Biochem Soc Trans, 2005. **33**(Pt 6): p. 1385-9.
275. Tontonoz, P. and L. Nagy, *Regulation of macrophage gene expression by peroxisome-proliferator-activated receptor gamma: implications for cardiovascular disease.* Curr Opin Lipidol, 1999. **10**(6): p. 485-90.
276. Medzhitov, R., P. Preston-Hurlburt, and C.A. Janeway, Jr., *A human homologue of the Drosophila Toll protein signals activation of adaptive immunity.* Nature, 1997. **388**(6640): p. 394-7.
277. Endemann, G., et al., *CD36 is a receptor for oxidized low density lipoprotein.* J Biol Chem, 1993. **268**(16): p. 11811-6.
278. Kunjathoor, V.V., et al., *Scavenger receptors class A-I/II and CD36 are the principal receptors responsible for the uptake of modified low density lipoprotein leading to lipid loading in macrophages.* J Biol Chem, 2002. **277**(51): p. 49982-8.
279. Ohnishi, K., et al., *Suppression of TLR4-mediated inflammatory response by macrophage class A scavenger receptor (CD204).* Biochem Biophys Res Commun, 2011. **411**(3): p. 516-22.
280. Geng, H., et al., *The effects of ox-LDL in human atherosclerosis may be mediated in part via the toll-like receptor 4 pathway.* Mol Cell Biochem, 2010. **342**(1-2): p. 201-6.
281. Chavez-Sanchez, L., et al., *Activation of TLR2 and TLR4 by minimally modified low-density lipoprotein in human macrophages and monocytes triggers the inflammatory response.* Hum Immunol, 2010. **71**(8): p. 737-44.
282. Stewart, C.R., et al., *CD36 ligands promote sterile inflammation through assembly of a Toll-like receptor 4 and 6 heterodimer.* Nat Immunol, 2010. **11**(2): p. 155-61.
283. Daynes, R.A. and D.C. Jones, *Emerging roles of PPARs in inflammation and immunity.* Nat Rev Immunol, 2002. **2**(10): p. 748-59.
284. Taketa, K., et al., *Oxidized low density lipoprotein activates peroxisome proliferator-activated receptor-alpha (PPARalpha) and PPARgamma through MAPK-dependent COX-2 expression in macrophages.* J Biol Chem, 2008. **283**(15): p. 9852-62.
285. Cristiano, L., A. Bernardo, and M.P. Ceru, *Peroxisome proliferator-activated receptors (PPARs) and peroxisomes in rat cortical and cerebellar astrocytes.* J Neurocytol, 2001. **30**(8): p. 671-83.
286. Karnati, S. and E. Baumgart-Vogt, *Peroxisomes in airway epithelia and future prospects of these organelles for pulmonary cell biology.* Histochem Cell Biol, 2009. **131**(4): p. 447-54.
287. Dixit, E., et al., *Peroxisomes are signaling platforms for antiviral innate immunity.* Cell. **141**(4): p. 668-81.

288. Beier, K., A. Volkl, and H.D. Fahimi, *TNF-alpha downregulates the peroxisome proliferator activated receptor-alpha and the mRNAs encoding peroxisomal proteins in rat liver.* FEBS Lett, 1997. **412**(2): p. 385-7.
289. Paintlia, M.K., et al., *Lipopolysaccharide-induced peroxisomal dysfunction exacerbates cerebral white matter injury: attenuation by N-acetyl cysteine.* Exp Neurol, 2008. **210**(2): p. 560-76.
290. Karin, M. and A. Lin, *NF-kappaB at the crossroads of life and death.* Nat Immunol, 2002. **3**(3): p. 221-7.
291. Li, X., et al., *PEX11 beta deficiency is lethal and impairs neuronal migration but does not abrogate peroxisome function.* Mol Cell Biol, 2002. **22**(12): p. 4358-65.
292. Baumgart, E., et al., *Mitochondrial alterations caused by defective peroxisomal biogenesis in a mouse model for Zellweger syndrome (PEX5 knockout mouse).* Am J Pathol, 2001. **159**(4): p. 1477-94.
293. Maxwell, M., et al., *Pex13 inactivation in the mouse disrupts peroxisome biogenesis and leads to a Zellweger syndrome phenotype.* Mol Cell Biol, 2003. **23**(16): p. 5947-57.
294. Faust, P.L. and M.E. Hatten, *Targeted deletion of the PEX2 peroxisome assembly gene in mice provides a model for Zellweger syndrome, a human neuronal migration disorder.* J Cell Biol, 1997. **139**(5): p. 1293-305.
295. Liu, X., et al., *Induction of apoptotic program in cell-free extracts: requirement for dATP and cytochrome c.* Cell, 1996. **86**(1): p. 147-57.
296. Garcia Fernandez, M., et al., *Early changes in intramitochondrial cardiolipin distribution during apoptosis.* Cell Growth Differ, 2002. **13**(9): p. 449-55.
297. Huttemann, M., et al., *The multiple functions of cytochrome c and their regulation in life and death decisions of the mammalian cell: From respiration to apoptosis.* Mitochondrion, 2011. **11**(3): p. 369-81.
298. Sakahira, H., M. Enari, and S. Nagata, *Cleavage of CAD inhibitor in CAD activation and DNA degradation during apoptosis.* Nature, 1998. **391**(6662): p. 96-9.
299. Cohen, G.M., *Caspases: the executioners of apoptosis.* Biochem J, 1997. **326 (Pt 1)**: p. 1-16.
300. Zha, J., et al., *Serine phosphorylation of death agonist BAD in response to survival factor results in binding to 14-3-3 not BCL-X(L).* Cell, 1996. **87**(4): p. 619-28.
301. Pilette, C., et al., *Oxidative burst in lipopolysaccharide-activated human alveolar macrophages is inhibited by interleukin-9.* Eur Respir J, 2002. **20**(5): p. 1198-205.
302. Hughes, H.P., *Oxidative killing of intracellular parasites mediated by macrophages.* Parasitol Today, 1988. **4**(12): p. 340-7.
303. Marriott, I. and Y.M. Huet-Hudson, *Sexual dimorphism in innate immune responses to infectious organisms.* Immunol Res, 2006. **34**(3): p. 177-92.
304. Rettew, J.A., Y.M. Huet-Hudson, and I. Marriott, *Testosterone reduces macrophage expression in the mouse of toll-like receptor 4, a trigger for inflammation and innate immunity.* Biol Reprod, 2008. **78**(3): p. 432-7.
305. Rettew, J.A., Y.M. Huet, and I. Marriott, *Estrogens augment cell surface TLR4 expression on murine macrophages and regulate sepsis susceptibility in vivo.* Endocrinology, 2009. **150**(8): p. 3877-84.

13. Ehrenwörtliche Erklärung

Hiermit erkläre ich, dass ich die vorliegende Arbeit selbständig und ohne unzulässige Hilfe oder Benutzung anderer als der angegebenen Hilfsmittel angefertigt habe. Alle Teststellen, die wörtlich oder sinngemäß aus veröffentlichten oder nichtveröffentlichten Schriften entnommen sind, und alle Angaben, die auf mündlichen Auskünften beruhen, sind als solche kenntlich gemacht. Bei den von mir durchgeführten und in der Dissertation erwähnten Untersuchungen habe ich die Grundsätze guter wissenschaftlicher Praxis, wie sie in der „Satzung der Justus-Liebig-Universität Gießen zu Sicherung guter wissenschaftlicher Praxis“ niedergelegt sind, eingehalten sowie ethische, datenschutzrechtliche und tierschutzrechtliche Grundsätze befolgt. Ich versichere, das Dritte von mir weder unmittelbar noch mittelbar geldwerte Leistungen für Arbeiten erhalten haben, die im Zusammenhang mit dem Inhalt der vorgelegten Dissertation stehen, oder habe diese nachstehend spezifiziert. Die vorgelegte Arbeit wurde weder in Inland noch im Ausland in gleicher oder ähnlicher Form einer anderen Prüfungsbehörde zum Zweck einer Promotion oder eines anderen Prüfungsverfahrens vorgelegt. Alles aus anderen Quellen und von anderen Personen übernommene Material, das in der Arbeit verwendet wurde oder auf das direkt Bezug genommen wird, wurde als solches kenntlich gemacht. Insbesondere wurden alle Personen genannt, die direkt und indirekt an der Entstehung der vorliegenden Arbeit beteiligt waren. Mit der Überprüfung meiner Arbeit durch eine Plagiatserkennungssoftware bzw. einer internetbasiertes Softwareprogramm erkläre ich mich einverstanden.

_____ _____

Ort, Datum Unterschrift